Performance, Combustion and Emission Analysis of a Compression Ignition Engine Fueled with Advanced Biofuel Blends

A thesis submitted in partial fulfillment of the requirement for the degree of

Master of Science in Mechanical Engineering

Submitted by

Minhaz Ahmed

Student ID: 22MME009

Supervisor: Prof. Dr. Mohammad Mizanur Rahman

Department of Mechanical Engineering

Chittagong University of Engineering and Technology

Chattogram-4349, Bangladesh

March, 2025

Approval

The thesis titled **"Performance, Combustion and Emission Analysis of a Compression Ignition Engine Fueled with Advanced Biofuel Blends"** submitted by Minhaz Ahmed, ID-22MME009, Session: 2022-2023 has been accepted as satisfactory in partial fulfillment of the requirement for the degree of Masters of Science (M.Sc.) in Mechanical Engineering dated on

Board of Examiners

1.	**Dr. Md. Mizanur Rahman** **Professor, Department of Mechanical Engineering, CUET**	**Chairman** **(Supervisor)**
2.	**Dr. Md. Arafat Rahman** **Professor, Department of Mechanical Engineering, CUET**	**Member** **(Co-supervisor)**
3.	**Head of the Department** **Department of Mechanical Engineering, CUET**	**Member** **(Ex-Officio)**
4.	**Dr. Md. Sanaul Rabbi** **Professor, Department of Mechanical Engineering, CUET**	**Member**
5.	**Md. Aminul Islam** **Associate Professor, Department of Mechanical Engineering, CUET**	**Member**
6.	**Dr. A.N.M. Mominul Islam Mukut** **Professor, Department of Mechanical Engineering, DUET**	**Member** **(External)**

Declaration

I, the undersigned, do hereby confirm to declare that the thesis is conducted and composed of myself and the work has not been submitted anywhere for other degrees or professional qualifications. To the best of my knowledge, contained materials were not written or published by anyone, except where due references are made.

Name: Minhaz Ahmed

Student ID: 22MME009

Acknowledgement

All praises are for Allah, the Lord of the universe, for supporting and providing me blessings for the completion of the present work.

I would like to express profound gratefulness to my supervisor Dr. Mohammad Mizanur Rahman, Professor, Department of Mechanical Engineering, Chittagong University of Engineering and Technology for his steady supervision, incredible direction, constant encouragement, and significant remarks. I would also like to acknowledge the unwavering support and insightful feedbacks provided by my co-supervisor Dr. Md. Arafat Rahman, Professor, Department of Mechanical Engineering, Chittagong University of Engineering and Technology.

I owe a debt of gratitude to Tafsirul Hassan, Assistant Professor, Department of Mechanical Engineering, Chittagong University of Engineering and Technology for the essential advice and invaluable guidance provided to shape the thesis. I would like to thank Dr. Md. Sanaul Rabbi, Professor, Department of Mechanical Engineering, Chittagong University of Engineering and Technology and Md. Aminul Islam, Associate Professor, Department of Mechanical Engineering, Chittagong University of Engineering and Technology for their critical assessment of this work.

I extend my sincere appreciation to the faculty and staff of Chittagong University of Engineering and Technology for providing a stimulating academic environment that facilitated my research endeavors. At long last, I would like to thank my parents for their unwavering support, consolation, and help all through my journey.

Abstract

Third-generation microalgae are considered superior to other biodiesel feedstocks. Biomass-to-liquid (BTL) diesel, a renewable fuel, has emerged as a promising alternative for transportation due to its unique properties that enhance engine performance and reduce NO_x emissions compared to conventional biodiesel. This study presents a numerical investigation into the effects of neat BTL diesel and four BTL diesel-microalgae biodiesel blends, prepared by mixing 20, 40, 60, and 80 vol% microalgae biodiesel into BTL diesel on the performance of a single-cylinder diesel engine. The study employs the RK multi-zone combustion model to simulate engine behavior across five injection timings (ITs) and validated against reliable experimental data. Neat BTL diesel demonstrated improved engine performance and exhaust characteristics compared to conventional diesel, except for NO_x emissions. The ignition delay, combustion duration, and premixed peak heat release rate for the microalgae-BTL blends increased by 11.04–67.24%, 0.66–13.03%, and 5.25–29.87%, respectively, while peak cylinder pressure decreased by 0.72–5.26% relative to pure BTL diesel. The microalgae-BTL blends caused brake-specific fuel consumption to rise by 2.14–7.51% across all ITs. Brake thermal efficiency decreased by 0.2–1.6% for ITs between 1° and 4° CA bTDC, but increased for ITs between 7° and 13° CA bTDC with higher biodiesel content in the blends. Additionally, the microalgae blends reduced CO_2, particulate matter (PM), and smoke emissions; however, the increased NO_x emissions compared to neat BTL diesel. The optimum IT is identified as 4° CA bTDC for improved performance and reduced PM and smoke with an acceptable NO_x trade-off.

সারসংক্ষেপ

তৃতীয় প্রজন্মের মাইক্রোঅ্যালগি অন্যান্য বায়োডিজেল ফিডস্টকের তুলনায় উন্নত বলে বিবেচিত হয়। জৈববস্তু থেকে তরল (BTL) ডিজেল, একটি নবায়নযোগ্য জ্বালানি, পরিবহনের জন্য একটি প্রতিশ্রুতিশীল বিকল্প হিসেবে আবির্ভূত হয়েছে কারণ এর অনন্য বৈশিষ্ট্যগুলি ইঞ্জিনের কর্মক্ষমতা বৃদ্ধি করে এবং প্রচলিত বায়োডিজেলের তুলনায় NO_x নির্গমন হ্রাস করে। এই গবেষণায় একটি একক-সিলিন্ডার ডিজেল ইঞ্জিনের কর্মক্ষমতার উপর ২০, ৪০, ৬০, ৮০ আয়তন % মাইক্রোএলগি বায়োডিজেলকে BTL ডিজেলে মিশিয়ে তৈরি করা চারটি BTL ডিজেল-মাইক্রোএলগি বায়োডিজেল মিশ্রণ এবং বিশুদ্ধ BTL ডিজেলের প্রভাব সম্পর্কে একটি সিমুলেশন ভিত্তিক গবেষণা তদন্ত উপস্থাপন করা হয়েছে। গবেষণায় পাঁচটি ইনজেকশন টাইমিং (IT) জুড়ে ইঞ্জিনের আচরণ পর্যবেক্ষণ করার জন্য RK মাল্টি-জোন দহন মডেল ব্যবহার করা হয়েছে এবং নির্ভরযোগ্য পরীক্ষামূলক তথ্যের ভিত্তিতে যাচাই করা হয়েছে। NO_x নির্গমন ব্যতীত, বিশুদ্ধ BTL ডিজেল প্রচলিত ডিজেলের তুলনায় উন্নত নিষ্কাশন বৈশিষ্ট্য এবং ইঞ্জিন কর্মক্ষমতা প্রদর্শন করেছে। মাইক্রোঅ্যালগি-বিটিএল মিশ্রণের জন্য ইগনিশন বিলম্ব, দহনের সময়কাল এবং প্রিমিক্সড পিক হিট রিলিজ রেট যথাক্রমে ১১.০৪-৬৭.২৪%, ০.৬৬–১৩.০৩% এবং ৫.২৫-২৯.৮৭% বৃদ্ধি পেয়েছে, যেখানে পিক সিলিন্ডারের চাপ বিশুদ্ধ বিটিএল ডিজেলের তুলনায় ০.৭২-৫.২৬% হ্রাস পেয়েছে। মাইক্রোঅ্যালগি-বিটিএল মিশ্রণের ফলে সমস্ত IT-তে ব্রেক-নির্দিষ্ট জ্বালানি ব্যবহার ২.১৪-৭.৫১% বৃদ্ধি পেয়েছে। ১° থেকে ৪° CA bTDC মধ্যে আইটি-তে ব্রেক তাপীয় দক্ষতা ০.২-১.৬% হ্রাস পেয়েছে, তবে মিশ্রণগুলিতে বায়োডিজেলের পরিমাণ বেশি থাকায় ৭° থেকে ১৩° সিএ বিটিডিসির মধ্যে আইটি-তে ব্রেক তাপীয় দক্ষতা বৃদ্ধি পেয়েছে। অধিকন্তু, মাইক্রোঅ্যালগি মিশ্রণগুলি CO_2, কণা পদার্থ (PM) এবং ধোঁয়া নির্গমন হ্রাস করেছে; তবে, বিশুদ্ধ বিটিএল ডিজেলের তুলনায় NO_x নির্গমন বৃদ্ধি পেয়েছে। উন্নত কর্মক্ষমতা এবং কম PM এবং ধোঁয়ার জন্য ৪° CA bTDC কে সর্বোত্তম IT হিসাবে চিহ্নিত করা হয়, যার সাথে গ্রহণযোগ্য NO_x ট্রেড-অফ থাকে।

List of Publications

The published articles from the thesis are as follow.

1. *Minhaz Ahmed, Md. Mizanur Rahman, Tafsirul Hassan, Md. Arafat Rahman,* **Effect of Injection Timing on a Diesel Engine Fueled with Biomass to Liquid Diesel and *Spirulina* Microalgae Biodiesel Blends**, Proceedings of 8^{th} International Conference on Mechanical, Industrial and Energy Engineering 2024, 02-04 January, 2025, Khulna, Bangladesh (Paper ID: 172).
2. *Abidur Rahman Adib, Md. Mizanur Rahman, Tafsirul Hassan, Minhaz Ahmed, Abdullah Al Rifat,* **Novel biofuel blends for diesel engines: Optimizing engine performance and emissions with C. cohnii microalgae biodiesel and algae-derived renewable diesel blends**, Energy Conversion & Management: X, 2024;23:100688.

Table of Contents

List of Tables

List of Figures

Nomenclature

BD100	Neat BTL diesel	**CTL**	Coal to liquid
BD20MB80	A blend of 20 vol.% BTL diesel and 80 vol.% microalgae biodiesels	**CZT**	Combustion zone temperature
BD40MB60	A blend of 40 vol.% BTL diesel and 60 vol.% microalgae biodiesels	**D100**	Neat diesel
BD60MB40	A blend of 60 vol.% BTL diesel and 40 vol.% microalgae biodiesels	**DEE**	Diethyl ether
BD80MB20	A blend of 80 vol.% BTL diesel and 20 vol.% microalgae biodiesels	**EGT**	Exhaust gas temperature
BMEP	Brake mean effective pressure	**FT**	Fischer Tropsch
BP	Brake power	**GTL**	Gas to liquid
BSFC	Brake specific fuel consumption	**HRF**	Heat release fraction
BSP	*Spirulina* microalgae biodiesel	**HRR**	Heat release rate
bTDC	Before top dead center	**IDP**	Ignition delay period
BTE	Brake thermal efficiency	**IT**	Injection timing
BTL	Biomass to liquid diesel	**LHV**	Lower heating value
CA	Crank angle	**NO_x**	Oxides of nitrogen
CD	Combustion duration	**PCP**	Peak cylinder pressure
CI	Compression ignition	**PHRR**	Peak heat release rate
CN	Cetane number	**PM**	Particulate matter
CO	Carbon monoxide	**SMD**	Sauter mean diameter
CO_2	Carbon dioxide	**SO**	Smoke opacity
CP	Cylinder pressure	**SO_x**	Oxides of Sulphur
CR	Compression ratio		

Chapter 1

Introduction

1.1 Background of the Study

Energy is one of the key elements of modern living and an important part in human well-being as well as economic development, as energy promotes economic progress. In 2030, the entire globe would require 50% more energy than it does now, based upon Shahid and Jamal [1] and the International Energy Agency (IEA) [2] research. There is a clear indication that the global energy need is climbing up continuously. The energy consumption by source globally from 1800 to 2023 is demonstrated in Fig. 1.1. The consumptions of all the suppliers of energy have raised so many times in past two centuries. Among these, fossil oils have been serving as the main source of the world's energy needs from long ago.

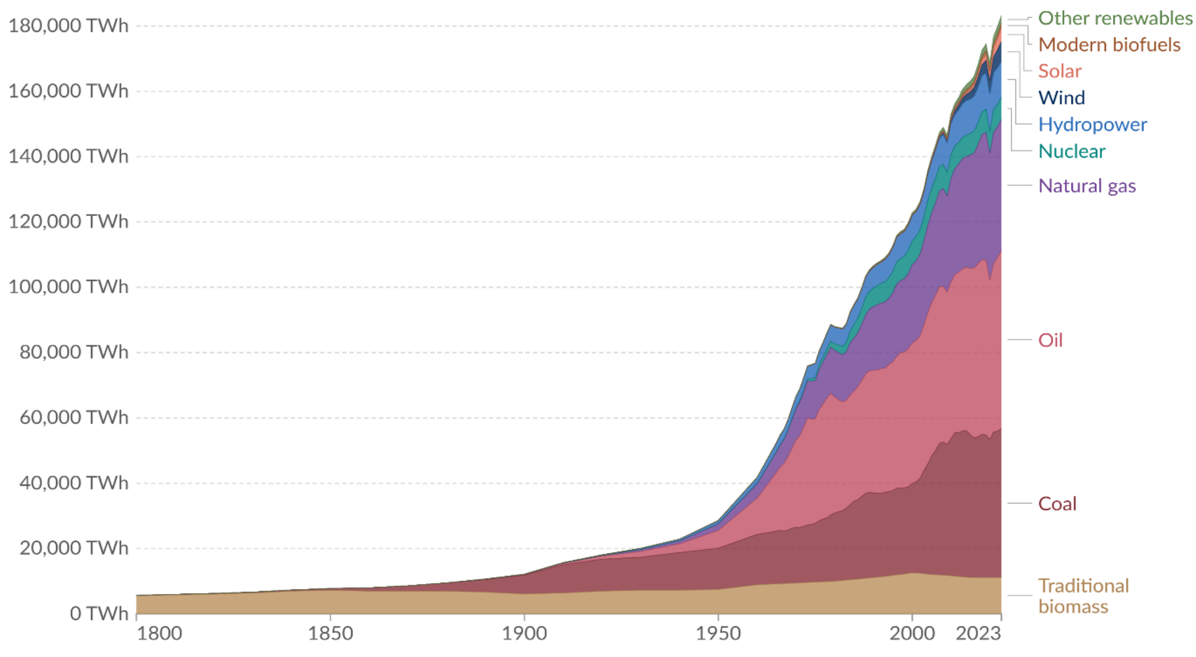

Figure 1.1. Scenario of major energy consumption by source worldwide [3].

The consumption of fossil oil in 1973 and 2023 were estimated 32722 TWh and 54564 TWh respectively, increasing by 66.75% in fifty years. Transportation sector is the second largest consumer of energy accounting for 30% of the total energy delivered worldwide after industrial sector [3]. The transportation industry has been expanding consistently over the last three decades, mainly as a result of the rising number of vehicles around the world. Diesel engine has become tremendously popular in automotive industry due to fuel efficiency, durability, heavy duty application, better engine performance, and heavy-duty applications.

However, the growing usage of fossil oil has become a global concern as there is a possible chance of energy crisis in near future because that crude oils are produced from non-renewable sources of energy [4]. Moreover, diesel engines are regarded as a significant contributor to air pollution in urban and suburban areas due to their emissions of carbon dioxide (CO_2), carbon monoxide (CO), nitrogen oxides (NOx), particulate matter (PM), sulfur oxides (SO_x), and black smoke, which are the primary cause of global warming and constitute hazards to human health [5,6]. Realizing these issues, experts around the world have conducted numerous scientific researches from long ago to invent alternative fuel source for diesel engine to tackle the possible energy crisis and negative ecological impacts. Biodiesel is one of the promising alternatives of conventional diesel studied by researchers till now. Biodiesel are made from biomass which can help mitigate climate change issues by quickly finishing the carbon cycle [7]. At present, biodiesel is getting attention for being renewable, biodegradable, and environment friendly [8]. In addition, PM, HC, and CO emissions are significantly reduced except NO_x for the application of biodiesel [9]. Utilizing biodiesel in combustion ignition (CI) engines improves complete combustion and lowers exhaust emissions because it is an oxygenated fuel. Biodiesel has some distinct advantages over petrodiesel. For instance, biodiesel has a higher cetane number (CN) and provides more lubrication; it also has a lower sulfur and aromatic content and produces fewer greenhouse gas emissions [10]. There are numerous feedstocks from which biodiesel can be extracted. Among these, third generation biodiesel feedstock or microalgae has been a point of immense interest for the researchers due to their higher lipid contents. Though biodiesel can tackle some issues associated with traditional diesel but it poses several disadvantages as well. For example, because of its larger density, higher viscosity, and lower calorific value, biodiesel, that lead to poor engine performance [11–14]. NO_x emission from biodiesel fueled engine is higher compared to neat diesel fueled engine [15]. Because biodiesel has a higher local oxygen concentration and a higher degree of unsaturation than neat diesel, it raises the adiabatic flame temperature, which increases the generation of thermal NO_x. NO_x is responsible for respiratory issues, acid rain, temperature rise, and impaired vision [16]. As despite many improvements there are still some problems that can not be solved by using biodiesel, researchers are trying to invent further sources of fuel that can reduce the limitations associated with biodiesel.

In past years, three approaches have been adopted to improve engine performance and limit emissions in diesel engine. The first technique was altering the engine hardware seen in contemporary diesel engines [17,18]. Nevertheless, engine modification is very challenging because of the engine's standard and complex design. In the second strategy, exhaust gas treatment equipment such filters, afterburners, catalytic converters, and exhaust gas recirculation (EGR) were implemented in road transportation [19,20]. However, application of exhaust gas treatment method requires periodic maintenance of the devices and modification of the exhaust system. The fuel adulteration approach is the last strategy to reduce emissions and improve performance. Various researchers are concentrating on improving fuel properties, combustion, performance, and emission characteristics with emulsification and fuel additives like nanoparticle, a promising additive having attractive properties [21]. Nanoparticle improves thermo-physical properties such as high surface to volume ratio, improves thermal conductivity, and enhances heat and mass transport properties [22]. Therefore, none the techniques are completely free of limitations.

In recent times, scientific researches are being conducted on several renewable sources to explore the potential of those to be applied as alternative fuel of CI engine. Investigations on several renewable diesel fuel like biomass to liquid (BTL) diesel, gas to liquid (GTL) diesel, and coal to liquid (CTL) diesel are carried on currently to observe their effect on performance, combustion, and emission characteristics of heavy-duty CI engine. Because these are derived from renewable biomass feedstocks, promote environmentally friendly energy objectives, and provide a clean substitute for conventional diesel, these fuels are known as renewable diesel. Renewable diesel is made from biomass, which includes organic substances including forestry residues, agricultural waste, food waste, and energy-producing plants. These renewable diesels can replace the conventional diesel due to their several novel characteristics. For example, these fuels exhibit better engine performance for having higher cetane number. Usage of these fuel sources improves engine emissions. Besides, combustion of renewable diesels in CI engine release lower amount of NO_x compared to biodiesel [23,24]. Therefore, the drawbacks associated with biodiesel can be overcome utilizing these renewable diesels. Several attempts have been made in current time to incorporate BTL diesel as alternative to traditional diesel.

1.2 Biodiesel

An alternative to fossil fuels, biodiesel is a flammable, sustainable, and nontoxic liquid fuel. Biodiesel can be produced out of straight vegetable oil, animal fats, and used cooking oil via transesterification technique. D6751 is the ASTM specification for pure biodiesel (B100) [25]. The process of transesterification involves an alcohol reacting with a triglyceride (fat or oil) to produce glycerol and esters. The major constituent in vegetable oils or fats is triglycerides. Triglycerides from vegetable or animal fat undergo a transesterification reaction with methanol, either with or without a catalyst, to produce fatty acid methyl ester (FAME) and glycerol as a byproduct. The base of a triglyceride is a glycerin molecule to which three long-chain fatty acids are joined. When the fatty acids react with alcohol, a mono-alkyl ester is produced. Long-chain fatty acid mono alkyl ester makes is known as biodiesel [26]. For transesterification, methanol is chosen over other short-chain alcohols due to its desirable chemical and physical characteristics, including being a polar molecule and the shortest carbon chain alcohol, as well as its affordability [14]. The transesterification reaction is shown in equation 1.1.

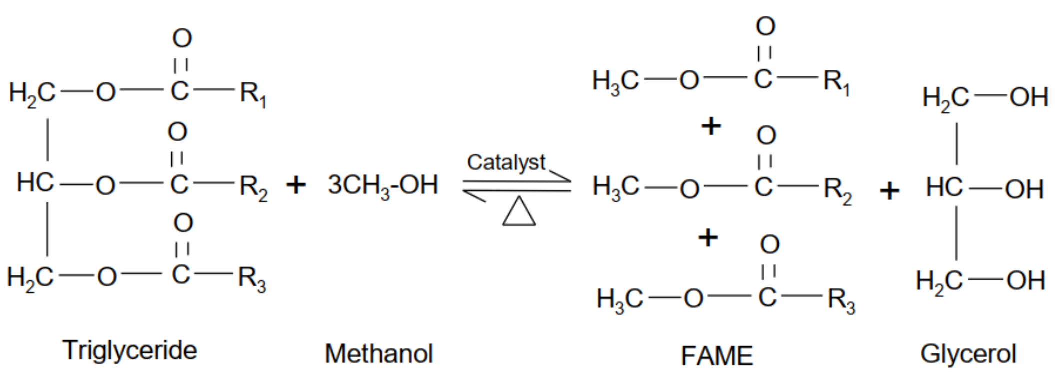

(1.1)

Biodiesel was first produced by Patrik Duffy in 1853 from vegetable oil. Peanut oil, a neat vegetable oil, was first applied as working fuel in compression ignition (CI) engine by Rudolf Diesel in 1893 considering as a potential automotive fuel [27,28]. The EN 14214 standard test methods are issued by the European Committee for Standardization (CEN). The requirements for biodiesel set by ASTM and EN are tabulated in Table 1.1. Pure vegetable oils have a number of disadvantages, like high viscosity, which causes poor atomization, fuel filter clogging, and injector coking. Nevertheless, biodiesel, which is made from esterified vegetable oils, can solve these problems.

Table 1.1. Biodiesel's ASTM and EN requirements [29].

Parameter	**Units**	**ASTM D6751 (USA)**		**EN 14214 (Europe)**	
		Limit	**Method**	**Limit**	**Method**
Kinematic viscosity (40 °C)	mm^2/s	1.9-6.0	D445	3.5-5.0	EN ISO 3104 / EN 14105
Density (15 °C)	Kg/m^3	-	-	860-900	EN ISO 3675 / EN ISO 12185
Flash point (closed cup)	°C	Min 93	D93	Min 101	EN ISO 2719 / EN ISO 3679
Flash point	°C	Min 130	D93	Min 120	EN ISO 3679
Cetane number		Min 47	D613	Min 51	EN ISO 5165
Water content	mg/kg	Max 500	D2709	Max 500	EN ISO 12937
Phosphorus content	mg/kg	Max 10	D4951	Max 10	EN 14107
Sulfur content	mg/kg	Max 15	D5453	Max 10	EN ISO 20846/ EN ISO 20884
Metals I (Na and K)	mg/kg	-	-	Max 5	EN 145308
Metals II (Ca and Mg)	mg/kg	-	-	Max 5	EN 145308
Acid number	mg KOH/g	Max 80	D664	Max 0.5	EN 14104
Free glycerol	mass%	Max 0.02	D6584	Max 0.02	EN 14105/ EN 14106
Total glycerol	mass%	Max 0.24	D6584	Max 0.25	EN 14105
Sulfated ash content	mass%	Max 0.02	D874	Max 0.02	ISO 3987
Methanol content	mass%	-	-	Max 20	EN 141110
Mono-glycerides	mass%	-	-	Max 80	EN 14105
Di-glycerides	mass%	-	-	Max 20	EN 14105
Tri-glycerides	mass%	-	-	Max 20	EN 14105

Ester content	mass%	-	-	Min 96.5	EN 14103
Iodine value	g I_2/100g			Max 120	EN 14111
Carbon residue	mass%	Max 0.05	D4530	-	-
Distillation 100% removed	°C	Max 360	D1160	-	-
Oxidation stability (100 °C)	hours	-	-	Max 6	EN 14112
Linolenic acid methyl ester	mass%	-	-	Max 12	EN 14103

1.3 Biodiesel Feedstocks

Biodiesel is seen as a highly promising substitute for diesel since its properties are comparable to those of diesel oil obtained from petroleum. Biodiesel consists of an alkyl ester derived from renewable resources, including vegetable oil, animal-based fat waste, and algae. Over 350 oil-bearing crops have been recognized as possible sources for the extraction of biodiesel worldwide. The abundance of feedstocks accessible for biodiesel synthesis is one of the most important aspects for producing biodiesel [1,30,31]. The widespread feedstocks of biodiesel are classified into three main categories- first, second, and third generation feedstocks of biodiesel. The three types of feedstocks categorized are described below in detail.

1.3.1 First Generation Biodiesel Feedstock

The term "first generation" refers to biodiesel produced from edible oils. Edible oils, such as those from soybeans, palm, sunflower, safflower, rapeseed, coconut, and peanut, are known as first-generation biodiesel feedstocks because they were the earliest crops utilized for biodiesel production. These oils are widely grown in various parts of the world, including as Malaysia, the United States, and Germany. More than 95% of the world's biodiesel is currently produced from edible oils, with rapeseed oil accounting for 84%, sunflower oil for 13%, palm oil for 1%, and other oils like soybean oil for the remaining 2% [32,33]. The main advantages of edible oil as biodiesel feedstock are wide availability and easiness of the conversation of edible oil to biodiesel.

However, they are threat to food chain, carbon storage, availability of land, and ecosystem. In addition, their application as feedstock is restricted by their usage in food industry, human diet, and high price. In recent years, the cost of vegetable oils has risen significantly, which affects the economic sustainability of the biodiesel industry. Additionally, the long-term use of edible oils for biodiesel is not sustainable due to the growing disparity between their demand and supply in various countries. For instance, if all the soybeans produced in the United States were dedicated to biodiesel production, it would only fulfill about 6% of the country's diesel needs [34].

1.3.2 Second Generation Biodiesel Feedstock

To lessen the dependence on edible oils for biodiesel production, an alternative approach is to use non-edible oils. The second-generation biodiesel refers to biodiesel derived from non-edible resources such as non-edible oil, grease, waste animal fats, and used cooking oil. By utilizing non-edible oils, competition with food production can be avoided, deforestation can be minimized, and they often prove to be more environmentally friendly and cost-effective compared to edible oils. They also have the advantage of producing valuable by-products and are generally more efficient. The availability of huge quantities of non-edible plant oil in nature has been noted globally [35]. According to Mohibbe Azam et al., 26 plant species are the most suited for usage as biodiesel that may be used for the manufacture of fatty acid methyl ester (FAME), while 75 plant species have seeds that contain more than 30% oil [36]. Second generation feedstocks also include animal fats like grease, waste oils, and animal fats like cattle tallow, chicken fat, and swine lard. By using various kinds of feedstock, there is no need to discard them. Compared to first-generation feedstocks, animal fat methyl esters offer a variety of benefits, including a higher cetane number, noncorrosive characteristics, clean and renewable attributes [37]. Furthermore, discarded cooking or frying oils are becoming more and more popular since, in most nations outside of the European Union (EU), they are a cheap feedstock for the generation of biodiesel. In addition, because it is unsuitable for human consumption, waste cooking oil (WCO) is a promising substitute for vegetable oil and a useful feedstock for the generation of biodiesel. Nowadays, it has been discovered that more than 60% of the WCO produced is disposed of inaccurately; even though there are no wide-ranging collection systems, its disposal in drainage systems or as garbage can sometimes be illegal and raise the cost as well as energy consumption of domestic waste water treatment systems that dispose of oil [38].

However, these categories of biodiesel content high amount of FFAs that reduce biodiesel yield. According to reports, there might not be enough second-generation feedstocks to meet the world's energy needs. Furthermore, biodiesel made from animal and vegetable fats performs poorly in cold climates [3,39,40]. Because animal fats may originate from contaminated animals, using them as a feedstock for biodiesel raises additional biosafety concerns [30].

1.3.3 Third Generation Biodiesel Feedstock

The third generation of feedstock for biodiesel has recently been identified to be microalgae. One such source that has been believed to be able to meet the constantly rising need for automotive fuel is microalgae biodiesel [41]. Lipids are vital components of microalgae used to produce biofuel, and in appropriate conditions, various species of microalgae may accumulate between 50 and 70 percent lipids by dry weight [42,43]. As a consequence of their high degree of saturation, microalgae lipids are primarily neutral lipids, and based on the strain, they may build up in the microalgal cell at various growth phases, making them a viable replacement for diesel fuel [44,45].

In comparison to edible and non-edible feedstocks, microalgae exhibit greater photosynthetic efficiency to produce biomass, better growth rates and productivity, and an increased oil content, making them a very promising feedstock. Microalgae can yield up to 25 times as much oil as oil palm and 250 times as much as soybeans [3]. They were additionally investigated for their ability to grow in household wastewater by consuming nutrients from it, which could help with the treatment of waste water [46]. Compared to earlier biodiesel sources, microalgae are reported to generate 19,000 to 57,000 l liters of oil per acre in a single year [47]. When compared to other biomass commodities like trees and plants, the expenses of collecting and transporting microalgae are relatively cheaper. Fields deemed improper for both first and second generation crops can support cultivation of algae. Microalgae can be harvested in a variety of habitats that are unsuited for other crop production, including brackish, saline water, as well as non-arable areas that are unsuitable for traditional farming [30]. Furthermore, they can be cultivated in bioreactors or on dairy farms [48]. They consume CO_2 from environment during their growth to conduct their biological process properly. Therefore, microalgae also contribute to establish green environment by reducing the amount of CO_2 in air. An effective biological system for capturing solar power for use in the synthesis of organic compounds is thought to be microalgae, which might be also easily chemically handled due to their tiny stature [49]. All these features of microalgae influenced to draw the attention of the researchers to establish microalgae biodiesel as a potential automotive fuel. The traditional organic solvent extraction approach is the first of several extraction techniques for biodiesel from microalgae. More sophisticated techniques include supercritical fluids, ultrasound, microwave irradiation, ionic liquids for oil extraction, and direct transesterification as well [50]. The different feedstocks of biodiesels are listed in Table 1.2.

Table 1.2. Different feedstocks of biodiesel [3,51–54].

First Generation Feedstock	Second Generation Feedstock	Third Generation Feedstock
Soyabean	Neem oil	*Chlorella vulgaris*
Rapeseed	Castor oil	*Spirulina platensis*
Sunflower	Karanja	*Spirulina maxima*
Peanut	Jatropha	*Chlorella protothecoides*
Safflower	Jojoba	*Euglena sanguinea*
Palm oil	Tobacco seed	*Azolla pinnata*
Cottonseed oil	Nagchampa	*Nannochloropsis gaditana*
Corn oil	Mahua	*Chlorella sorokiniana*
Coconut oil	Tung	*Chroomonas salina*
Rice bran oil	Waste cooking oil	*Nannochloropsis sp.*
Mustardseed oil	Beef tallow	*Haematococcus pluvialis*
	Poultry fat	*Chlorella protothecoides*
	Fish oil	Stoechospermum marginatum
	Rubber seed	*Nodularia spumigena*
	Mahua	*Botryococuus braunii*
	Syringa	*Euglena sanguinea*
	Moringa	

1.4 Lipid Content in Microalgae Cells

The unit cells of microalgae are comprised of complex components like protein, carbohydrate, lipid, and different chemical pigments. Lipid content is the main factor upon which potential of a source to be used as biodiesel depends strongly and microalgae species are reported to contain 30-80% of lipids in general [42]. Lipids can be extracted easily using organic solvent extraction technique because of their properties of being insoluble in polar compounds but soluble in nonpolar compounds as hydrophobic chain exists in their structure. They are divided into two groups – neutral lipid and polar lipid [55]. Microalgae experience biochemical transformations throughout their various growth stages. In contrast to glyco- or phospholipids, the buildup of neutral lipids during development is preferable for the synthesis of biodiesel. Additionally, a high level of polyunsaturated fatty acid (PUFA) content may negatively impact the qualities of biodiesel. Different techniques of lipid extraction are demonstrated in Fig. 1.2.

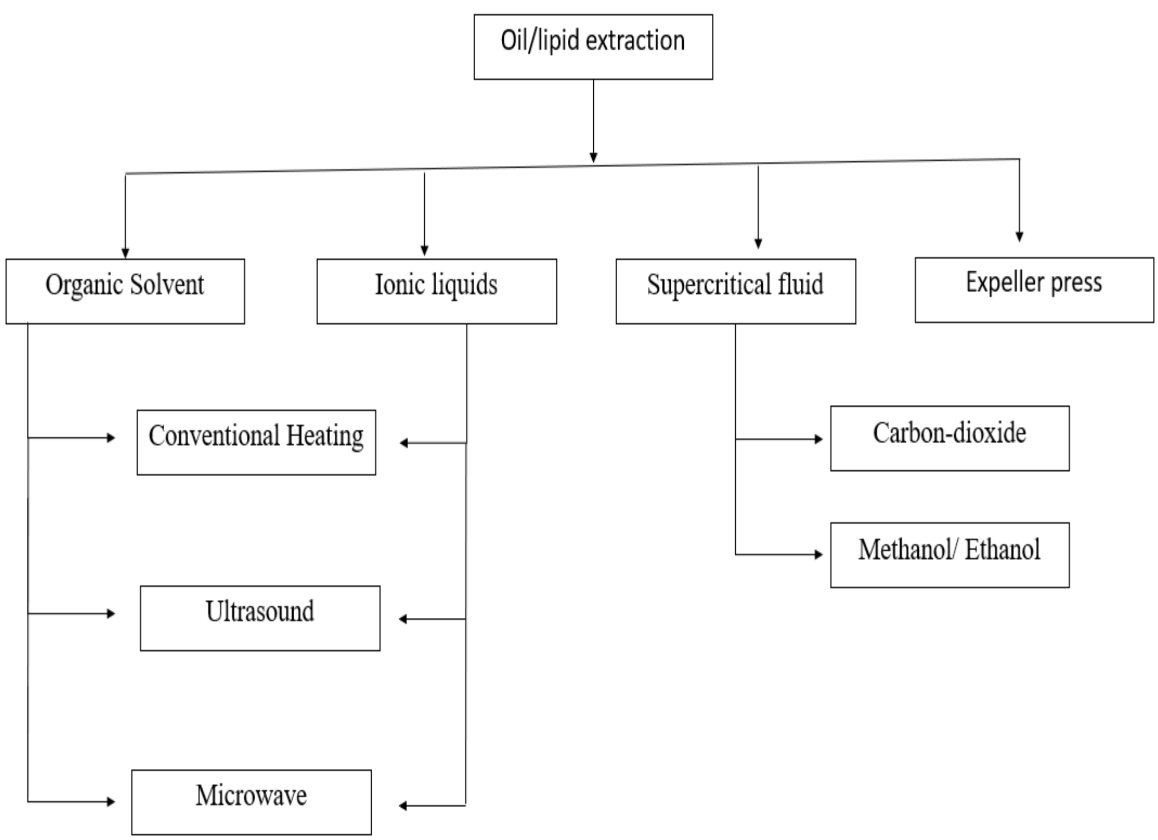

Figure 1.2. Different lipid extraction techniques [50].

In essence, organic solvent extraction is a mass transferring procedure where lipid molecules permeate cell walls and dissolve in organic solvent. Mechanical acoustic waves with extremely high energy are called ultrasonic waves. The strong attraction between molecules is broken by the tremendous power of ultrasonic waves, which also create cavitation bubbles. The molecules' and ions' dipole moment and ionic conduction are affected by microwave extraction. It offers the advantage of heating the sample consistently because it has a non-contact heat source [56]. Fluids that have liquid-like solubility and gas-like diffusivity are employed in supercritical fluid extraction (SFE). Numerous natural substances can be dissolved by them. Oil yield of different microalgae spices are presented in Table 1.3.

Table 1.3. Oil yield of different microalgae species.

Microalgae	Treatment method	Oil yield (%)	Ref.
Chlorella Vulgaris	microwave	10	[57]
	ultrasound	52	[58]
Chlorella protothecoides	microwave	21.9	[58]
	ultrasound	42	[58]
Nannochloropsis oculata	microwave	26.51	[59]
	ultrasound	30.12	[58]
	acid	33.8	[59]
	autoclave	28.6	[58]
Chlorella sp.		28-32	[60]
Crypthecodinium Cohnii		20	[60]
Brotryococcus braunii		25-75	[60]
Dunaliella primolecta		23	[60]
Spirulina Plantesis	soxhlet	12-23.3	[61]

1.5 Microalgae Cultivation and Biodiesel Production

Commercially microalgae cultivation started just several decades ago. There are two types of culture systems: open systems are outdoor constructions like ponds and lagoons, and closed systems are tubes or vessels that are subjected to artificial or solar radiation [62]. Different microalgal species respond differently to different levels of light intensity because they need different amounts of light energy to perform photosynthesis. The light intensity range for cultivating microalgae is 76–600 mol/m^{2}s [63]. Carbon, nitrogen concentration and carbon-to-nitrogen ratio significantly influence their growth rate.

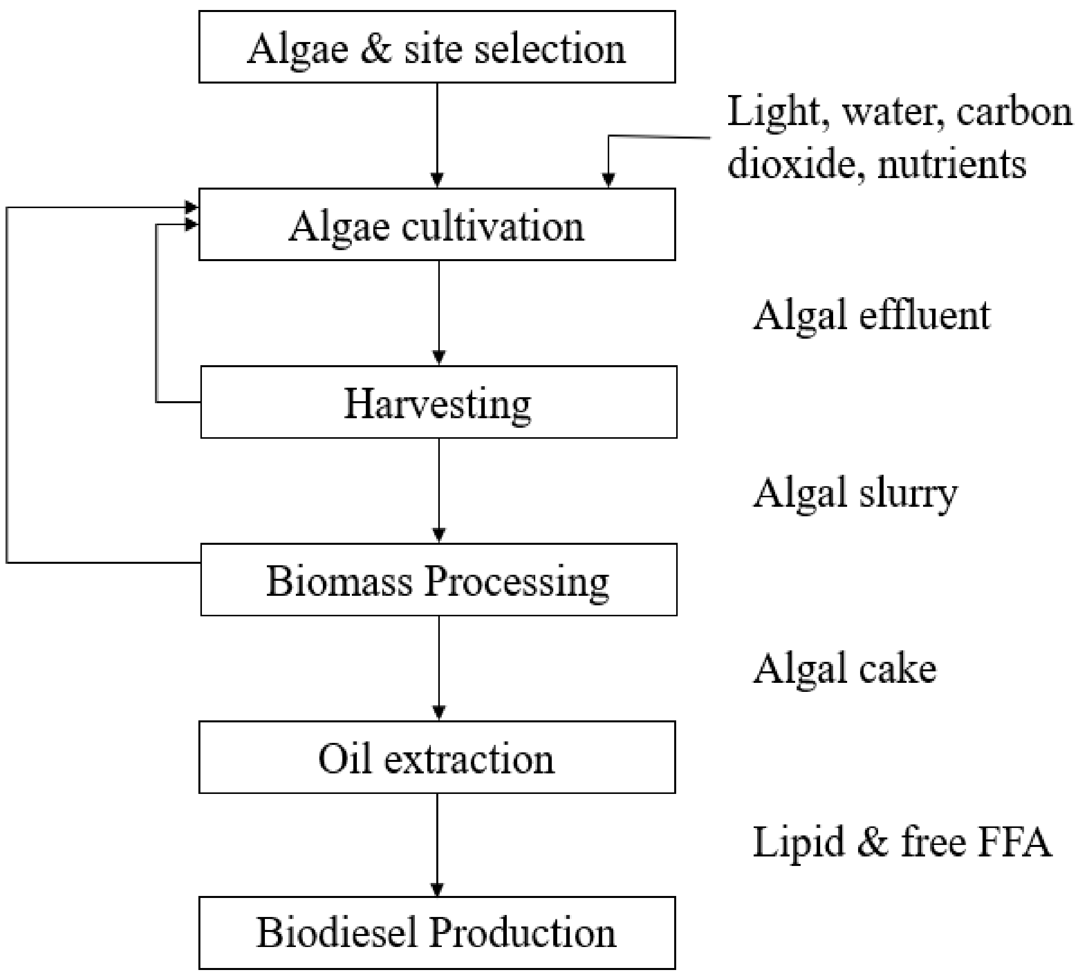

Figure 1.3. Stages of converting microalgae into biodiesel.

Closed photobioreactors and open systems for microalgae growth phases are combined in hybrid systems, which lessen environmental pollution and make biomass production easier. The most effective system is determined by the biological conversion method, technology, and microalgae strain. For the microalgal biomass to be further processed into biofuels, water must be eliminated from the algal culture following lipid synthesis. Extracting oil from algae and harvesting algae from tanks are difficult and highly energy-intensive processes. The cost of harvesting makes up between 20% and 30% of the total production expenses [47,53,64]. Harvesting microalgae can be divided into two categories. Using methods like flocculation, flotation, or sedimentation, biomass is separated from the bulk culture during the first phase, known as bulk harvesting. Following that, methods like centrifugation and filtering are used to concentrate the biomass slurry. Fig. 1.3 shows all the stages from selection of algal species to production of biodiesel to be applied as transportation fuel.

Microalgae can be converted into biodiesel using chemical and biological processes. There are two ways to transesterify them: direct single-stage procedures and traditional two-stage methods [65]. The traditional process for turning microalgae into biodiesel involves choosing species of the algae with a lipid percentage between 15 and 40%. After selection of microalgae strain, necessary light, water, CO_2, and other necessary element should be ensured for effective microalgae cultivation. After removal of water from the algae they should be dried properly. Then, oil is extracted from the dried algae using any appropriate extraction technique. After that crude extracted oil can be turned into biodiesel by transesterification process.

1.6 Biomass to Liquid Diesel

Microalgae biodiesels have superior physio-chemical properties than the first and second generation feedstocks. Nevertheless, there are some disadvantages associated with microalgae as well. For example, microalgae pose lower cetane number, higher density and higher viscosity compared to conventional diesel. Such aspect of microalgae biodiesel result in poorer engine performance than diesel. Additionally, though microalgae reduce the emissions of CO_2, PM, and smoke but they raise the emission of NO_x [4]. Researchers are putting effort to overcome these drawbacks of microalgae and very recently renewable diesels are reported to be viable solution of those problems as outcome of the scientific investigations. Renewable diesels are synthetic fuel produced from biomass, a renewable source. Biomass is solely naturally formed, renewable carbon source and a significant part of a fossil fuel alternatives [66]. Biomass to liquid (BTL) diesel, gas to liquid (GTL) diesel, and coal to liquid (CTL) diesel are typical renewable diesels have been studied by the researchers. Renewable diesels are produced by two step procedures: gasification of dry biomass and conversion of gaseous product to liquid fuel by Fischer-Tropsch (FT) process [23].

The method called "biomass to liquid" turns biomass into liquid biofuels. BTL fuels have unique qualities and these are even higher grade than fossil fuels in terms of properties. They are excellent because they have zero particulate matter emissions, low NOx emissions, much reduced CO_2 emissions, and a product quality that can be adjusted (Octane and cetane number). Because of these, vehicles can use them either pure or in combination with other fuels without requiring engine modifications [67]. The main benefits of the resulting synthetic biofuel are its high biomass yield (up to 4000 l/ha), its high potential to cut CO_2 emissions by over 90%, and its high quality, which is unaffected by any restrictions on its use in engines built today or those anticipated to be built in the future [68]. The world's first commercial BTL facility, using the Choren Carbo-V® process, is now being built in Frieberg, Sax. Currently, research and development regarding BTL diesel in Europe is gaining traction. Properties of BTL fuel are listed in Table 1.4.

Table 1.4. Main properties of BTL diesel [23,24,69].

Properties	Value
Cetane Number	84-99
Density (kg/m^3)	775-785
Surface Tension (mN/m at 25ºC)	24.96
Viscosity (Pa-s at 25ºC)	2.0976
Cloud Point (ºC)	-5 to -30
Lower Heating Value (MJ/kg)	43.9
Oxygen Content	0

1.6 BTL Diesel Production

In general, the FT synthesis of BTL diesel involves three primary phases. Initially, biomass undergoes gasification to produce biomass-derived syngas, or bio-syngas which is mainly a mixer of carbon mono-oxide and hydrogen. In a subsequent stage, the bio-syngas undergoes a cleaning procedure to eliminate contaminants, producing a clean bio-syngas that satisfies the conditions of FT synthesis. Green diesel, or renewable diesel and other clean biofuels are finally produced by putting the cleaned bio-syngas into a FT catalytic reactor [47,70]. The steps of BTL production via FT process is shown in Fig. 1.4.

The process of gasification can be used to transform carbonaceous feedstock into gas mixtures that is called syngas. Wood and agricultural waste are only two examples of the biomass feedstocks that can be used to create bio-syngas. Every kind of biomass has distinct qualities. Pre-treatment, which usually consists of drying, size reduction, and screening, is required prior to gasification [71]. More surface area and porous structures per unit of biomass will be produced by smaller biomass particle sizes, which will aid in heat transfer and the conversion of biomass during the gasification process. Different hydrodynamics, gasification agents, and operating circumstances are used in the construction of various gasifier types. Updraft fixed bed type, fluidized-bed type, downdraft fixed bed type, and entrained flow type are the most commonly utilized varieties of gasifiers [72]. The biomass's cellulose, hemicelluloses, and lignin components undergo thermochemical breakdown in the first phase of the gasification process. The char produced in the first phase is then gasified, and additional equilibrium processes take place.

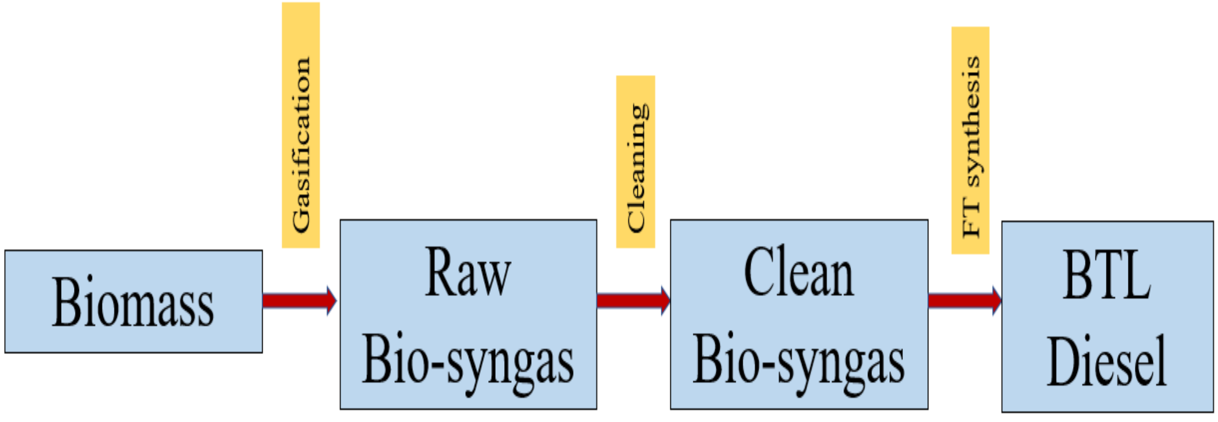

Figure 1.4. Flow diagram of BTL diesel production.

Pretreatment of the biomass feedstock and optimization of the gasification methods result in the efficient production of bio-syngas with the required levels of hydrogen and carbon monoxide. Nevertheless, the raw bio-syngas will exhibit certain contaminants and that must be eliminated in order to satisfy the FT synthesis requirements as they can reduce the FT activity in the bio-syngas catalytic conversion.

Syngas can be converted into higher hydrocarbons, particularly liquid transportation fuels, using the well-established and highly skilled FT process. Green diesel and other long-chain hydrocarbons are created by gasifying biomass and using the bio-syngas for FT synthesis. Co-based catalysts are the preferred catalyst for FT synthesis because they produce higher productivity than Fe-based catalysts at high conversion levels [66]. In order to produce BTL, biomass must first be ground and dried into pellets, which are further separated into gas and solid components.

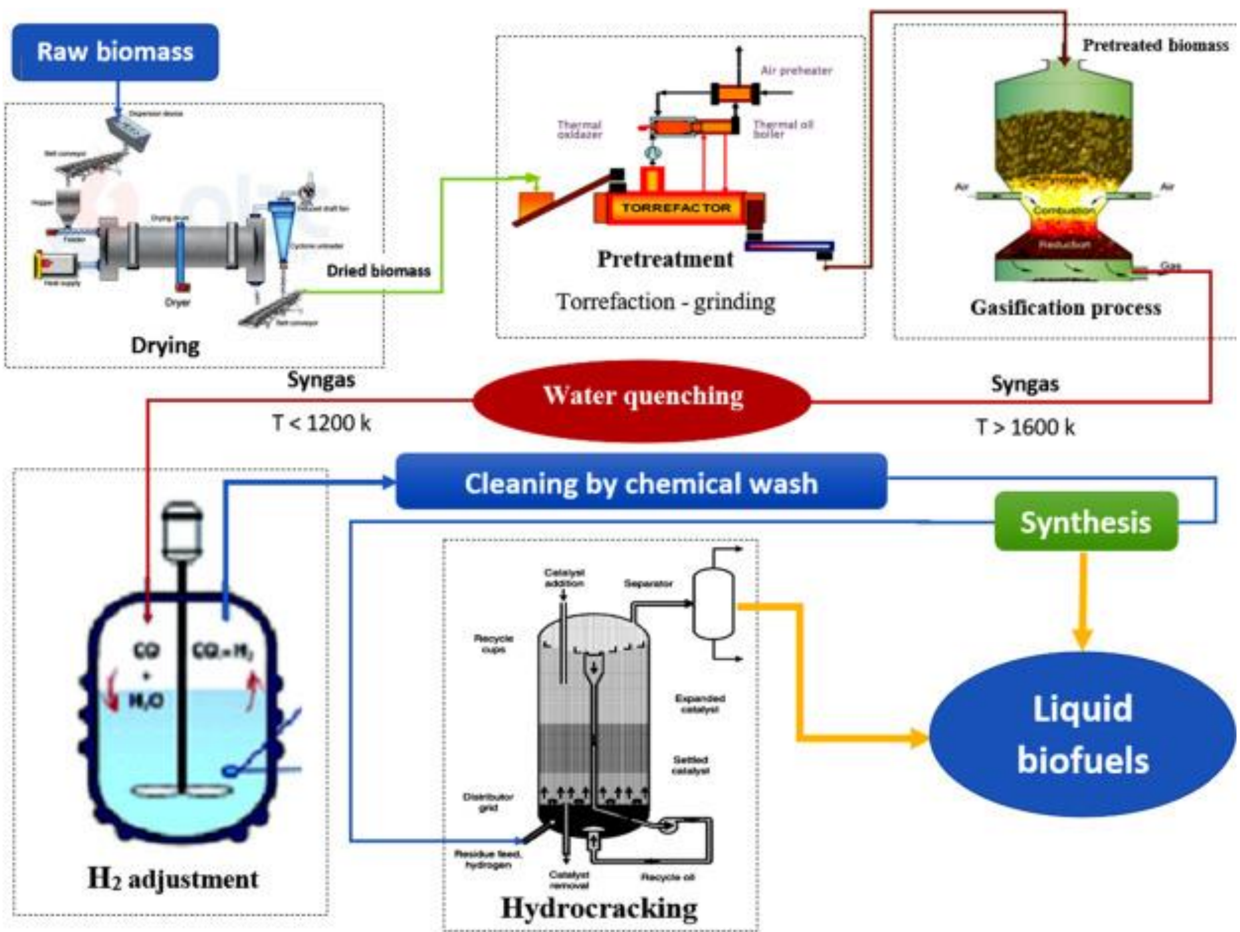

Figure 1.5. Steps of BTL synthesis [73].

Through the use of FT processes, where the gas is refined and liquefied produces a paraffin-like liquid that has been isomerized for stability. The fuel specifications can be adjusted to better suit the needs of the engine [73]. At the Kaiser Wilhelm Institute, Franz Fischer, Hans Tropsch, and Helmut Pichler invented the FT process in 1923 when they interacted synthesis gas across a cobalt catalyst to produce distillate oils, gasoline, and diesel [74]. Fig. 1.5 demonstrates the flow line of all the steps of BTL production sequentially.

1.7 Prospect of BTL Fuel

5 tons of biomass are needed to produce 1 ton solar diesel, and 13,000 tons of this diesel annually require 50,000 hectares of biomass. Four million tons of solar diesels, or 13% of the country's current diesel consumption, could be produced on one million hectares of set-aside land in Germany [75]. The production of grain and fodder is not in conflict with BTL fuels, which are essentially CO_2-neutral and can be easily tailored to meet the needs of internal combustion engines. In a crude-oil refinery, there are several options for using feedstocks obtained from biomass, and advancements in biofuel production technologies will enable a shift to a sustainable global economy [76]. However, high investment costs, poor energy density, infrastructure constraints, limitations on photosynthetic productivity, and land competition with food production are among challenges associated with biofuel production using BTL processes.

1.8 Diesel-RK Software

A professional thermodynamic full-cycle engine simulation program, Diesel-RK is made for a variety of real-world applications, such as engine system design and generic multicylinder engine concept analysis. The internal combustion engine department at Bauman Moscow State Technical University began developing the Diesel-RK software in 1981–1982. The software was designed from the start as a mean for optimization research, thus the effectiveness and speed of the mathematical models and algorithms used—many of which were original author’s codes—were given special attention. The software is intended for internal combustion engine designers and analyzers. Numerous engines of different kinds and uses have been tested to ensure the software is competent. Numerous computational processes were added to the program to meet the needs of industrial firms, including Russia's largest engine designers. The first Diesel-RK program was released in 1991 which was financed by A. Surion. Because of its user-friendly interface and contemporary combustion model, it was extensively utilized by top Russian engine manufacturers [77].

The Diesel-RK software is a commercial software that can be used by both novices and expert researchers. It has settings wizards that make establishing empirical coefficients and input data easier. Calculation model calibration and computational research are made easier by these wizards, which automatically generate data files based on general engine information. For researchers performing rapid engine design analyses and students with little expertise, this is incredibly beneficial. The RK-model, one of the sophisticated mathematical models for diesel combustion used by this software, takes into account injection features such as fineness of fuel spray in cylinder, interface with air swirling and wall structures, and spray direction across the piston bowl.

Moreover, the program contains algorithms for "Fuel Spray Visualization." This code gives the user the ability to visually examine the evolution of the fuel sprays and their interactions with the cylinder walls. For a specific fuel supply characteristic and swirl intensity, the code is useful for planning the geometry of the piston bowl and for selecting the appropriate dimension, quantity, and orientation of injector nozzles. Fig. 1.6 exhibits the interface of Diesel-RK software.

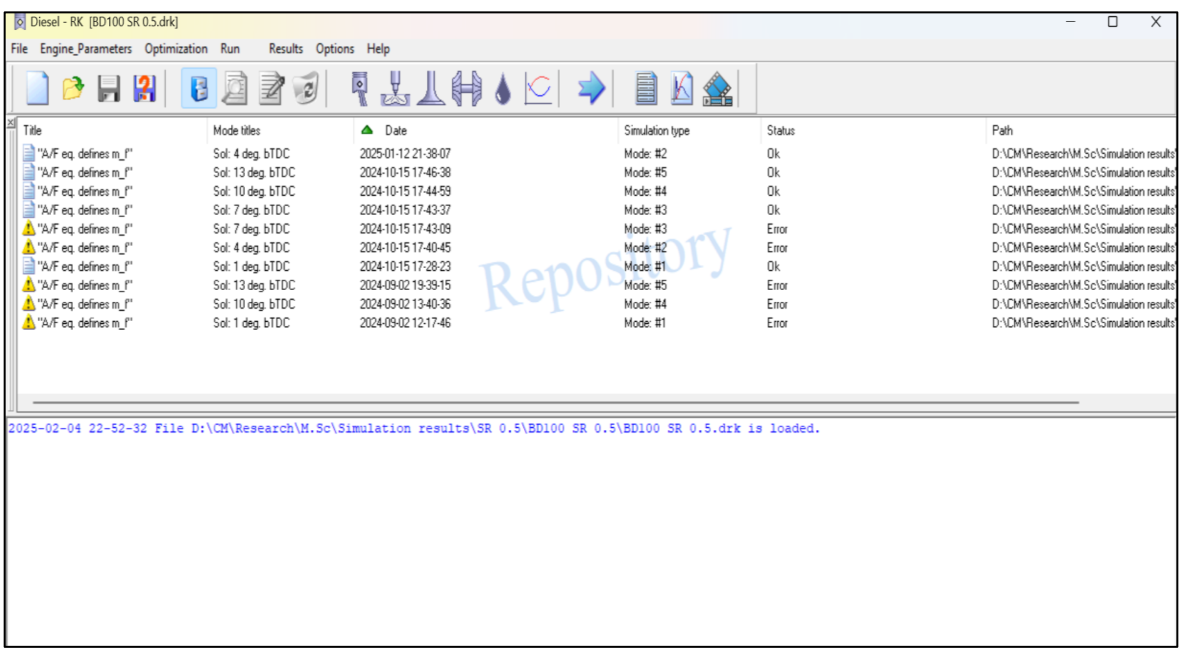

Figure 1.6. Interface of Diesel-RK.

1.9 Features of Diesel-RK

Diesel-RK numerical tool can be employed to design direct injection diesel engine, spark ignition engine, 2-stroke engine having uniflow and loop scavenging system, gas engine, and dual fuel engine. In order to estimate consumption of engine fuel, analyze graphs of torque, analyze combustion, performance, and emissions, create dual fuel engine mixtures, predict knock, optimize valve timing, and convert diesel engines into gas engines, the DIESEL-RK solver, a feature of the software is utilized. The key features of the tool are described below:

A "Fuel Spray Visualization" algorithm built into the DIESEL-RK helps engineers to model how fuel spray interacts with surrounding sprays, air swirl, and combustion chamber walls. Evaluation outcomes can be stored as animated GIF files, AVI files, or Windows graphic files. Detailed visualization is made possible by the 3D tool's analysis of the spatial evolution of sprays, which identifies characteristic zones and examines their influence on the rate of heat release. The intersection zones of spray spatial are marked in fig. 1.7 by green dots. This feature is very useful for big size marine engines. With 14 nonlinear search methods, DIESEL-RK provides an integrated multiparametric and multidimensional optimization process that enables 1D and 2D parametrical search investigations for optimization computations.

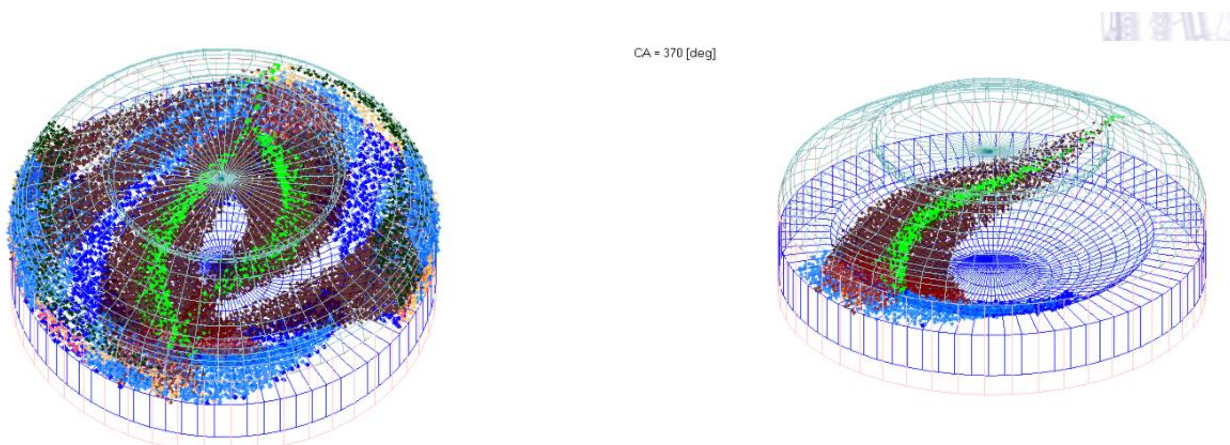

Figure 1.7. Spray spatial intersection zone [77].

Various fuels, including mixtures of biofuels and diesel oil, are supported by the DIESEL-RK combustion model. Biofuel blends' physical characteristics are used to simulate the evaporation and combustion processes as well as to simulate spray development. Sequential

Injection Profiles are supported in heat Release and NO_x simulations by DIESEL-RK, which enables the simulation of engines with up to five distinct fuel injection systems (A B, C, D, and E), each with its own configurations, nozzles, and cycle fuel mass. Fig. 1.8 shows the interface for selecting desired operating mode from several ones.

1.10 Diesel-RK Computational Models

A number of simulation models are developed to evaluate the engine performance, emission, and combustion parameters of diesel engine. The RK-model is used to simulate blend production and combustion in CI engines. Prof. Razleytsev established the RK-model simulation approach between 1990 and 1994. The RK model considers the following- the heading of sprays in the combustion cylinder; the dynamic of fuel spray development; the dynamic and pattern of the swirl; the configuration of the injection profile, including multiple injections.

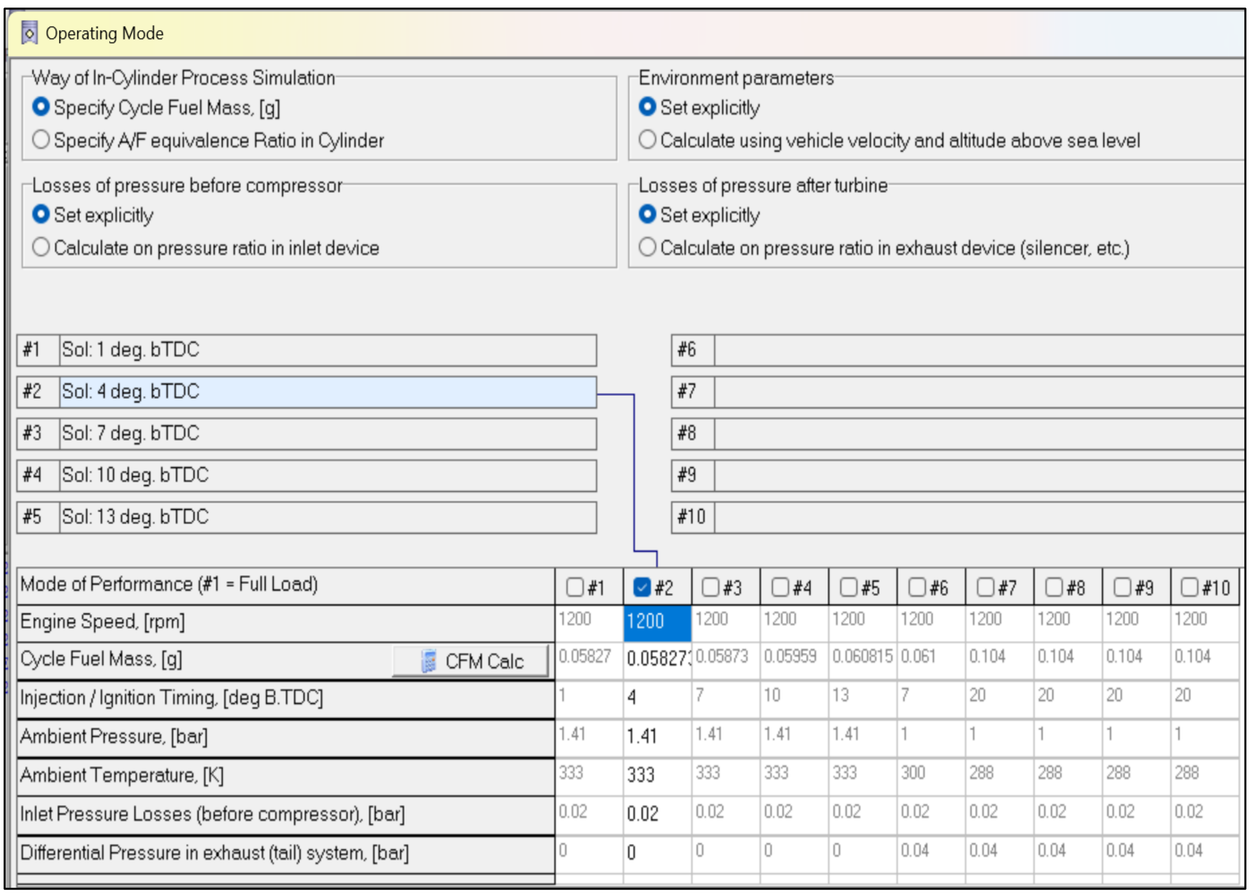

Figure 1.8. Operating modes in Diesel-RK.

For accurate prediction in engines with large EGR, multiple injection, and HCCI, NO emission computation uses Prof. Zvonov's Zeldovich mechanism and Detail Kinetic Mechanism (DKM), which is supported by Diesel-RK local release. The gas exchange model optimizes valve timing and predicts the best intake and exhaust ports configuration by taking into account non-steady gas flow, engine port design, nearby cylinders, and pulse converter design. Using Woschni's formula, heat transfer equations, and valve, piston, and manifold-controlled ports and manifolds, heat transmission is simulated for many kinds of surfaces. With exceptional precision, Diesel-RK is a program that models the operation of different internal combustion engines. Data entry and engine model calibration are made easier by using the Wizard of New Project Creation to create input data and eliminating the need for an initial setup of empirical coefficients.

1.11 Novelty Statement of the Study

The preceding discussion emphasizes the viability of BTL diesel and biodiesel derived from Spirulina microalgae as fuel for CI engines. A research gap regarding the impact of utilizing BTL diesel and microalgae biodiesel in diesel engines is realized by going through intensive literature review. As far as the author is aware, no investigation has been done on how blended fuel consisting of algae derived biodiesel and BTL diesel influence the attributes of CI engine. To address this gap, a numerical analysis is carried out utilizing the Diesel-RK software to assess the performance, emission characteristics, and combustion of a CI engine fueled with the blends of BTL diesel and *Spirulina* microalgae biodiesel.

1.12 Objectives

The principal goal of the study is to numerically investigate the performance, combustion, and emission parameters of a diesel engine fueled with the blends of BTL diesel and *Spirulina* microalgae biodiesel. The specific objectives of the study are as follow.

- To examine the effect of neat BTL diesel on the combustion, performance, and emission parameters of a diesel engine.

- To evaluate the effect of the microalgae biodiesel blended with BTL diesel on the combustion, performance, and emission parameters of a diesel engine.
- To evaluate the effect of variation of injection timing on the characteristics of a diesel engine fueled with the blends of BTL diesel and microalgae biodiesel.

1.13 Scopes and Limitations

1.13.1 Scopes

An ecologically friendly, sustainable, and biodegradable alternative fuel is biodiesel which reduces significantly the releases of PM, HC, and CO from diesel engine. Because biodiesel contains oxygen in its fuel, it improves full combustion and lowers exhaust emissions when used in CI engines. Biodiesel's widespread use in the automotive industry is being constrained due to some issues and worries. As an instance, biodiesel shows poor performs in diesel engines due to its higher viscosity, density, and lower calorific value as compared to petroleum-based diesel. Additionally, engines running on biodiesel release higher amount of NO_x than those running on petroleum-based fuel. NO_x is responsible for respiratory issues, acid rain, global warming, and impaired vision.

Researchers are trying to overcome the mentioned limitations for long time. In recent time, various scientific researches are being conducted to investigate the potential of several renewable diesels like BTL, GTL, and CTL to be adopted as transportation fuel. These renewable fuels have higher cetane number and superior physiochemical properties that leads to better engine performance with respect to conventional diesel. Moreover, many recent studies reported that the emission of NO_x decreases when renewable fuel BTL diesel is applied in CI engine compared to microalgae biodiesel. Therefore, the limitations associated with microalgae biodiesel can be overcome applying BTL diesel.

1.13.2 Limitations

While BTL diesel provides many benefits such as renewability, improved emission, and better performance, there are some constraints to utilize them as alternative fuel. The complex production process of BTL diesel by gasification as well as FT method is costly making them expensive than conventional diesel. The extensive production of biomass for BTL diesel could result in altered land use, habitat loss, and higher water usage. The widespread commercialization of BTL diesel will take time due to the existing challenges associated with the technology involved in its synthesis. Therefore, supply of biomass is not widely available right now.

1.14 Thesis Outline

The thesis is organized in a manner described below.

Chapter 1 includes the brief introduction of the background, the alternative fuels, and the simulating software involved in the study.

Chapter 2 is dedicated to review the previous literatures that discuss the effect of third generation microalgae biodiesel on the diesel engine's performance, emission, and combustion characteristics. The influence of renewable diesels on attributes of CI engine are also reviewed in this chapter.

Chapter 3 discusses the methodology involved in this study in details. The properties of the test fuels are mentioned. The numerical models and equations involved in the study are discussed in detail. Specifications of all the test engines are listed. The validations of the numerical tool are incorporated. Finally, the chapter is concluded by summarizing the whole research outline.

Chapter 4 includes the collected data and their data reduction process from numerical investigation. At first measured combustion parameters are tabulated. Then, the measured values of the performance attributes are tabulated. Finally, the levels of emissions of different exhaust gases are shown.

Chapter 5 discusses all the results of the study which is the main part of the thesis. The effect of *Spirulina* microalgae blended BTL diesel on engine performance, combustion, and emission characteristics are discussed in details. Finally, chapter 5 is closed by manifesting the comparison of the present finding with the previously reliable finding of various authors.

Chapter 6 summarizes the finding of the thesis work and conveys the recommendation for future work.

Chapter 2
Literature Review

2.1 Introduction

A large number of scientific studies has been conducted from very long time earlier in search of alternative fuels for heavy duty diesel engine. Among various alternative fuels investigated till present date, biodiesel is one of the promising and highly potential fuel to replace conventional diesel. Moreover, several renewable diesels have been investigated in very recent time by the researchers and considered as a source of transportation fuel that can overcome the shortcomings of the microalgae biodiesel. These literatures are reviewed thoroughly in this chapter. The effect of microalgae biodiesel and BTL diesel on the performance, combustion, and exhaust characteristics of auto ignition engine has been focused in the following description.

2.2 *Spirulina* Microalgae

Spirulina, additionally referred to as *Arthrospira*, are blue-green and multicellular algae with a spiral appearance [78].

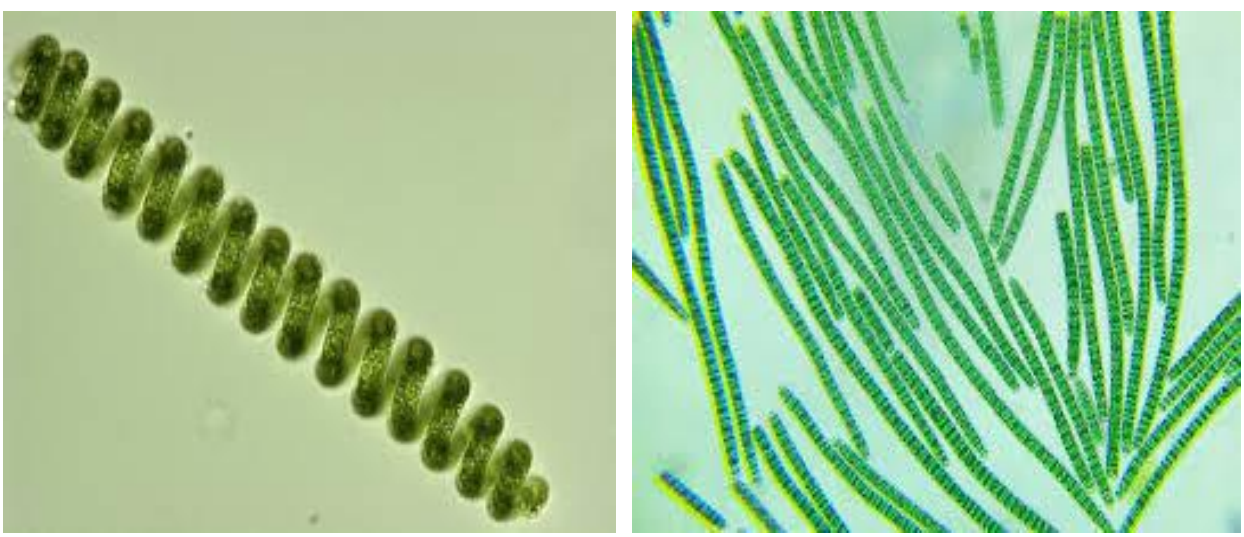

Figure 2.1. *Spirulina* microalgae [78].

P. J. Turpin separated *Spirulina* from a clean water source in 1827. Fig. 2.1 represents the photographic view of *Spirulina* microalgae. A bluish green, septal, helical shaped microalga was discovered by Wittrock and Nordstedt in 1844 adjacent to the Montevideo city of Uruguay, formerly known as *Spirulina platensis*.

They breed through binary fission and primarily autotrophic due to their photosynthetic nature. Plenty of helical filaments are present in them; which range in length from 50 to 500 μm and have a diameter of roughly 3 to 12 μm [79]. *Spirulina*'s smooth, exposed body surface makes it straightforward for basic enzymatic systems to break down [80]. Although Gomont recognized the aseptate and septal forms of the genus *Spirulina* and *Arthrospira* respectively in 1892, their helical morphology led to their reunification under the *Spirulina* name in 1932 [81]. The term "*Spirulina*," which has been used for the majority of global researches on these microalgae, is widely used by scientists, producers, and consumers.

2.3 Properties of *Spirulina* Microalgae

Physical and chemical properties of *Spirulina* microalgae were evaluated and described in various scientific researches. Mostafa et al. in their study evaluated the characteristics of *Spirulina* microalgae that was cultivated and grew in a research center regarding microbiology. A 19.55% lipid content was identified by the authors in *Spirulina platensis*, which may have resulted from stress-induced culture in the lack of a nitrogen supply and 10 g/L salinity levels. The yields of the specified pigments such as allophycocyanin, C-phycocyanin, carotenes and chlorophyll in this study were roughly 0.54, 10.99, 0.74, and 0.57 wt. % respectively. Furthermore, it provided the approximate weight percentages of 53.3, 11.57, and 2.74% for total proteins, carbs, and nucleic acids, accordingly. All of the findings suggested using the biomass following the separation of lipids as a supplement to livestock feed, while using pigments for organic coloring and medicinal purposes [82].

Morsy et al. conducted a scientific experiment to investigate the food value of *Spirulina* and discussed the physio-chemical characteristics of this algal species. *Spirulina*'s high alkalinity makes it a practical resolve to most diets' pH difficulties [83]. Table 2.1 contains the properties of the microalgae reported by the authors.

2.4 FAME Composition of *Spirulina*

The general chemical name for biodiesel produced from renewable resources through the transesterification process is Fatty Acid Methyl Ester (FAME). The composition of FAME in *Spirulina* microalgae reported by Rajak et al. is enlisted in Table 2.2. The main fatty acid in *Spirulina platensis* was found C16:0 (palmitoyl fatty acid group). In contrast, stearic fatty acid group, had the minimum quantity among other fatty acids. Since they have greater cetane numbers, lowered melting points, and are less likely to oxidize, smaller chain and saturated fatty acids are recommended for the preparation of biodiesel fuel. Nonetheless, Spirulina platensis is a promising feedstock for the production of biodiesel fuel due to its palmitoyl fatty acid dominance.

Table 2.1. Properties of *Spirulina* [83].

Properties	Values
Lipid content	7.2 %
Protein	61.5 %
Carbohydrate	12.8 %
Moisture content	5.4 %
Ash content	7.1 %
pH	6.9
Color	Bluish green
Odor	Similar to marine weed

Table 2.2. FAME composition of Spirulina [84,85].

FAME	Composition (wt%)
Palmitic (C16:0)	41.25
Linolenic (C18:2)	17.5
Linoleic	12.5
Ecosenoic (C20:0)	1.25
Oleic (C18:1)	4.0
Eicosic (C20:1)	4.4

Stearic (C18:0)	0.98
Myristic (C14:0)	2.56
Behenic (C22:0)	6.65
Caprylic	3.92
Lignoceric	3.97
PUFA	2.11

2.5 Properties of *Spirulina* Microalgae Biodiesel

Plenty of researches have been conducted with the aim of exploring the potential of biodiesel derived from *Spirulina* microalgae. Table 2.3 shows the properties of the *Spirulina* microalgae derived biodiesel determined in the previous scholarly studies [86]. Prior to being widely adopted, an extensive examination of algal biodiesel's characteristics and compatibility for use in diesel engines is essential. The properties of the biodiesel extracted from any resource should comply with the well-established ASTM standards to be considered acceptable as automotive fuel. Because physio-chemical properties of fuels directly influence the in-cylinder combustion, performance, and exhaust attributes of automotive engines. Due mainly to a greater oxygen content, algae biodiesel exhibits a kinematic viscosity of 44.7% and a density of 5.1% higher than regular diesel.

Table 2.3. Properties of *Spirulina* Microalgae Biodiesel [82,86,87].

Parameters	Values
Density (kg/m^3) at 15ºC	861
Kinematic viscosity (mm^2/sec)	3.9
Flash Point	128
Cetane Number	52
LHV (MJ/kg)	36.5
C (%)	78.3
H (%)	12.6
O (%)	9.1

These extra oxygen atoms affect the density of algae biodiesel, in contrast to diesel fuel, which does not include them. Additionally, the produced biodiesel's higher oxygen content promotes more intense molecular interactions than diesel, which makes the molecules of the biodiesel more viscous. Furthermore, compared to diesel fuel, algal biodiesel has a significantly greater flashpoint and a lower heating value. Brake thermal efficiency in CI engines is greatly influenced by the fuel's density, viscosity, and calorific value. Because biodiesel is denser and more viscous, it may inject more fuel into the combustion chamber, which raises the in-line pressure. However, power and fuel consumption are impacted negatively by its somewhat lower calorific value [88].

2.6 FTIR Spectrometer Analysis of *Spirulina* Biodiesel

Mostafa et al. in their investigation conducted FTIR analysis of the produced *Spirulina* biodiesel and compared with Egyptian Petro-diesel. The photographic view of the analysis is represented in Fig. 2.2. Aliphatic hydrocarbons with comparable molecular structures primarily made up both diesel and biodiesel. The spectra of biodiesel, like those of algal oil, display cis isomers.

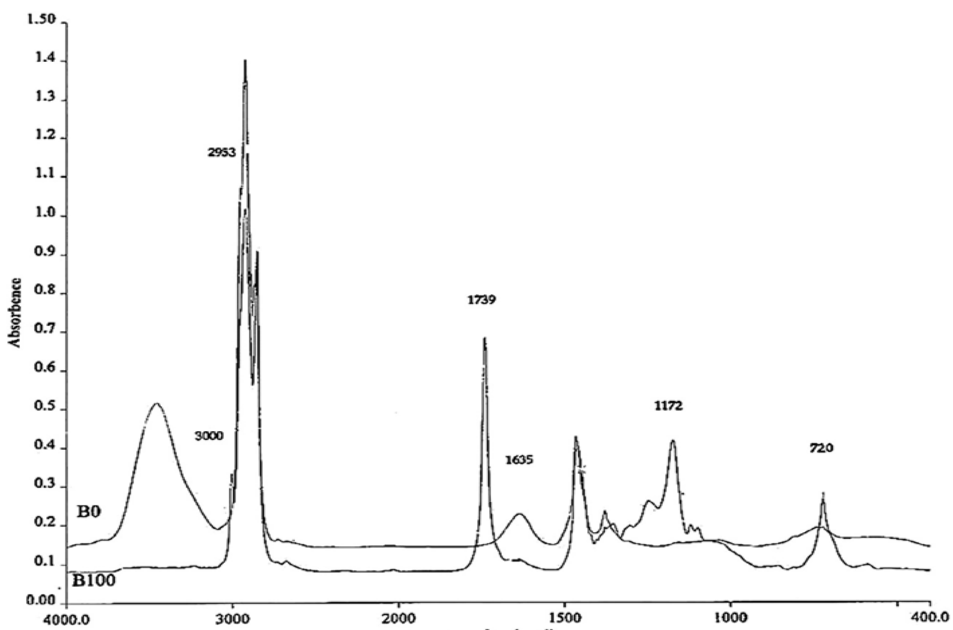

Figure 2.2. FTIR spectrometry for biodiesel and diesel [82].

However, FTIR spectra show differences between the two, with biodiesel exhibiting overlapping peaks in the 1000 cm^{-1} to 1300 cm^{-1} range, unlike diesel oil. Complete transesterification in biodiesel spectra is indicated by the lack of a peak greater than 3000 cm^{-1}, which belongs to the OH radical of carboxylic acid. The stretch bands for aromatic hydrogen (=C-H) and aromatic (C=C) which do not exist in biodiesel spectra appear at around 2953 and 1635 cm^{-1}, respectively, in regular diesel spectra [82].

2.7 Effect of Microalgae Biodiesel on Engine Combustion

A good deal of scholarly works is available on the effect of microalgae biodiesels over the performance, combustion and emission characteristics of a diesel engine. Rajak et al. investigated the usage of *Spirulina* microalgae biodiesel as an environmentally beneficial and renewable substitute for petroleum fuel in diesel engines, by assessing its performance, combustion, and emission properties. A four-stroke, single-cylinder diesel engine is utilized in the studies, and it is fed *Spirulina* biodiesel and its blends under various load conditions. Despite having a slightly lower peak cylinder pressure (PCP) and heat release rate (HRR), combustion characteristics of *Spirulina* biodiesel were similar to diesel fuel. The ignition delay period (IDP) shortened for microalgae blends compared to neat diesel [84]. Nautiyal et al. conducted a scientific experiment to figure out how *Spirulina* biodiesel affects the performance, combustion, and emission characteristics of diesel engines. A naturally aspired four stroke single cylinder diesel engine was utilized as test setup. The IDP for neat biodiesel decreased to 7.3ºCA from 10ºCA for regular diesel. Biodiesel-diesel blends showed a reduced HRR than basic diesel. The combustion durations (CD) for basic diesel, B10, B20, and B100 blends were 37.5, 38, 38, and 40 ºCA, correspondingly [88]. A numerical analysis was conducted by Rajak et al. on the engine characteristics of a CI engine powered by diesel and algae-biodiesel blended fuels at different compression ratios of 16.5 to 18.5 using the commercial Diesel-RK software. A single cylinder four stroke direct injection diesel engine is investigated numerically at full load. *Spirulina* microalgae and its blend (D80B20) produced equivalent cylinder pressures to diesel at various compression ratios of 16.5, 17.0, 17.5, 18.0, and 18.5. Compared to base diesel, alternative fuel showed a shorter IDP and CD at full load [89]. The graphical representations of CD and IDP for regular diesel, neat biodiesel and diesel-biodiesel blend prepared by the authors using the data resulted from the numerical investigation are presented in Fig. 2.3.

The experimental study of Suresh aimed to design an electrostatic precipitator mechanism to reduce nanoparticle discharges in emission from a diesel engine using Al_2O_3 nanoparticle-enriched *Spirulina* algae biodiesel-diesel combination. The biodiesel was mixed with diesel at concentration of 15% and 30% and employed to a naturally aspired single cylinder CI engine to test the engine performance, combustion and environmental parameters. The PCP for algae biodiesel blends were found slightly lower than regular diesel. Conventional diesel exhibits the highest peak HRR owing to its high energy content and efficient combustion. The 15% and 30% algae-derived biodiesel blends have slightly reduced HRR peaks, perhaps due to biodiesel's lower calorific value. As an efficient catalysts for combustion, the nanoparticles promote fuel atomization and foster improved air-fuel mixing, both of which raise the rate of combustion [90]. The purpose of the investigation conducted by Munimathan et al. was to identify the attributes of a reactivity-controlled compression ignition (RCCI) engine employing low- and high-reactive fuels, *Spirulina* algal biodiesel and methane-enriched hydrogen. A four-stroke single cylinder direct ignition CI engine was utilized as the test setup. By enhancing the oxygen content in the methane and hydrogen, biodiesel and dimethyl ether boost the reactivity of the combination. The hydrogen and methane fuel mixture's fast flame speed causes high cylinder pressure. The remarkably low density of hydrogen showed tendency to decrease the CD and cause a significant engine HRR. When there is minimal load, it displayed a negative HRR as a result to the high reactive fuel [91]. Chaurasiya et al. demonstrated the influence of variation of the injection timing (IT) on the characteristics of a single-cylinder diesel engine. They carried numerical research for the fuel blends prepared by mixing 5% h_2 with 95% of ordinary diesel, nbutanol (nB), diethyl ether (DEE), and spirulina microalgae. PCP and IDP for the blend of microalgae increased gradually with the advancement of IT. As injection timing advances, the level of SFC for 5%H95%DEE gradually rises, but the level of SFC for 5%H95%nB shows an inverse tendency. 5%H95%DF exhibits the greatest exhaust gas temperature (EGT) at 29.5 deg. b TDC, subsequently followed by 5%H95%SMA, 5%H95%nB, and 5%H95%DEE at 713.82, 710.66, 676.37, and 619.41 K, respectively. Results are contrasted with diesel fuel [92].

In the study of Rajak et al., a single cylinder, 4-stroke, water-cooled, naturally aspirated, and direct injection compression ignition diesel engine's combustion, performance, and emission characteristics are all taken into account. At a steady engine speed of 1500 rpm, the engine is tested with multiple mixtures of diesel and *Spirulina* blends. The PHRR value for diesel was observed as 93.54 J/⁰CA which reduced by biodiesel blends to 87.1, 69.3, 68.9, 66.2 and 63.2 J/˚CA for B20, B40, B60, B80 and B100 fuel samples respectively. The PCP reduced slightly for the microalgae blended fuels compared to pure diesel. The amount of reduction raised higher with the increase of the proportion of bioidiesel [84,93]. Krishania et al. explored the performance, combustion, and emissions of an auto ignition engine fueled with biodiesel blends from several first, second, and third generation oil feedstocks and compared them with diesel fuel. The study numerically examined the attributes of a diesel engine running on B20 blend fuel from various feedstocks at different CR's at 1500 rpm and *Spirulina* microalgae was one of them. The CP raised for microalgae compared to regular diesel at all three CR's of 16.5, 17.5, and 18.5. AT CR of 16.5, the HRR resulted from microalgae blend reduced by 0.9 deg/J with respect to traditional diesel. Similar tendency exhibited by microalgae for CR of 17.5 and 18.5 also. The analysis concluded that increasing CR resulted in a decrease in IDP for all fuels assessed. Microalgae biodiesel featured shorter IDP than diesel fuel attributed to increased CN and oxygen levels. The Maximum rise of pressure rate of the generation biodiesel blends is found lesser than that of gasoline and declines with a rising proportion of alternative fuels due to biodiesel's less intensive pre-combustion phase compared to gasoline fuel. With a corresponding CR of 16.5, the maximum rise of pressure rate for diesel was determined to be 6.1, whereas the MRPR for *Spirulina* biodiesel was determined to be 5.6. Finally, the authors marked as conclusion that among the second and third generation feedstocks, which used as a blend of B20 and *Spirulina* microalgae and Jatropa biodiesel improved the combustion, performance and ecological indicators of the CI engine. Optimum outcomes were resulted for CR of 17.5 [94]. Rajak et al. applied blends of *Spirulina* Microalgae oil, containing 20, 40, 60, and 80 Vol% of biodiesels with diesel, as alternative fuel in a diesel engine. The IDP of all microalgae biodiesel and diesel mixture is higher than that of diesel. Compared to biodiesel, the cylinder's PHRR rise is greater for fuels samples containing *Spirulina* microalgae. Neat diesel, SMB1, SMB2, SMB3, SMB4, and SMB5 fuel samples displayed PCP of 94.04 bar, 91.9 bar, 90.39 bar, 89.7 bar, 88.7 bar, and 88.0 bar, respectively [95]. The variation of CP and HRR with load determined by the authors are shown in Fig 2.4.

Using blends of hydrogen, ammonia, and microalgae biodiesel, the study of Subbiah et al. evaluated the performance of an auto ignition engine with an emphasis on combustion characteristics, energy consumption, emissions, and braking thermal efficiency. In terms of combustion, the blends containing hydrogen and ammonia showed the maximum cylinder pressure and heat release rate.

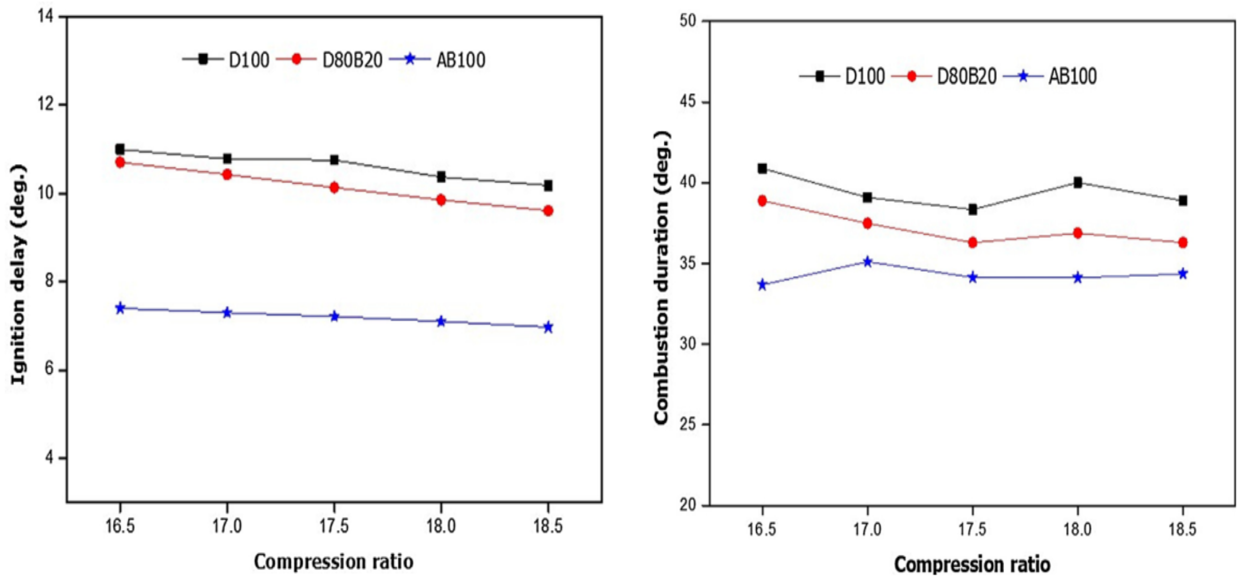

Figure 2.3. Variations IDP and CD with respect to CR (reported by Rajak et al.) [89].

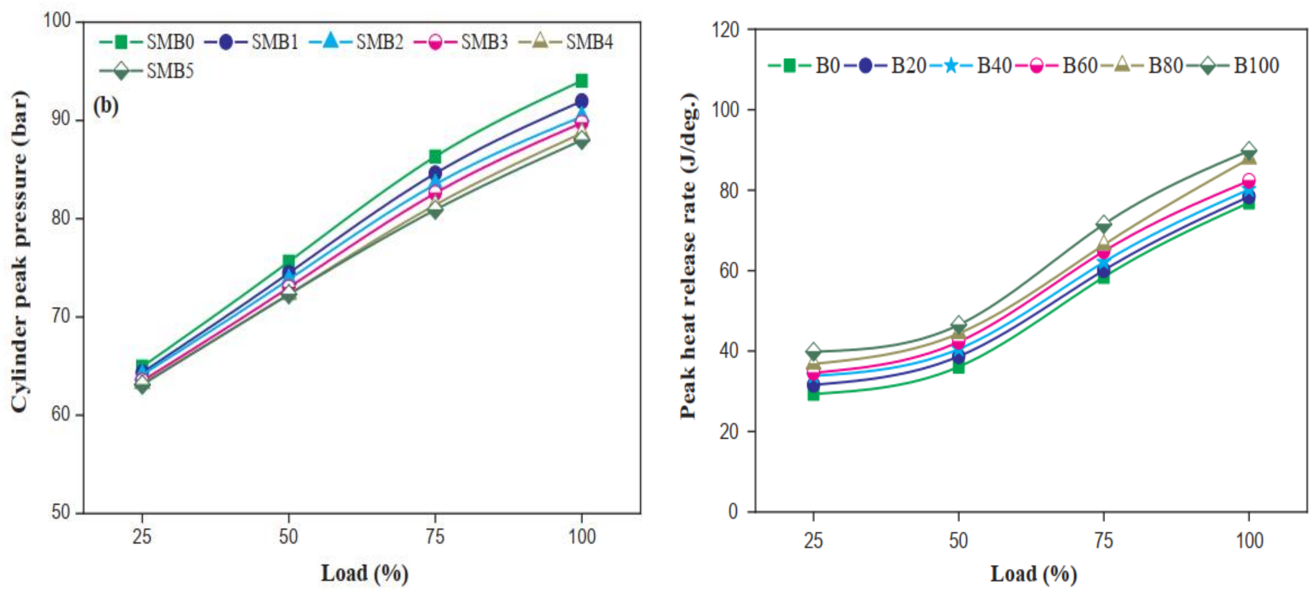

Figure 2.4. PCP and PHRR for the fuel blends with load (reported by Rajak et al.) [95].

Cylinder pressure was somewhat lowered in ammonia mixes when EGR was used. Because biodiesel blends have a lower heating value than clean diesel, they lowered the HRR. Another explanation for the lower HRR levels is an increase in the biodiesel's viscosity. Because of the improved combustion process and increased rate of energy release, B30A exhibited a 9.8% improvement in HRR. The B30H's high calorific value is probably the reason for the 13.8% increase in HRR caused by the hydrogen content when compared to the other mixes [96].

2.8 Effect of Microalgae Biodiesel on Engine Performance

According to the study of Rajak et al., the most efficient blend was B20% (20% microalgae *Spirulina* biodiesel and 80% diesel), which resulted in lower exhaust gas temperature (EGT), brake thermal efficiency (BTE), and higher specific fuel consumption (SFC) when compared with diesel. In comparison to B0, the brake thermal efficiency of B100 was relatively low [84]. Nauitiyal et al. reported that at full load, the BTE of algal biodiesel-diesel blends of B10, B20, and B100 and base diesel were 26.79%, 25.97%, 26.51%, and 27.19%, respectively, indicating similar performance. Increase in engine load resulted in higher efficiency due to higher in-cylinder temperature [88]. The findings of Rajak et al. denotes that applying algal biodiesel resulted in a 6.56% drop in brake torque compared to 18.73 N-m recorded with neat diesel at CR16.5. Brake torque decreased by 1.7%, 0.44%, and 0.55% for D80B20 blend, and 7.71%, 6.66%, 7.90%, and 8.32% for neat biodiesel at CR17, CR17.5, CR18, and CR18.5, respectively. Moreover, diesel demonstrated a lesser SFC than both biodiesel and its blend because of its greater density and smaller calorific value, resulting in more fuel injection at the same time and pressure [89].

Experimental findings of Suresh indicated that increasing the biodiesel content in the mixture resulted in an 11.3% increase in BSFC and a 10.4% loss in BTE with respect to base diesel. Biodiesel blended fuels have poorer thermal efficiency due to low calorific value, limiting the generation of power during burning. Nonetheless, addition of nanoparticle resulted BTE close to base diesel and decreased the SFC as well [90]. The BSFC and BTE found by the authors are presented in fig. 2.5. Based to the experimental findings of Munimathan et al., the BTE was 37.84%, the BSFC was 182 g/kWh, and the EGT was 320 ºC. With the help of their superior fuel properties, fuel mixtures are suggested to enhance engine performance. With the increment of the percentage of hydrogen in the fuel mixture, the BTE increased gradually. Rising the engine load also elevated the BTE [91]. Chaurasiya et al. reported that the SFC for the *Spirulina* microalgae blended fuel is almost similar or slightly smaller to regular diesel blended fuel. Similarly, the hydrogen enriched microalgae blend showed BTE almost close or slightly higher than the hydrogen enriched diesel blend [92].

Performance analysis in the scholarly work of Rajka et al., indicated that in comparison to neat diesel, the engine's BTE at B20 blend decreased by 0.63% at CR17.5. At full load situation of the engine, the BTE for pure diesel, B20, B40, B60, B80, and B100 fuel blends were determined 33.51%, 33.3%, 33.18%, 33.0%, 32.5%, and 32.1%, respectively. Compared to pure diesel, the overall efficiency decreased at B100% was roughly 4.2% which is because of lower heating value of biodiesel. The SFC escalated while using *Spirulina*-diesel fuel blends compared to neat diesel. Physio-chemical properties of biodiesel play significant role to monitor the engine SFC [84,93]. Krishania et al. found that with the advancement in injection timing (IT) of fuel, B20 blend from the first, second, and third generation of biodiesel including microalgae derived biodiesel blend showed a decrease in BTE, EGT, and elevation in SFC. The BTE with 100% load was 32.92% for *Spirulina* biodiesel and 33.42% for pure diesel at CR of 16.5. As the engine load increased, the BTE also increased. This is because a higher load causes the cylinder temperature to rise. However, the values of EGT for microalgae were close to those of regular diesel at higher engine loads [94]. Rajak et al. applied blends of *Spirulina* Microalgae oil, containing 20, 40, 60, and 80 Vol% of biodiesels with diesel, as alternative fuel in a diesel engine. The effect of microalgae biodiesel on the attributes of a 4-stroke and single cylinder direct ignition CI engine is tested for varying engine loads. The incorporation of *Spirulina* microalgae biodiesel to diesel results in a spike in BSFC and a 3.03% decrease in BTE at 100% load.It has been noted that under the each tested engine load, the indicated thermal efficiency of all test mixture of microalgae and diesel fuel is smaller than that of neat diesel. The indicated thermal efficiency showed a sequential drop with the increment of engine load [95].

Uslu et al. explored the effect of incorporating third generation *Spirulina* microalgae biodiesel and Fe_3O_4 nanoparticle on the performance and emission indicators of a single cylinder water cooled direct ignition CI engine. Algal biodiesel was blended into diesel at varying ratios of 10% and 20% separately, and Fe_3O_4 nanoparticle was added to 20% biodiesel blend at three distinguished amounts- 25, 50, and 75 ppm step by step. The engine parameters are tested for variable loads of 25% and 100% individually maintaining fixed CR and speed. The application of biodiesel and nanoparticle both boosted the BMEP and BTE. The greatest increases were obtained with 20MAB80D75IO fuel in comparison to diesel, at averages of 28.64% and 13.18%, correspondingly. These parameters improved averagely by 3.85% and 12.85% with the 20MAB80D, accordingly.

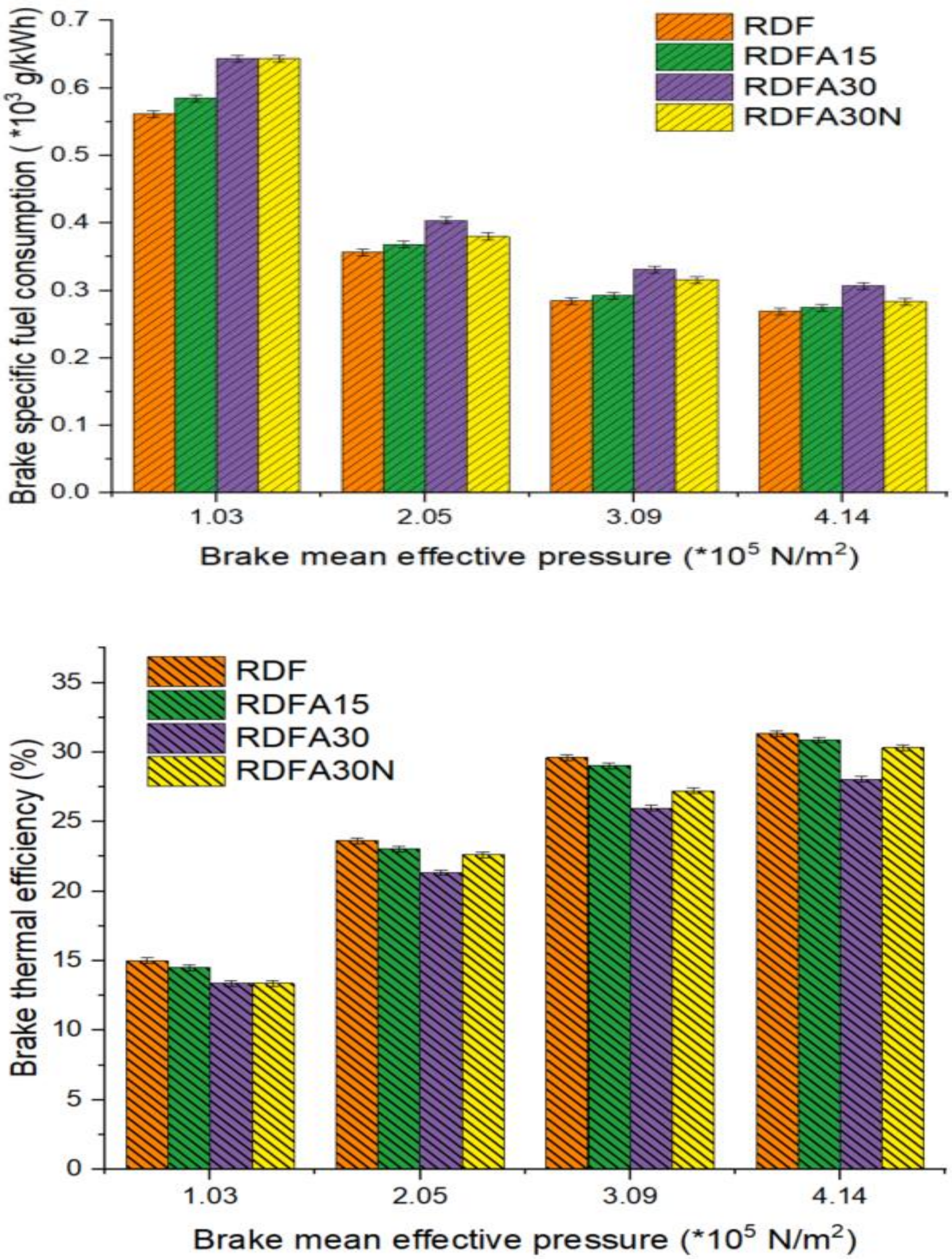

Figure 2.5. BSFC and BTE vs. BMEP (from literature) [86].

However, the BSFC response dropped with Fe_3O_4 nanomaterial and rose with algal biodiesel. When contrasting it with BSFC diesel, it demonstrated an average drop of 19.02% for 20MAB80D75IO fuel. A mean rise of 11.31% was observed with the 20MAB80D [97].

Alzubaidi et al. looked into the impact on emission and performance parameters of a 4-stroke auto ignition engine fueled by mixing *Spirulina* biodiesel with diesel at different ratios. The findings demonstrate that the fuel blend with ratio 10 of biodiesel/diesel escalates the BTE by 1.7%, whereas, decreases the BSFC and exhaust gas temperature (EGT) by 12.7 and 3.45%, respectively, with respect to base diesel at CR of 14 [98]. An experimental work was carried out to examine the prospective of the blend of *Spirulina* microalgae biodiesel (80% diesel & 20% biodiesel) as alternative fuel of diesel engine by Garg et al. at CR of 18. Under varying load conditions and with different ITs of 20◦, 23◦, 25◦, and 28◦ bTDC (before top dead center), the performance and emission parameters were evaluated. At full load, the biodiesel blend's peak BTEs for ITs of 20°, 23°, 25°, and 28° bTDC were estimated to be 26.79%, 23.77%, 24.77%, and 25.09%, respectively, against 27.76% for neat diesel [87].

2.9 Effect of Microalgae Biodiesel on Engine Emissions

According to Rajak et al., when *Spirulina* biodiesel is used instead of diesel fuel, CO, CO_2, and HC emissions were reduced. The NO_X emissions were less than those of diesel in CR17.5. As the amount of oxygen in the biofuel or biodiesel increased, the amount of smoke that was released reduced, helping to ensure full combustion. The CO emission rate dropped as the engine load increased [84]. In the investigation of Nautiyal et al., *Spirulina* biodiesel considerably reduced CO and HC emissions while also reducing smoke opacity due to its oxygen content. However, the release of NO_x after combustion increased for biodiesel. Injection timing, oxygen incorporated fuel, and a higher flame temperature all contribute to the increased NOx levels [88]. The emission analysis of Rajak et al. indicated that utilizing D80B20 at 100% load with CR17.5 led to 4.5% lower CO_2 emissions compared to D100 (pure diesel). CO_2 emissions elevated as cylinder clearance volumes lowered owing to higher CR. Particulate matter (PM) emission was lowered for biodiesel. On the other hand, the NO_x released by neat microalgae biodiesel and its blend were comparatively higher in quantity than conventional diesel all CR’s except for 17.5. Therefore, CR 17.5 was considered as the optimum operating condition for biodiesel application [89].

From emission analysis of the study conducted by Suresh it is observed that microalgae biodiesel lowered the emission of hydro-carbons and CO, meanwhile increasing the exhaust of NO_x. For the minimum brake mean effective pressure (BMEP) of 1.03 bar, release of NOx dropped by 1.8% and 9.2% for 15% and 30% biodiesel blends accordingly. Under a maximum engine load of 4.14 bar, emissions of HC were minimum for each fuel sample [90]. In the investigation of Munimathan et al., smoke, CO_2, NOX, and HC emission levels were detected as 610 ppm, 8.9 ppm, 48 ppm, and 25 HSU, respectively. With the help of this fuel blend, emissions were successfully reduced. Based on the results, the fuel combination including 15% hydrogen and 1% methane, which makes up 20% of the low-rank fuel, produced the optimal engine characteristics [91]. According to the findings of Chaurasiya et al., the CO_2 emission dropped slightly for biodiesel blend compared to diesel incorporated blend. At all operating conditions. Smoke level in engine exhaust significantly reduced by biodiesel. However, NO_x emission resulting from engine exhaust increased for all cases emitting the highest amount for the most advanced IT [92].

In a nutshell, the microalgae spirulina biodiesel concept had significantly lower emission parameters than diesel in [84,93]. The level of HC, CO and BSN dropped significantly for microalgae blends with respect to diesel. From the emission analysis section of the study carried by Krishania et al., level of smoke emission was observed to be lower for *Spirulina* microalgae biodiesel with respect to conventional diesel at CR of 17.5 and 18.5. The PM was determined to be 0.78 g/KWh for diesel and 0.766 g/KWH for spirulina at CR17.5. According to the study, for all fuel assessments, a decrease in PM emissions was noted as CR climbed. Compared to diesel fuel, every biodiesel in the current investigation had decreased PM emissions. The findings also showed that the emission of both NO_x and SO_2 harmful gases from test engine were decreased for algal biodiesel with respect to pure diesel [94]. Rajak et al. mentioned in their experiment that for *Spirulina* bioidesel, the estimated PM emissions were 0.285, 0.226, 0.201, 0.20, 0.18, 0.18, and 0.167 g/KWh, respectively, according to greater load. When SMB1 and SMB5 are compared to pure diesel, the PM emissions are reduced by 20.7% and 41.4%, respectively. Emissions of smoke and NO_X dropped when spirulina microalgae biodiesel was added. Since SMB1 has a lighter mixture and superior combustion than diesel, it can reduce NO_X emissions by up to 4.9% and Bosch Smoke Number (BSN) emissions by up to 5.4% [95].

Uslu et al. examined the impacts of adding microalgal biofuel to diesel fuel, as well as the effects of varying Fe_3O_4 concentrations on diesel engine responses at various engine loads. As byproducts of incomplete combustion, *Spirulina* biodiesel and nanoparticle tended to lower emissions of HC and carbon monoxide CO. Comparing 20MAB80D75IO blend to gasoline, a mean decrease of 24.21% and 57.36% were obtained, respectively. On average than that of D100, while the NOx generated by 20MAB80D was 3.83% higher.

The average decreases with the 20MAB80D were 20.14% and 22.62%, respectively. On the other hand, 20MAB80D75IO produced NO_x that was 11.63% greater than D100, while 20MAB80D produced NOx that was 3.83% higher [97]. According to Alzubaidi et al., though the emissions of CO and CO_2 were close to those of base diesel, the NO_x emission slightly raised for biodiesel by 2.4%. In general, there was a noticeable decrease in CO_2 and NO_X emissions when algae biodiesel was added to conventional fuel. On the other hand, CO and UHC emissions rose. B10 displays a little lower UHC value at 25% load with 14.5 CR (58 ppm Vol.), which is 12% lower than B0 [98]. Garg et al. found in their investigation that the HC and CO_2 emissions dropped, whereas, the release of NO_x increased for microalgae. While the release of NO_x rose for microalgae, the emissions of HC and CO_2 dropped with respect to neat diesel [87].

Suubiah et al. noticed in their study that the NO_x emissions increased as a result of the combustion temperature being raised by the hydrogen present in the combustion products.

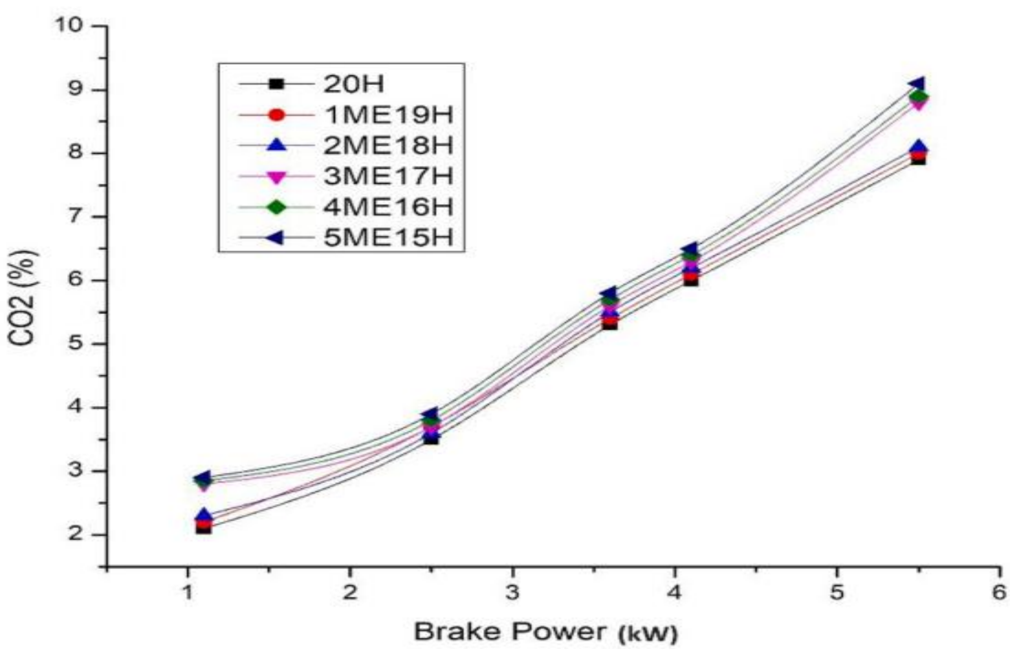

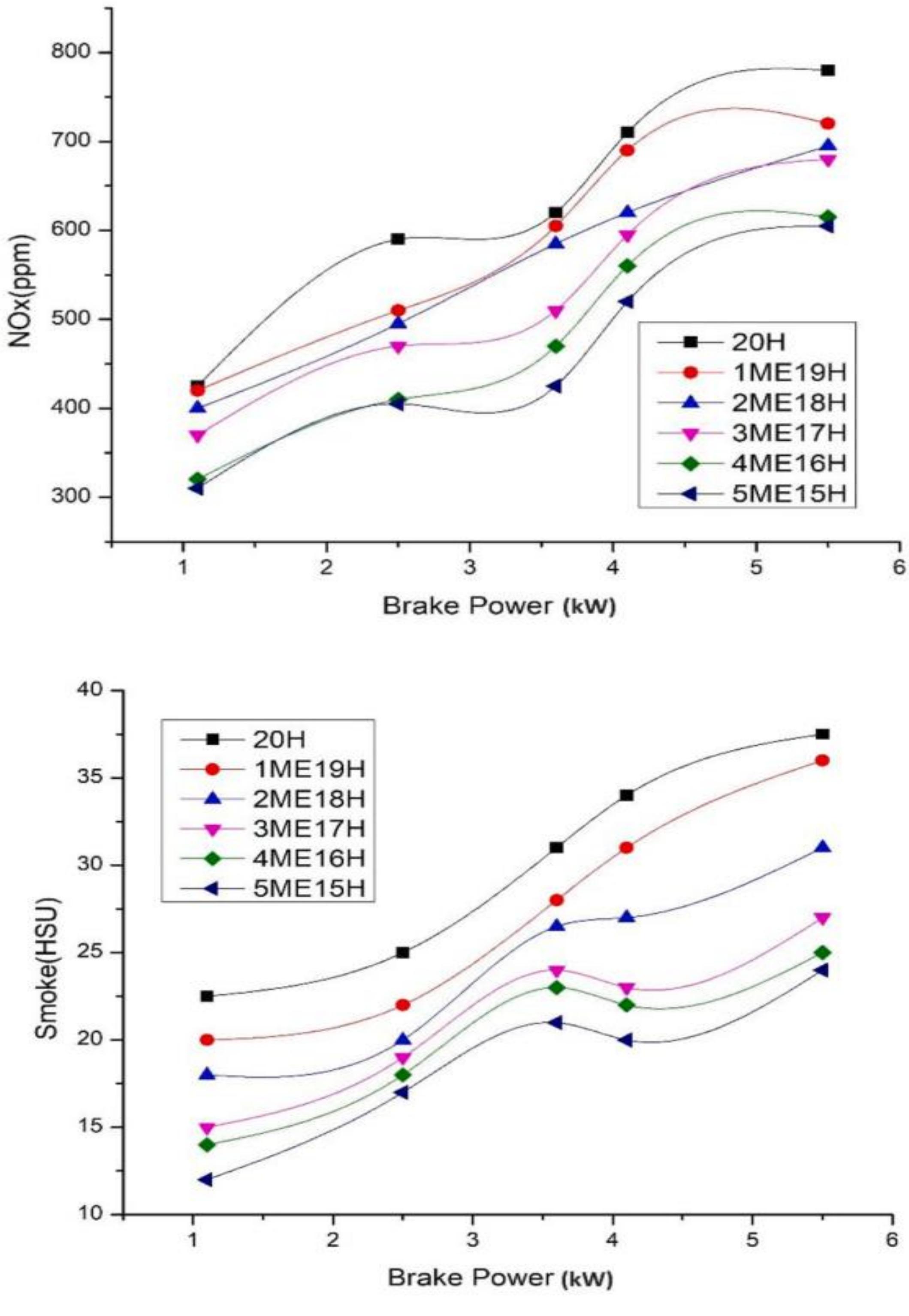

Figure 2.6. Emissions of CO_2, NO_x and Smoke vs. BMEP (from literature) [91].

All braking power levels saw a decrease in the production of most emissions, including hydrocarbon and carbon monoxide emissions, when biodiesel blends were used. When EGR was used, the combustion temperature dropped and the combustion time rose. In comparison to hydrogen blends, ammonia blends with EGR thus reported the lowest NO_x emissions [96].

2.10 Biomass to Liquid Diesel

As discussed already, microalgae biodiesel can overcome some limitations associated to petroleum fuel. On the other hand, several other difficulties are generated from its applications like comparatively poor engine performance and increased NO_x emissions. Therefore, remarkable scientific studies are being conducted recently to minimize the shortcomings of microalgae biodiesel. As a result, renewable diesels like BTL, GTL, and CTL diesels have come to light as noble alternative fuel sources due to their several outstanding characteristics. They are renewable and cleaner fuel sources that poses very high cetane number, a significant parameter to measure fuel's potential. These alternative fuels are not naturally derived rather these fuels are produced by gasification and FT approaches, hence subsequently known as 'Synthetic Fuel'. These synthetic fuels are highly compatible to diesel engine. These fuels can be applied to existing traditional engines without altering engine hardware and this feature is marked as 'drop in' characteristics.

Renewable diesels are mainly long chain paraffinic hydrocarbons. BTL diesel comes with remarkable qualities that help in improving engine combustion and performance attributes. It can also improve the engine emissions leading to environmentally friendly cleaner combustion. These features of BTL diesel are highlighted in several scholarly literatures. The physio-chemical properties of BTL diesel are listed in table 2.4 collected from previous literature.

Table 2.4. Properties of BTL diesel [24,69,99].

Properties	Values
Flash Point (℃)	57
Dynamic Viscosity (mpa-s) @ 40℃	1.84
Kinematic Viscosity (mm^2/s) @ 40℃	2.36
LHV (Mj/Kg)	44

Density (kg/L)	0.875
Surface Tension (mN/m)	29.2
Water Content (%mass)	0.00238
Sulphur Content	~0
Oxygen Content	0

2.11 Effect of BTL Diesel on the Characteristics of Diesel Engine

Currently, a few numbers of researchers have conducted scientific investigations to examine the compatibility of renewable diesels to the CI engine. Various forms of biomass, including vegetable oils from different sources, leftover cooking oils, and fats, can be converted into renewable fuels, an alternative fuel [100]. FT synthesis is being used to improve and optimize the production of synthetic fuel in response to the expanding need for liquid hydrocarbon fuels and the diminishing reserves of fossil fuels. GTL technology bases itself on F-T synthesis, which is the process that turns synthesis gas—also known as syngas, a mixture of hydrogen and carbon monoxide that can be produced from natural gas, coal, or biomass—into ultra-clean fuels and chemicals with additional benefits [101].

Rimkus et al. tested the in-cylinder, performance, and ecological characteristics of a diesel engine fueled with the blends of BTL diesel and conventional diesel. The study used a 4-cylinder Audi 1.9 TDI direct ignition diesel engine. The winter diesel fuel (EN 590, designated as D1 in the Fig. 2.7) and the diesel (85% vol.) and BTL (15% vol.) blend (designated as D2 in the Fig. 2.7) that were bought from gas stations were used in the experiments. In comparison to pure diesel, experimental studies on the combustion process using diesel and BTL fuel blend that operated at typical speed and load but at varying braking torque revealed that engine efficiency rose by 2.0% and brake specific fuel consumption decreased by 2.6%. Moreover, because of the fuel's weaker BTL chain structure and a smaller C/H ratio, the exhaust gas's CO_2 levels decreased by about 1.1% and its HC levels dropped by 3–7%. Besides that, the shorter fuel IDP brought on by the BTL fuel's higher CN and lower oxygen content resulted in a 12–20% decrease in the premixed combustion phase's PHRR and a lower maximum combustion temperature, which in turn decreased the NO_x concentration by about 9–12% [99]. The BSFC and BTE measured by the authors are presented in Fig. 2.7.

Effect of diesel, biodiesel, and BTL fuels were examined by Ogunkoya et al. in a single-cylinder CI engine at a fixed speed of 2000 rpm and three engine loads, which corresponded to 0 bar, 1.26 bar, and 3.77 bar brake mean effective pressure (BMEP). Exhaust emissions, combustion, and engine performance parameters were all evaluated by the authors. A single cylinder air-cooled diesel engine with a displacement of 418 cc, a compression ratio of 19:1, a bore of 86 mm, and a stroke of 72 mm was used for the experiment. When BTL was applied in the CI engine, the mechanical efficiency and indicated work were marginally reduced at low engine loads, but increased at higher loads. In comparison to both diesel and biodiesel, BTL also exhibited better BTE and poorer BSFC. Except for NO_x and no-load circumstances, the study indicated that BTL emissions improved. Except at 0 bar BMEP, BTL exhibited lower emissions of HC, CO, and CO2 than diesel and biodiesel. The smoke's opacity (SO) dramatically increased at 3.77 bar BMEP. The IDP of BTL was found larger than that of biodiesel, although it was shorter than that of diesel fuel. Engine operating conditions had varying effects on cumulative heat release, in-cylinder pressure, and HRR [24]. Henry et al.'s experiment included evaluating the potential of 100% Sun Diesel in a single-cylinder heavy-duty direct-injection CI engine as well as a Mercedes A-Class (MY1999) diesel vehicle. Sun diesel improved the engine emissions by dropping the amount of NO_x and PM significantly in engine exhaust compared to conventional diesel. PM emission was measured using the min-dilution tunnel gravimetric method (BG1). The Sun Diesel engine's in-cylinder pressure peaking before conventional diesel, with higher peak pressure and somewhat lower mean effective pressure, indicated variations in the combustion process. FT's lower boiling hydrocarbons and Sun Diesel's lower premixed burning percentage may help to reduce NO_x output through quick evaporation and a lower gas mixture temperature [69]. The emission parameters measured by the authors are shown in Fig. 2.8.

Niemi et al. investigated the effect of a wood based renewable diesel (CTO) blends on the attributes of a CI engine. Without changing engine parts or performance, the study investigated the effects of various blends of CTO renewable diesel (HB) in commercial low sulfur diesel fuel oil (DF), abbreviated as DF, HB10, HB20, HB50, and HB100, on the operation and exhaust emissions of a contemporary common-rail non-road diesel engine. The study focused on a four-cylinder, common-rail diesel engine, especially an AGCO POWER 44 AWI, which was turbocharged and intercooled. Crude tall oil (CTO), a wood waste from chemical pulping, is used to make wood-based renewable diesel. It contains natural extractive components such as fatty acids, rosin acids, sterols, and neutral compounds. The more CTO renewable fuel the fuel blend contained, the lower the cycle-averaged CO and HC emissions. The CTO renewable fuel's greater cetane number and significantly lower amount of aromatic components were thought to be the primary causes. The exhaust smoke was very low—nearly insignificant for all fuels—because of the high-NO_x setting. With the exception of idle, where higher HB concentration decreased emissions of ultrafine particle numbers, the study did not find any discernible trends in the exhaust

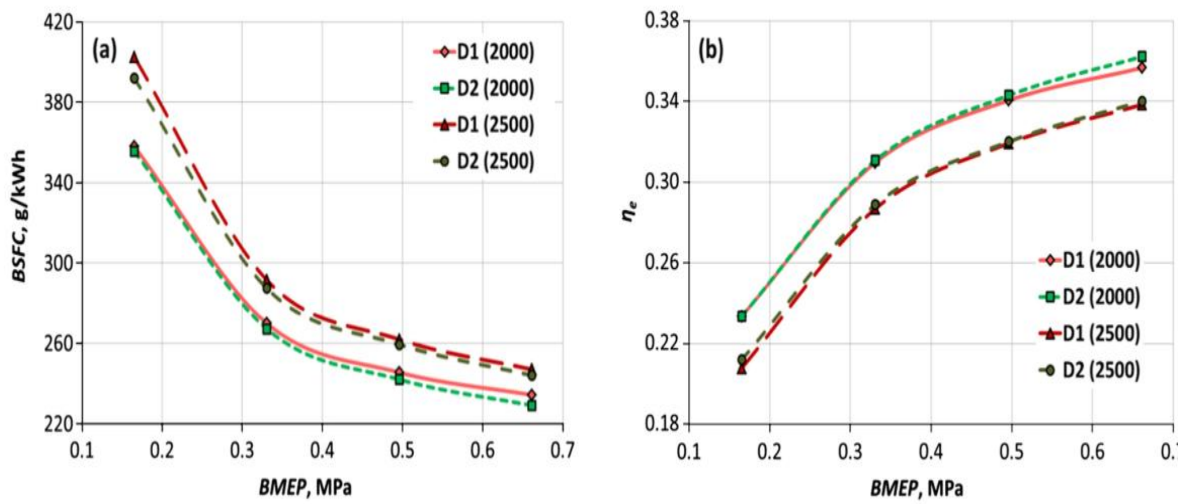

Figure 2.7. Variations of (a) BSFC & (b)BTE for neat diesel (D1) and BTL-diesel blend (D2) (from literature) [99].

particle size distributions. The share of renewable fuels climbed, as well as the peak particulate number. The primary goal was to investigate how the performance and exhaust emissions of contemporary common-rail diesel engines are impacted by mixtures of fossil and renewable diesel. The ISO8178 standard's NRSC cycle was followed when conducting the performance and emission measurements [102]. According to related research by Miers et al., Sun Diesel's pre-mixed combustion phase peak value decreased with an advance in injection timing [103].

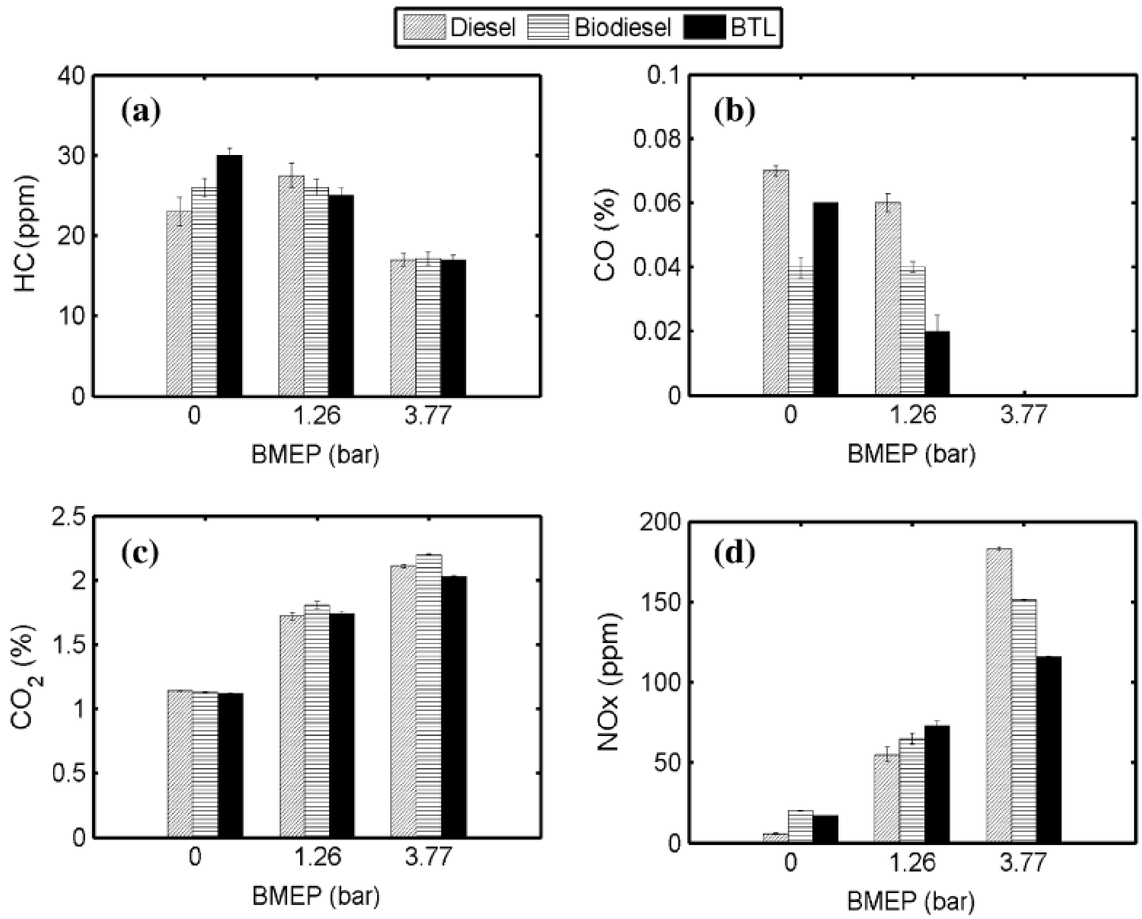

Figure 2.8. Emissions parameters with respect to BMEP (from literature) [24].

When using neat vegetable oils with pump-line-nozzle injection systems, Soltic et al. demonstrated that the various physical characteristics of the fuels have a significant impact on the injection system and can also cause longevity issues [104].

Mizushima et al. used a portable emission measurement system (PEMS) to assess emissions from a heavy-duty diesel vehicle running on alternative fuel, such as FAME, HVO, and BTL, in the real world. This heavy-duty transport truck had a maximum payload capacity of three tons, and it was equipped with an unmodified diesel engine with a displacement of 2999 cm^2. The PEMS was installed in the vehicle's cargo area to monitor exhaust gas emissions while driving on public roads. Weather and driving behavior have an impact on NO_x emission characteristics, according to the study. Hot and humid weather produced low NO_x emissions, but cold and low humidity conditions produced high emissions. When driving carelessly without using eco-driving techniques, NO_x emissions rose and surpassed the 2009 regulation limit in Japan. While the emission characteristics of biofuels such as HVO and BTL were either the same or slightly elevated, FAME dramatically enhanced NOx emissions in these biofuels. Consequently, paraffinic hydrocarbon biofuels are appropriate for heavy-duty diesel cars, whereas FAME is not [105].

2.12 Conclusion

The literature review on the third generation *Spirulina* microalgae biodiesel feedstock highlights its potential as a sustainable energy solution. Several scientific investigations have showed that the microalgae biodiesels can be a solution to the risk of decline of fossil fuels in near future. They are compatible to diesel engine and can improve emissions of most of the harmful gases leading to cleaner and environmentally friendly combustion. Additionally, the less explored novel renewable diesels are gaining attraction in recent times due to their significant characteristics. These are derived from renewable biomass resources and have properties even better than biodiesel. BTL diesel, a renewable diesel, have been studied by a few researchers and reported to exhibit better engine performance compared to diesel. The review of previous studies indicates that there is a lack of research work combining the renewable diesel and microalgae biodiesel for the application of alternative fuel of CI engine. The current study is motivated by this gap of research and focused to observe the influence of the addition of renewable diesel into microalgae derived biodiesel for diesel engine.

Chapter 3

Methodology

3.1 Test Fuel Properties

The performance, combustion, and emissions of a diesel engine are evaluated for pure diesel, BTL diesel, and blends of *Spirulina* microalgae biodiesel and BTL diesel for five different ITs at constant swirl ratio of 0.5 using Diesel-RK simulation software. Six different test fuels are investigated termed as D100 (neat diesel), BD100 (neat BTL diesel), BD80MB20 (a blend of 80 vol% BTL diesel and 20 vol% *Spirulina* microalgae biodiesel), BD60MB40 (a blend of 60 vol% BTL diesel and 40 vol% *Spirulina* microalgae biodiesel), BD40MB60 (a blend of 40 vol% BTL diesel and 60 vol% *Spirulina* microalgae biodiesel), and BD20MB80 (a blend of 20 vol% BTL diesel and 80 vol% *Spirulina* microalgae biodiesel). All the considered fuel blends satisfy ASTM standards. Table 3.1 illustrates the properties of the test fuels.

Table 3.1. Properties of test fuels [84,106,107].

Property	D100	BD100	*Spirulina* microalgae biodiesel	BD20MB80	BD40MB60	BD60MB40	BD80MB20
LHV (MJ/kg)	42.98	44.58	41	41.64803006	42.32757	43.04096	43.79081981
Kinematic viscosity (mm^2/s)	2.95	1.55	5.26	4.119598914	3.226444	2.526931	1.97907616
Dynamic viscosity (Pa.s)	0.0025	0.00118	0.00453	0.003461425	0.002645	0.002021	0.001544277
Density (kg/m^3)	851.4	761.2	861	841.04	821.08	801.12	781.16
Cetane number	47	80	52.2	57.76	63.32	68.88	74.44
Surface Tension (N/m)	0.0274	0.02496	.03336	0.030192	0.028884	0.027576	0.026268

C (%)	0.8659	0.8579	0.7746	0.79126	0.80792	0.82458	0.84124
H (%)	0.1267	0.1254	0.1221	0.12276	0.12342	0.12408	0.12474
O (%)	0	0	0.1033	0.08264	0.06198	0.04132	0.02066
C/H	6.8343	6.8413	6.344	6.4456	6.5461	6.6456	6.7439

The physico-chemical properties of the fuel blends tested in this numerical study are determined using equations (1) to (4). The Grunberg-Nissan mixing rule [108], initially put forth by Arrhenius [109], serves as a method for ascertaining the viscosity of blends [110–113]. Cetane number, density, heating value, and elemental composition of the fuel blends are all estimated using Kay's mixing rule.

$$CN_b = \sum_{k=1}^{3} Z_k CN_k \tag{3.1}$$

$$D_b = \sum_{k=1}^{3} Z_k D_k \tag{3.2}$$

$$ln\, \mu_b = \sum_{k=1}^{3} Z_k\, ln\, \mu_k \tag{3.3}$$

$$HV_b = \frac{\sum_{k=1}^{3} X_k D_k HV_k}{\sum_{k=1}^{3} X_k D_k} \tag{3.4}$$

In the equations, Z_k stands for mixing ratio, CN_k, D_k, μ_k, and HV_k indicate known values like cetane number, density, viscosity, and heating value of pure fuel, and CN_b, D_b, μ_b, and HV_b indicate the equivalent estimated properties of the fuel blends.

3.2 Engine Specifications

For experimental analysis, a single cylinder, four stroke, direct injected (DI) diesel engine based on a Cummins N series production engine used by Singh et al. is chosen to validate the numerical software [114]. The main specifications of the engine are listed in Table 3.2. The selected model Cummins N-14, DI diesel engine has 2.34 L displacement volume in a cylinder, 13.97 cm bore, 15.24 cm stroke length, 30.48 cm connecting rod and 8 holes contain in equally spaced with cylindrical cup (tip) piston bowl. The diesel fuel is directly injected into the cylinder using a common rail, pilot valve actuator fuel system at rail pressure of 1200 bar, at 152° Spray pattern angle. The eight equally spaced nozzle orifice diameter is around 0.196 mm. A quiescent charge is produced by the cylinder head with a swirl ratio approximately 0.5 near the TDC. In addition, the bowl depth and width are 9.78 cm and 1.55 cm respectively with simulated compression ratio (16:1) and Geometric compression ratio (11.2:1). The reason behind selecting this engine is the availability of all the required engine specifications.

Table 3.2. Engine Specifications.

Engine base type	Cummins N-14, DI Diesel
Number of cylinders	1
Number of intake valves	2
Number of exhaust valves	1*
Number of holes	8, equally spaced
Bore × Stroke, cm	13.97×15.24
Displacement, L	2.34
Connecting rod Length, cm	30.48
Bowl width, depth, cm	9.78, 1.55
Simulated compression ratio	16:1
Geometric compression ratio	11.2:1
Swirl ratio	0.5
Combustion chamber	Quiescent, direct injection
Cup(tip) type	Mini sac
Fuel injector type	Common rail, pilot valve actuated
Nozzle orifice L/D	5
Nozzle orifice diameter, mm	0.196
Rail pressure, bar	1200 or 1600
Spray pattern included angle	152°

3.3 Computational Models

The investigation of the current study is carried on a numerical tool named Diesel-RK. The software uses a quasi-dimensional multizone model of combustion to investigate the attributes of the CI engine for the alternative fuels. Temperature, pressure, and other necessary properties are assessed for time or CA. The software uses thermodynamic models, which are founded on the first law of thermodynamics, to examine the performance attributes of engines. Heat transfer and engine frictions are measured on the basis of semi-empirical equations. The various simulation models utilized here are provided in Table 3.3, while the governing equations are expressed in Table 3.4. The simulation models are selected on the basis of previous literature.

Table 3.3. Simulation models for different engine parameters.

SL. No.	Parameters	Simulation Models	Ref.
1	Heat Transfer	Woshchni's formula	[115]
2	Combustion	Multizone model	[116]
3	Ignition Delay	Tolstov's mechanism	[117]
4	NOx	Zeldovich mechanism	[118]
5	PM	Alkidas mechanism	[119]
6	Soot	Razleytsev mechanism	[120]
7	Smoke	Bosch and Hartridge	[121]

Table 3.4. List of governing equations used in Diesel-RK.

SL. No.	**Equation name**	**Main equation**	**Nomenclature**
1	Mass balance	$\frac{dm}{dt} = \sum_i \dot{m}_i$	$\dot{m}_i$ = mass flow rate of the i^{th} species in kg/sec.
2	Species balance	$Z_i = \frac{m_i}{m}$	m = overall mass contained within the control cylinder
3	Species equations	$\frac{d(mZ_i)}{dt} = \sum_j m_j Z_i^j + \dot{s}_{gen}$	$\dot{s}_{gen}$ = net generation of the k^{th} species in kg/s

4	k[th] species net generation	$\dot{s}_{gen} = \Omega_k W_m v$	Ω_k = molar rate (mol/sec), v = specific volume (kg/m^3) and W_m = weight (kg/mol)
5	Species balance equations	$\dot{Z}_i = \sum_j \left(\frac{\dot{m}_j}{m}\right)\left(Y_i^j - Y_i^{cyl}\right) + \frac{\Omega_i W_m}{D}$	D = density (kg/m^3)
6	Energy balance	$\frac{d(mu)}{dt} = -p\frac{dv}{dt} + \frac{dQ_{ht}}{dt} + \sum_j \dot{m}_j h_j$	$\frac{d(mu)}{dt}$ = internal energy, $p\frac{dv}{dt}$ = displacement work, $\frac{dQ_{ht}}{dt}$ = heat transfer and $\sum_j \dot{m}_j h_j$ = enthalpy flux
7	Brake specific fuel consumption	$BSFC = \frac{\dot{m}_f}{\mathrm{BP}}$	$\dot{m}_f$ = mass flow rate (kg/s) and BP = brake power (kW)
8	Frictional mean effective pressure (MEP$_f$)	$MEP_f = \alpha + \beta CP_{max} + \gamma S_v$	α, β, γ = coefficients, CP_{max} = peak cylinder pressure (bar) and S_v = mean piston velocity (m/s)
9	Heat released in ignition delay period	$\tau = 3.8 \times 10^{-6}(1 - 1.6 \times 10^{-4}.n)\sqrt{\frac{T}{P}} exp\,(\frac{E_a}{8.312T} - \frac{70}{CN + 25})$	P = pressure, (bar), T = temperature (K), E_a = activation energy, τ = time (sec) CN = cetane number and n = engine speed (rpm)
10	Heat released in premixed combustion	$\frac{dx}{d\tau} = \phi_0(B_0\frac{m_f}{v_i}(\sigma_{ud} - x_0)(0.1\sigma_{ud} + x_0)) + \phi_1\frac{d\sigma_u}{d\tau}$	$\frac{dx}{d\tau}$ = HRR (J/sec), m_f = fuel mass per cycle, x_0 = fraction of burnt fuel during ID, σ_u and σ_{ud} = fuel fractions evaporated at ID, ϕ_0, ϕ_1, ϕ_2, and ϕ_3= crank angle, B_0, B_1, B_2, and B_3 = empirical constants
11	Heat released in controlled combustion	$\frac{dx}{d\tau} = \phi_1\frac{d\sigma_u}{d\tau} + \phi_2 B_2\frac{m_f}{v_c}(\sigma_u - x)(\alpha - x)$	x = fraction of fuel burnt, α = air-fuel ratio
12	Heat released in late combustion	$\frac{dx}{d\tau} = \phi_3 B_3 K_T(1 - x)(\xi_b\alpha - x)$	K_T = evaporation constant, ξ_b = air efficiency
13	Zeldovich mechanism	$O_2 \rightleftharpoons 2O$ $N_2 + O \rightleftharpoons NO + N$ $N + O_2 \rightleftharpoons NO + O$	

14	NO concentration during the combustion	$\frac{d[A]}{dt} = \frac{2.333 \times Pe^{-\frac{38020}{T_b}}[N_2]_e[O]_e\left\{1-\left(\frac{[NO]}{[NO]_e}\right)^2\right\}}{NRT_b\left(1+\frac{2365}{T_b}.e^{\frac{2365}{T_b}}.\frac{[NO]}{[O_2]_e}\right)}$	$\frac{d[A]}{dt}$ = volumetric concentration of NO, N = angular velocity (rpm), R = constants, T_b = temperature
15	Soot formation	$\left(\frac{d[A]}{dt}\right)_K = 0.004\frac{q_c}{V}\frac{dx}{dt}$	V = volume (cc), $\frac{dx}{dt}$ = HRR in J/deg, q_c = cycle fuel mass (kg)
16	$Summary\ of\ emission$	$Summary\ of\ emission, SOE = C_{PM}\left(\frac{PM}{J}\right) + C_{NO}\left(\frac{NO_X}{L}\right)$	C_{PM} and C_{NO} = constants using of J = 0.15 and L = 7
17	$Smoke\ Number$	$Bosch\ Smoke\ Number, [PM] = 565Y_{pm}\left(ln\frac{10}{10-BN}\right)^C$	C = constant of 1.206, PM= Particulate matter, Y_{pm} = constant and BN = Bosch Number
18	$Hartridge\ Smoke\ Level$	$Hartridge\ Smoke\ Level = C[1-0.954e^{(-2.4226[C])}]$	

3.4 Governing Equations

Thermodynamic models are based on the first law of thermodynamics and are used to analyze the performance characteristics of engines in Diesel-RK software. Pressure, temperature, and other required properties are evaluated for crank angle (CA) or time. Engine friction and heat transfer are taken into account using semi-empirical correlations derived from experimental results. The combustion process inside the engine is simulated using a quasi-dimensional multi-zone model. The model takes into account the following conservation equations, as described by Fiveland and Assanis [116].

3.4.1 Conservation of Mass

The net mass flux within the system boundaries is the mass change rate inside any open system, and it can be stated mathematically as Eq. (3.5),

$$\frac{dm}{dt} = \sum_{k} \dot{m}_k \tag{3.5}$$

where $\dot{m}_k$ is the mass flow rate of the kth species in kg/sec.

3.4.2 *Conservation of Species*

The species conservation formula, which considers evaluating and destroying every species within a combustion chamber based on mass fraction, is defined as Eq. (3.6).

$$Y_k = \frac{m_k}{m} \tag{3.6}$$

where m_k represents the mass of the kth species and m represents the overall mass contained within the control cylinder.

The species equations, written as equation (3.7) are derived from their multidimensional counterparts by ignoring species diffusion term and is consistent with the zero-dimensional assumption and.

$$\frac{d(mY_k)}{dt} = \sum_{j} m_j Y_k^j + \dot{s}_{gen} \tag{3.7}$$

where $\dot{s}_{gen}$ states the net generation of the ith species in kg/s [116]. Net generation of the ith species is given by equation (3.8).

$$\dot{s}_{gen} = \Omega_i W_m v \tag{3.8}$$

where Ω_i, v, and W_m denote the rate of molar in mol/sec, specific volume in kg/m^3, and weight in kg/mol.

The equations have been created on a mass basis to follow the evolution of species in the combustion chamber. The combination of equation (3.7) and (3.8), and the continuity equation finally gives a species conservation equation that can be rewritten as equation (3.9) [116].

$$\dot{Y}_k = \sum_j \left(\frac{\dot{m}_j}{m}\right)\left(Y_k^j - Y_k^{cyl}\right) + \frac{\Omega_k W_m}{\rho} \tag{3.9}$$

3.4.3 Conservation of Energy

The energy equations must be evaluated to establish the rate of change of energy inside the system, as shown in equation (3.10), where, $\frac{d(mu)}{dt}$, $p\frac{dv}{dt}$, $\frac{dQ_{ht}}{dt}$ and $\sum_j \dot{m}_j h_j$ state the internal energy, displacement work, heat transfer, and enthalpy flux respectively. The widespread equation of energy for an open thermodynamic system can be expressed in the ways of Fiveland and Assanis [116].

$$\frac{d(mu)}{dt} = -p\frac{dv}{dt} + \frac{dQ_{ht}}{dt} + \sum_j \dot{m}_j h_j \tag{3.10}$$

Some presumptions are also required to solve the equations mentioned above. The energy conservation formula is given for the cylinder volume from when the inlet valve closes to when the exhaust valve opens. Pressure is taken to be uniform inside the cylinder throughout both the compression and expansion phases, with fixed unburned and burned gas zones in chemical equilibrium. Burned and unburned zones are believed to be divided by an infinitely thin flame front during flame propagation, with no heat exchange between the two regions. All gases are deemed perfect. Due to the high temperatures generated during engine combustion, the high pressures cause a counterbalance to a deviation from the ideal gas law [122].

3.4.4 Engine Friction Model and Specific Fuel Consumption

McAulay et al. recommended that overall loss inside the single-cylinder CI engine varied linearly with PP and piston speed [123]. Chen and Flynn suggested a similar correlation for modeling engine friction [60]. Diesel-RK software has the option to use different friction models. Chen and Flynn provide a simplified formula that considers most of the losses regarding friction mean effective pressure (FMEP). Associated losses are necessary to evaluate FMEP in equation (3.11) and specific fuel consumption in equation (3.12) [123] where constants α, β, γ depend upon engine geometry. P_{max} and S_v are the peak cylinder pressure (PCP) in bar and mean piston velocity in m/s, respectively. Datta and Mandol used the values of α, β, and γ as 0.1 bar, 0.005, and 0.142 bar-s/m respectively [122].

$$FMEP = \alpha + \beta P_{max} + \gamma S_v \tag{3.11}$$

Once the FMEP has been determined, the BMEP can be obtained using the indicator diagram's IMEP. The displacement volume of the cylinder used in the simulation is then used to assess brake power (P_b) [122]. Mathematically, BSFC can be written as equation (3.12) where $\dot{m}_f$ is the mass flow rate (kg/s) and P_b is the brake power (kW).

$$BSFC = \frac{\dot{m}_f}{P_b} \tag{3.12}$$

3.4.5 Heat Release Model

The Diesel-RK modeling tool employs a multi-zone combustion model in-cylinder HRR, separated into four phases: ignition delay period, premixed combustion, controlled combustion, and burning phases, as shown in equations (3.13) to (3.14) [93,117,124]. Their physical and chemical features differ, but each affect the HRR. When calculating the heat release in the cycle, the combustion process of the fuel is split, having unique physical and chemical features that limit the burning speed [125]. These are as follows:

a) Ignition Delay Period

The first phase of heat release is the IDP, which is estimated using a modified Tolstov's equation [115,117,119,126,127]. The IDP is based on equation (3.13) because it divides the start of combustion (SOC) and the beginning of injection inside the engine's cylinder. In general, ID can be a complex process involving a combination of temperature, pressure, air-fuel ratio, and fuel characteristics. The compression caused by piston motion causes significant changes in CP and temperature during the IDP [128].

$$\tau = 3.8 \times 10^{-6}(1 - 1.6 \times 10^{-4}.n)\sqrt{\frac{T}{P}}exp\,(\frac{E_a}{8.312T} - \frac{70}{CN + 25}) \tag{3.13}$$

Where, P, T, E_a, τ, CN, and n denote the pressure, temperature, activation energy of fuel, time in seconds, cetane number, and engine speed in rpm respectively.

b) Premixed Combustion Period (Changed Formation)

Throughout the premixed combustion phase, the HRR is given by Eq. (3.14) where x_0 is the fraction of burnt fuel during ID, σ_u, σ_{ud} are the fuel fractions evaporated at ID, $\frac{dx}{d\tau}$ states HRR in J/sec, A_0, A_1, A_2, and A_3 is empirical constants. x is a fraction of fuel burnt, ϕ_0, ϕ_1, ϕ_2, and ϕ_3 are the crank angle, ξ_b is air efficiency, m_f is the fuel mass per cycle, and α is air-fuel ratio.

$$\frac{dx}{d\tau} = \phi_0(A_0\frac{m_f}{v_i}(\sigma_{ud} - x_0)(0.1\sigma_{ud} + x_0)) + \phi_1\frac{d\sigma_u}{d\tau} \tag{3.14}$$

c) Controlled Combustion Period (Changed Formation)

During the mixing-controlled combustion period, the HRR can be obtained as equation (3.15).

$$\frac{dx}{d\tau} = \phi_1\frac{d\sigma_u}{d\tau} + \phi_2 A_2\frac{m_f}{v_c}(\sigma_u - x)(\alpha - x) \tag{3.15}$$

d) Burning Period

After the fuel injection, at the late combustion phase, the HRR is given by equation (3.16), where K_T is the evaporation constant.

$$\frac{dx}{d\tau} = \phi_3 A_3 K_T(1 - x)(\xi_b\alpha - x) \tag{3.16}$$

3.4.6 NO_X Formation Modelling

This analysis takes into account the thermal NO exploitation chain Zeldovich mechanism. It comprises a step-by-step computation of the equilibrium composition of combustion products in the burned gas zone for the eighteen species [93,129]. The NO concentration in the combustion product is determined using the Zeldovich mechanism given in Eq. (3.20).

NO and NO_2 are usually grouped as NO_x emissions. Of all the oxides of nitrogen, NO is the most influential in diesel engine emissions [118]. Therefore, in this study, only the NO formation is considered for use in the Zeldovich mechanism. The designed steps are shown below [125]:

i. Step-by-step determination of the equilibrium composition of the products of combustion for eighteen species in the zone of burnt gas
ii. Applying the chain Zeldovich mechanism, the kinetic calculation of thermal nitrogen oxide formation is made.

$$O_2 \rightleftharpoons 2O \tag{3.17}$$

$$N_2 + O \rightleftharpoons NO + N \tag{3.18}$$

$$N + O_2 \rightleftharpoons NO + O \tag{3.19}$$

The rates of the reactions depend on the concentration of atomic oxygen. The volume concentration of NO in combustion products formed in a current calculation step is obtained from the following equation.

$$\frac{d[C]}{dt} = \frac{2.333 \times Pe^{-\frac{38020}{T_b}}[N_2]_e[O]_e\left\{1 - \left(\frac{[NO]}{[NO]_e}\right)^2\right\}}{NRT_b\left(1 + \frac{2365}{T_b}.e^{\frac{2365}{T_b}}.\frac{[NO]}{[O_2]_e}\right)} \tag{3.20}$$

Formation of $\frac{d[C]}{dt}$ strongly depends on temperature, N is the angular velocity in revolution per minute. The equilibrium concentrations of the eighteen species are calculated at every time step. The overall system of equations includes the fourteen equilibrium equations, three material balance equations, and Dalton's equation of partial pressure.

3.4.7 Formation of Soot and Particulate Matter

The formation of soot is a significant problem in diesel engines, and it is formed due to incomplete combustion of hydrocarbon fuels [130]. Soot is a fine dispersion of black carbon particles in a vapor carrier. Soot is formed mainly due to the chain destructive transformation of molecules of fuel diffusing from the surface of drops to the front of a flame and high-temperature thermal polymerization and dehydrogenization of a vapor-liquid core of evaporating drops. Soot particles form, grow, and oxidize due to chemical reactions during combustion [125]. Exhaust soot concentration related to normal conditions are given in Eq. (3.22) as follows:

$$[C]_H = \int_{\theta_B}^{480} \frac{1}{6n} . \frac{d[C]}{dt} . \left(\frac{0.1}{p}\right)^{\gamma} d\theta \tag{3.22}$$

The level of soot formation can be expressed as Hartridge smoke level or Bosch smoke number (BSN) or Factor of absolute light absorption coefficient. Hartridge smoke level is calculated using equation (3.23) as follows:

$$Hartridge\ Smoke\ Level = C[1 - 0.954e^{(-2.4226[C])}] \tag{3.23}$$

The soot formation rate in the burning zone is calculated using the following equation (3.24) as mentioned by Alkidas [119].

$$\left(\frac{d[C]}{dt}\right)_K = 0.004 \frac{q_c}{V} \frac{dx}{dt} \tag{3.24}$$

where V, $\frac{dx}{dt}$, and q_c are volume in cc, HRR in J/deg, and cycle fuel mass in kg, respectively.

Alkidas [119] also presented a correlation for PM emission as a function of BSN and is given by equation (3.25).

$$Bosch\ Smoke\ Number, [PM] = 565Z_{pm}\left(ln\frac{10}{10-BN}\right)^{C} \tag{3.25}$$

where C is a constant of 1.206, Z_{pm} is a constant, and BN is Bosch Number.

Another important equation is the air pollutant emissions, which is the summary of PM and NOx emissions shown in equation (3.26) where, C_{PM} and C_{NO} are constants, using of J = 0.15 and L = 7.

$$Summary\ of\ emission, SE = C_{PM}\left(\frac{PM}{J}\right) + C_{NO}\left(\frac{NO_X}{L}\right) \tag{3.26}$$

3.5 Computational Model Setup

The Diesel R-K software has been used to conduct this numerical investigation to examine the effect of renewable BTL diesel and blends of microalgae biodiesel/BTL diesel on conventional diesel engine. Before starting the simulations for specific operating conditions, the engine model should be set and fuel properties are to be defined. The model of test engine is set in the numerical software according to the engine specifications mentioned in Table 3. 2. Then, the properties of the neat fuels and blended fuels derived from previous literature and mathematical equations are utilized as input data to prepare the fuel library. The fuel injector is equipped with eight equally spaced holes and the orifice diameter of the nozzle is considered 0.192 mm. Nozzle discharge co-efficient is 0.7. After incorporating the fuel properties, the simulations were performed for the six test fuels individually. For each test fuel, engine simulations were executed for five different ITs of 1, 4, 7, 10, and 13° bTDC at swirl ratio of 0.5. During each test run of the simulation, the load and injection pressure are maintained constant at 3.82 bar BMEP and 1200 bar respectively. Cycle fuel mass of different fuel blends is adjusted in such a way that the load remains fixed. Injection pressure is kept constant by varying the injection duration. The engine parameters like sauter mean diameter (SMD), combustion duration (CD), IDP, CP, HRR, heat release fraction (HRF), combustion zone temperature (CZT), BSFC, BTE and EGT are determined for each test fuels.

Additionally, among emission parameters the amount of CO_2, NO_x, PM, and smoke in exhaust are measured. Table 3.5 includes the input parameters required in the study to conduct simulation.

Table 3.5. Input parameters of simulation.

Sl. No.	**Parameter**	**Value**	**Unit**
1	Bore size	13.97	cm
2	Stroke size	15.24	cm
3	Connecting rod length	30.48	cm
4	Compression ratio	16	-
5	Load	~3.82	bar BMEP
6	Speed	1200	rpm
7	Spray pattern included angle	152	degree
8	Nozzle orifice diameter	0.196	mm
9	Number of injector holes	8, equally spaced	
10	Fuel injection pressure	~1200	bar
11	Intake temperature	333	K
12	Intake pressure	1.41	bar
13	Swirl ratio	0.5	
14	Fuel injection timing	1, 4, 7, 10, 13	° CA bTDC
15	Intake valve open	703	º CA
16	Intake valve close	195	º CA
17	Exhaust valve open	485	º CA
18	Exhaust valve close	27	º CA
19	Piston bowl design	cylindrical	
20	Cylinder linear temperature	420	K
21	Cylinder head temperature	470	Degree
22	Coolant temperature	368	K
23	Piston wall temperature	500	K

3.6 Numerical Tool Validation 1

The numerical software is validated with the single cylinder Cummins N-14 diesel engine using the findings of the experiment conducted by Singh et al. [114]. The numerical findings were validated for neat diesel. The technical specifications of the engine are mentioned in Table 4. The values of Peak CP, PHRR of premixed combustion phase, IDP, and NO_x emission for pure diesel at IT of 7 º bTDC and swirl ratio 0.5 obtained by Singh. et al. experimentally are considered for validation. Simulation is performed in Diesel-RK software for neat diesel keeping the operating conditions same and the values of Peak CP, PHRR, IDP, and NO_x emission are collected. The experimental values of Peak CP, PHRR of premixed combustion phase, IDP, and NO_x emission observed by Singh et al. are 78.54 bar, 235.16 J/deg, 3.994 º CA, and 582 ppm respectively, while the values of these parameters obtained by simulation are 80.7 bar, 237.2 J/deg, 4.027 º CA, and 592 ppm respectively. The values of Peak CP, PHRR, IDP, and NO_x obtained numerically differ by only 2.75%, 0.87%, 0.83%, and 1.72% respectively from experimental values as presented in Table 3.6. Fig. 3.1(a-d) shows the graphical representations of the experimental and numerical findings simultaneously. There is a good agreement of the numerical results with the experimental ones. For well-calibrated models, the permissible error margin between experimental and numerical findings is usually between 5 to 10% [4,131,132].

Table 3.6. Comparison of experimental and numerical results.

Parameters	Experimental	Numerical	Deviation (%)
Peak CP (bar)	78.54	80.7	2.75
PHRR (J/deg)	235.16	237.2	0.87
IDP (° CA)	3.994	4.027	0.83
NO_x (ppm)	582	592	1.72

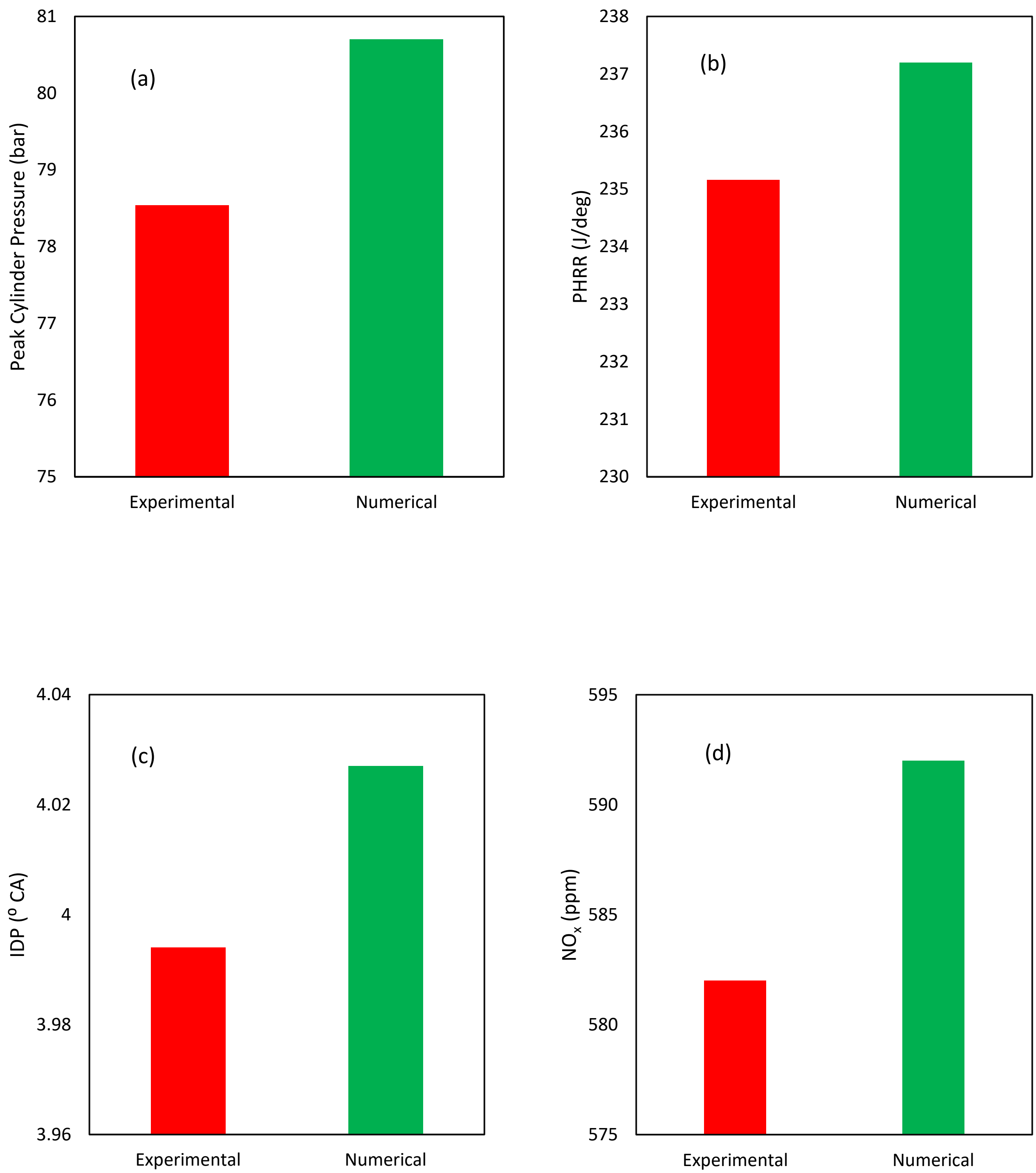

Figure 3.1. Validation of the numerical tool.

3.7 Numerical Tool Validation 2

An experimented is conducted for neat diesel in the diesel engine setup existing in the 'Heat Engine Laboratory' of Department of Mechanical Engineering, CUET to validate the numerical findings again. A naturally aspirated CI engine (Hatz 1 B30-2 Model) with a single-cylinder, DI, four-stroke has been used as a test engine for the experimental analysis to validate the numerical tool for second time. Table 3.7 and Fig. 3.2 demonstrate the specifications and schematic arrangement of the test engine setup, respectively. The experimental validation conducted for neat diesel.

Model TFCP 132SB-2 asynchronous motor with frequency converter serves as dynamometers for the test engine. Elastic claw couplings transfer power from the test engine to the dynamometric brake. In addition, a test stand (Model GUNT CT 110, 7.5 kW) from G.U.N.T. Gerätebau is used to investigate and experiment on test engines up to 7.5 kW power. Air consumption is measured by a 20.6 mm orifice meter at the air box, and fuel consumption is measured by a flow meter sensor (Huba control type 680-out signal 0-10 Volts direct current (VDC)) at the bottom with a measuring tube. The test stand shows engine torque and speed. A proximity switch (WATCHENDORFF proximity sensor, type PNP-N. O, Sn 4 mm, 10-30 VDC, and 200 mA) monitors the speed at the brake mechanism connection. The FLINTEC ZLB-200Kg-C3, electric force sensor, measures torque-proportional force, while electronics calculate engine torque using the lever arm near the sensor. The three temperatures, ambient, fuel, and exhaust gas, are monitored by the K-type thermocouples, calibrated and positioned at the intake port, fuel line, and exhaust port of the test setup. Finally, a PC data acquisition system (Model USB-AD16f) collects, stores, and analyzes speed, torque, brake power (BP), fuel consumption, BSFC, BTE, air/fuel ratio, fuel temperature, and EGT and displays it on a PC with LabVIEW software (GUNT software).

The test engine is warmed with pure diesel for 10 minutes before the experiment to ensure steady-state analysis. Thus, the EGT is tested until it approaches a constant value to maintain that condition [133]. Each test is repeated ten times to increase the measurement's reliability. The mean values of the results are taken with great concern for accuracy.

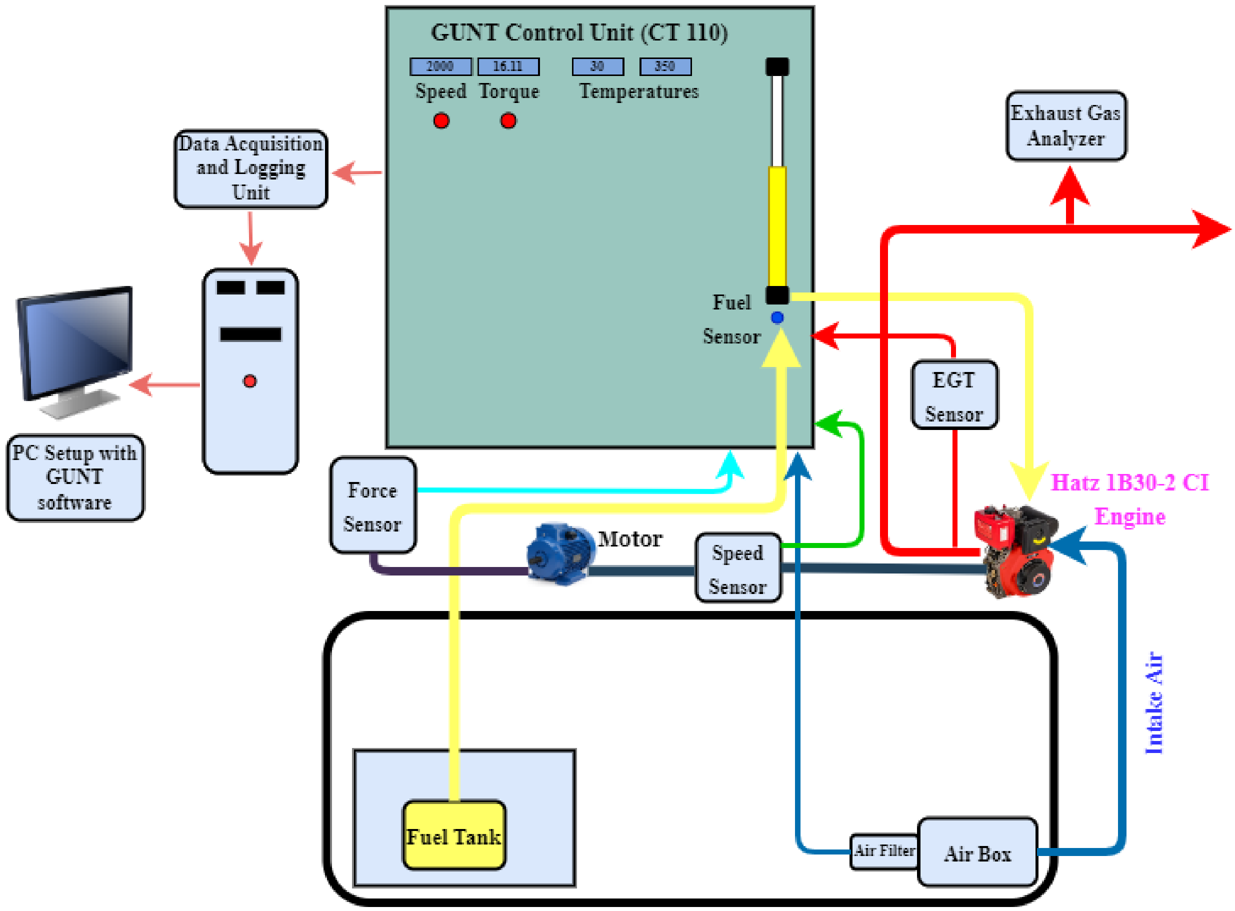

Figure 3.2. Schematic arrangement of the engine setup.

Table 3.7. Engine Specifications.

Item	**Specification**
Manufacturer	Motorenfabrik Hatz
Model	1 B30-2
Engine type	Air-cooled, 4-stroke, DI, CI engine
Number of Cylinder	1
Aspiration	Natural
Displacement	347 cm^3
Bore	80 mm
Stroke	69 mm

Rod length	114.5 mm
Crank radius	34.5 mm
Power output	5.4 kW @ 3600 rpm
Compression ratio	21.5:1
Oil capacity	1.1 L
Stop solenoid	12 V
Noise level	95 dB (A)

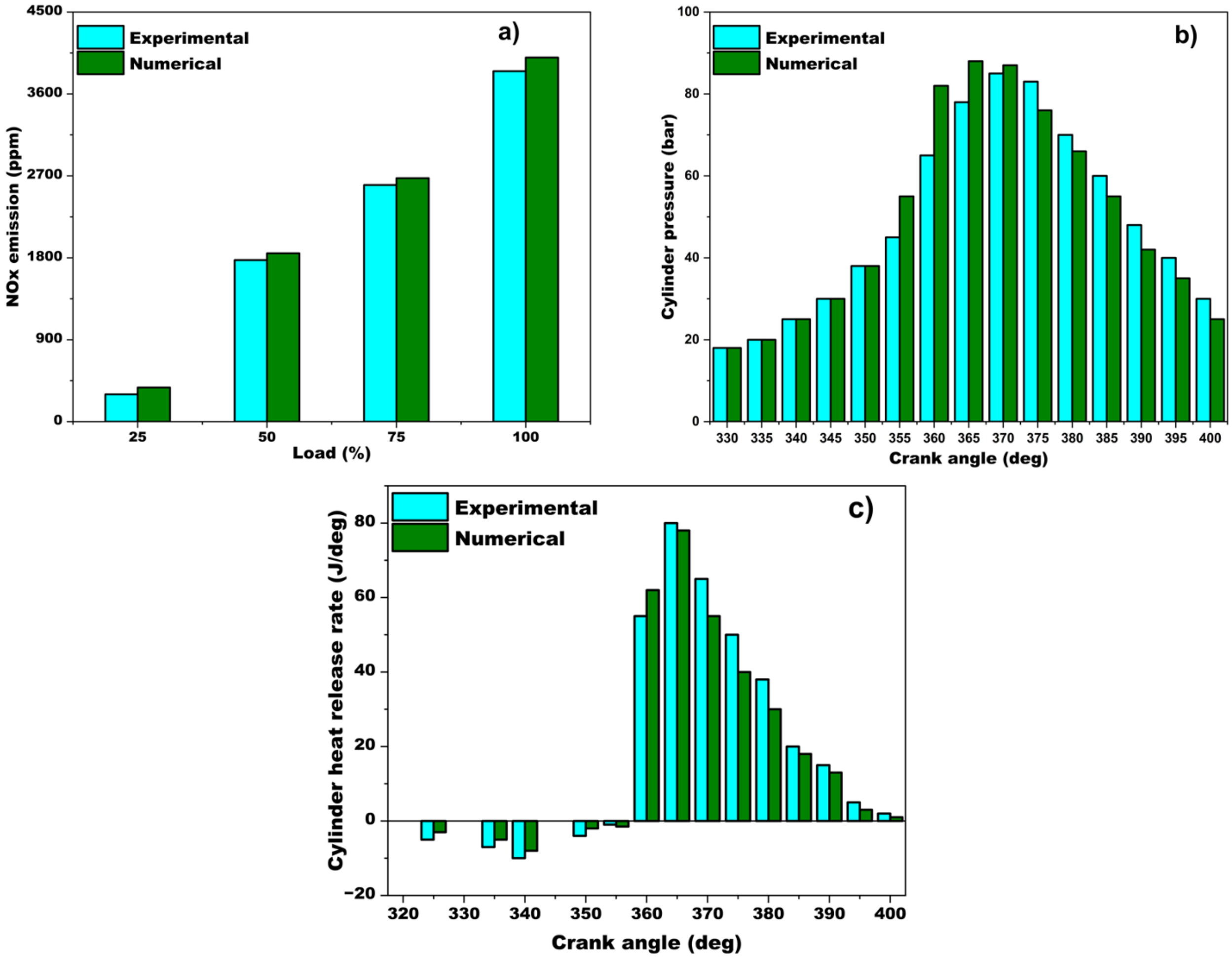

Figure 3.3. Validation of the numerical tool.

Table 3.8. Validation of the numerical tool at full throttle condition.

Parameter	Experimental	Numerical	Error Deviation (%)
BSFC (g/kWhr)	255.7	248.30	2.9
BTE (%)	33.74	34.114	1.1
EGT (K)	553	571.34	3.2

The diesel-RK tool validation is performed for performance characteristics using neat diesel fuel for 2000 rpm at full throttle conditions to ensure the reliability of the numerical tool. Engine parameters such as BTE, BSFC, and EGT are calculated for tool validation, as depicted in Table 3.8. Under full-throttle conditions, the experimental and numerical values of BSFC are determined to be 255.7 and 248.30 g/kWhr, respectively, resulting in a difference of about 2.9%. Similarly, the BTE and EGT results differ only by approximately 1.1% and 3.2%, respectively, which is less than 5%, indicating the simulation's reliability.

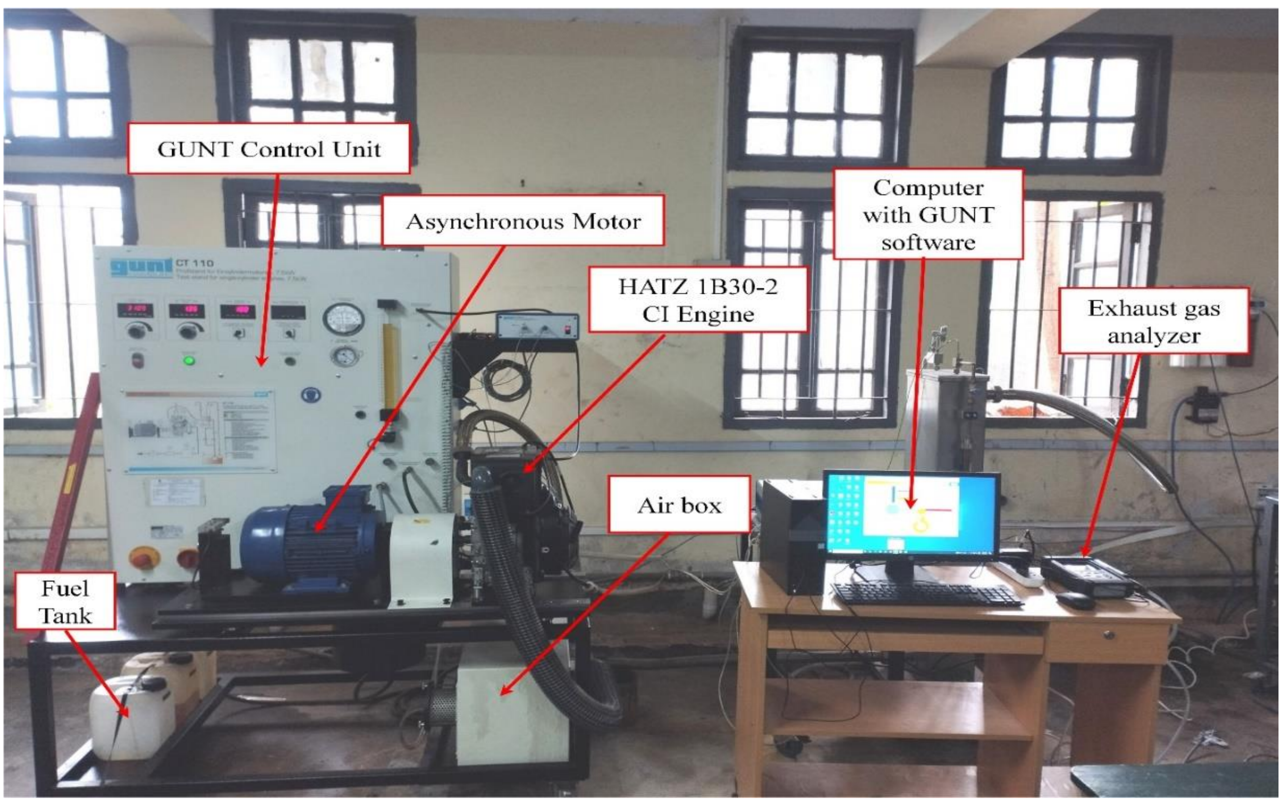

Figure 3.4. Photographic view of engine setup.

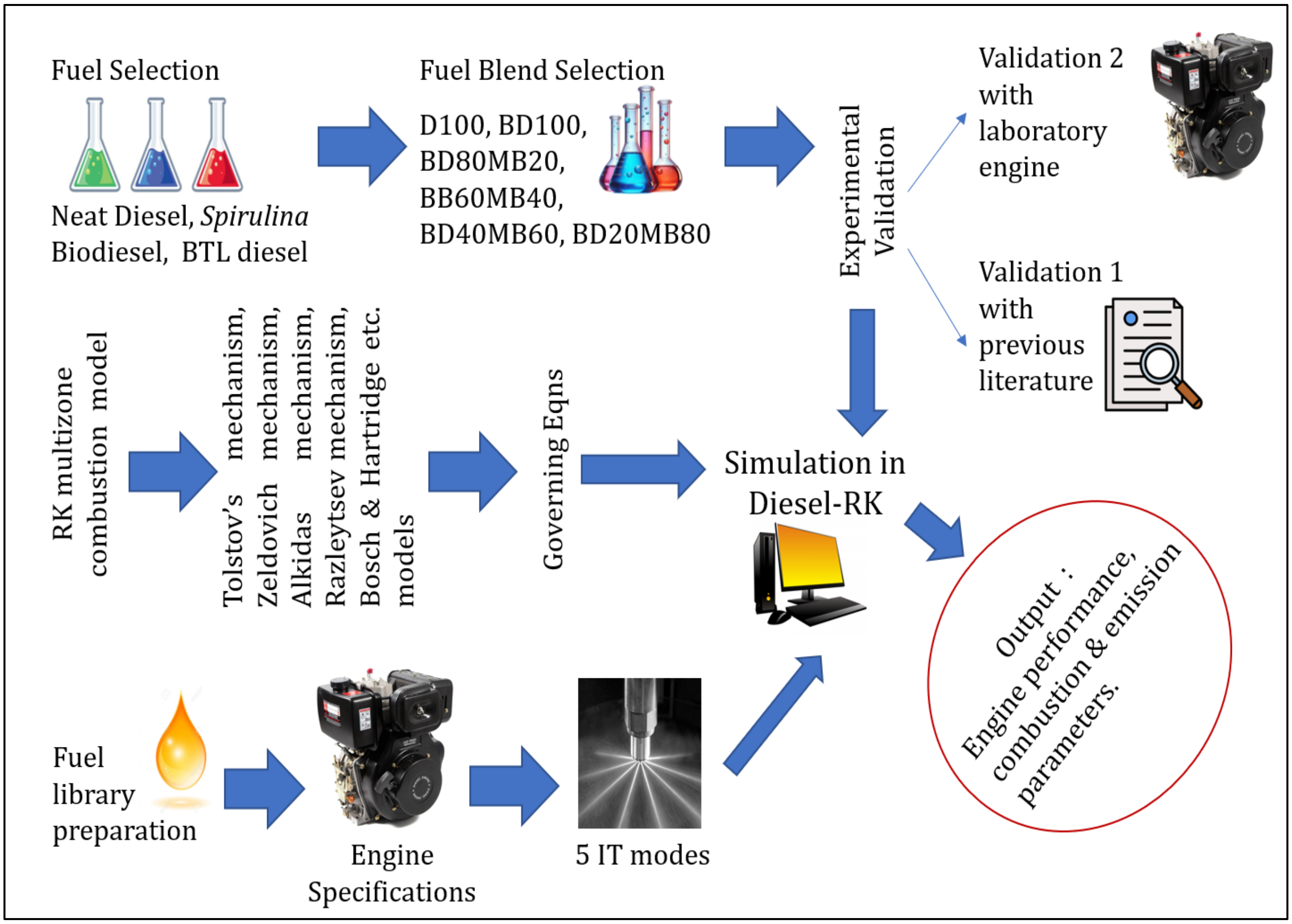

Figure 3.5. Flow diagram of methodology.

Chapter 4
Data Collection and Analysis

4.1 Introduction

The combustion, performance, and emissions attributes of the CI engine are measured numerically in the Diesel-RK software. Among combustion parameters the sauter mean diameter, the ignition delay period, the heat release rate, the heat release fraction, the cylinder pressure, the combustion duration, and the combustion zone temperature are measured. Various engine performance parameters including the brake specific fuel consumption, the brake thermal efficiency, and the exhaust gas temperature are determined. Finally, the emissions of CO_2, NO_x, smoke and particulate matters are calculated and analyzed.

4.2 Combustion Parameters

In the combustion stroke of diesel engines, the chemical energy of the fuel is turned into mechanical energy. The performance and emission parameters of a diesel engine is closely dominated by the combustion of fuel. Proper combustion attributes of fuel in a CI engine leads to better engine performance and improved emissions of the harmful gases. Combustion of fuel is a complex phenomenon which is generally influenced by fuel's characteristics, engine hardware, IT, SR, CR, etc. SMD, IDP, HRR, HRF, CP, are CZT are calculated numerically to analyze the combustion characteristics of the CI engine designed for the current investigation. All these parameters are measured for the six different fuel samples (neat diesel, neat BTL diesel and four blends of BTL diesel-microalgae biodiesel) considered in the study at five different ITs (1, 4, 7, 10, and 13° bTDC). After completing the simulation for a specific operating condition, the resulted combustion parameters are stored in 'Table of engine parameters' section of Diesel-RK software as shown in fig. 4.1. The measured values of SMD, IDP, and CD engine parameters can be collected from that section. The graphical representations of the CP, HRR, and HRF with respect to CA are available in 'Fuel injection and heat release' section. The values of each point of the graphs can be imported to Microsoft Excel afterwards. The measured values of SMD, IDP, and CD of the fuel samples at five different ITs are presented in the Table 4.1, 4.2, and 4.3 respectively.

```
---------------------------- COMBUSTION ----------------------------
 3.9236     - A/F_eq   - Air Fiel Equival. Ratio (Lambda) in the Cylinder
0.25487     - F/A_eq   - Fuel Air Equivalence Ratio in the Cylinder
 80.446     - p_max    - Maximum Cylinder Pressure, bar
 1527.0     - T_max    - Maximum Cylinder Temperature, K
 9.0000     - CA_p.max - Angle of Max. Cylinder Pressure, deg. A.TDC
 15.000     - CA_t.max - Angle of Max. Cylinder Temperature, deg. A.TDC
 1.6283     - dp/dTheta- Max. Rate of Pressure Rise, bar/deg.
0.12078     - Ring_Intn- Ringing / Knock Intensity, MW/m2
 12545.     - F_max    - Max. Gas Force acting on the piston, kg
System:    Common Rail
 1201.5     - p_inj.max- Max. Sac Injection Pres. (before nozzles), bar
 655.19     - p_inj.avr- Mean Sac Press. for Total Fuel Portion, bar
 13.231     - d_32     - Sauter Mean Diameter of Drops, microns
 4.0000     - SOI      - Start Of Injection or Ignition Timing, deg. B.TDC
 9.5450     - Phi_inj  - Duration of Injection, CA deg.
 1.8697     - Phi_ign  - Ignition Delay Period, deg.
            -   ...    - calculated by modified Tolstov method   :   1.9
 2.1303     - SOC      - Start of Combustion, deg. B.TDC
0.00307     - x_e.id   - Fuel Mass Fraction Evaporated during Ignit. Delay
 30.200     - Phi_z    - Combustion duration, deg.
                         Phi_z 5%=  1.6;  Phi_z 50%=  8.8;  Phi_z 95%= 20.2
0.89460     - Rs_tdc   - Swirl Ratio in the Combustion Chamber at TDC
0.50000     - Rs_ivc   - Swirl Ratio in the Cylinder at IVC
 5.4332     - W_swirl  - Max. Air Swirl Velocity, m/s  at cylinder R=   49
```

Figure 4.1. Values of calculated combustion parameters in Diesel-RK.

Table 4.1. Calculated values of SMD for different test fuels at various ITs.

Operating Conditions	**D100**	**BD100**	**BD80MB20**	**BD60MB40**	**BD40MB60**	**BD20MB80**
IT1	15.446	13.29	14.04	14.84	15.622	16.398
IT4	15.379	13.232	13.979	14.744	15.553	16.398
IT 7	15.409	13.257	14.006	14.73	15.581	16.425
IT10	15.535	13.37	14.121	14.897	15.715	16.565
IT13	15.771	13.559	14.319	15.07	15.894	16.756

Table 4.2. Calculated values of IDP for different test fuels at various ITs.

Operating Conditions	D100	BD100	BD80MB20	BD60MB40	BD40MB60	BD20MB80
IT1	4.5076	1.8858	2.1033	2.4027	2.7175	3.1462
IT4	4.4108	1.8691	2.0744	2.3603	2.7023	3.0941
IT 7	4.4824	1.8977	2.1068	2.3994	2.7512	3.2063
IT10	4.7799	2.0284	2.26118	2.5797	2.9096	3.406
IT13	5.2755	2.2339	2.4612	2.8147	3.2062	3.7296

Table 4.3. Calculated values of CD for different test fuels at various ITs.

Operating Conditions	D100	BD100	BD80MB20	BD60MB40	BD40MB60	BD20MB80
IT1	33	30	30.2	30.8	31.8	34
IT4	33.2	30.2	30.2	30.6	31.6	34
IT 7	33	30	30.4	30.8	31.8	34
IT10	33.6	30.6	30.8	31	32	34.6
IT13	33.8	31.2	31	31.6	32.6	35.2

4.3 Performance Parameters

Performance parameters of internal combustion engine indicate how well chemical energy of fuel is transformed into mechanical works. Better engine performance leads to higher amount of work available in crankshaft. Generally, a high-performance engine consumes less fuel and produces higher amount of power. Performance parameters are closely linked to combustion of engine. BSFC, BTE, and EGT are measured for analyzing the performance of the test engine. Similar to the combustion attributes the performance attributes are also available in 'Table of engine parameters' section in Diesel-RK software as per Fig. 4.2. The resulted values of BSFC, BTE, and EGT are shown in Table 4.4, Table 4.5, And Table 4.6. The performance parameters of each test fuels are determined for five different ITs.

```
 ---------------- PARAMETERS OF EFFICIENCY AND POWER ---------------
  1200.0     - RPM      - Engine Speed, rev/min
  8.9349     - P_eng    - Piston Engine Power, kW
  3.8186     - BMEP     - Brake Mean Effective Pressure, bar
  71.107     - Torque   - Brake Torque, N m
 0.05827     - m_f      - Mass of Fuel Supplied per cycle, g
 0.23479     - SFC      - Specific Fuel Consumption, kg/kWh
 0.31538     - SFC_ISO  - Specific Fuel Consumption in ISO, kg/kWh
 0.34394     - Eta_f    - Efficiency of piston engine
  5.4214     - IMEP     - Indicated Mean Effective Pressure, bar
 0.48830     - Eta_i    - Indicated Efficiency
  6.0800     - Sp       - Mean Piston Speed, m/s
  1.2276     - FMEP     - Friction Mean Effective Pressure, bar (Intern.Exp)
 0.75673     - Eta_m    - Mechanical Efficiency of Piston Engine
```

Figure 4.2. Values of Calculated performance parameters in Diesel-RK.

Table 4.4. Calculated values of BSFC for different test fuels at various ITs.

Operating Conditions	**D100**	**BD100**	**BD80MB20**	**BD60MB40**	**BD40MB60**	**BD20MB80**
IT 1	0.24696	0.23478	0.23959	0.24486	0.24977	0.25477
IT 4	0.2455	0.2348	0.23951	0.24429	0.24899	0.2536
IT 7	0.24591	0.23659	0.24125	0.24599	0.25037	0.25439
IT 10	0.24817	0.24006	0.24486	0.24902	0.25322	0.25706
IT 13	0.25163	0.24509	0.25168	0.25418	0.2581	0.26092

Table 4.5. Calculated values of BTE for different test fuels at various ITs.

Operating Conditions	D100	BD100	BD80MB20	BD60MB40	BD40MB60	BD20MB80
IT 1	33.916	34.395	34.312	34.159	34.051	33.929
IT 4	34.118	34.392	34.323	34.238	34.159	34.085
IT 7	34.061	34.132	34.076	34.002	33.969	33.978
IT 10	33.751	33.639	33.574	33.588	33.587	33.626
IT 13	33.287	32.949	32.664	32.907	32.952	33.128

Table 4.6. Calculated values of EGT for different test fuels at various ITs.

Operating Conditions	D100	BD100	BD80MB20	BD60MB40	BD40MB60	BD20MB80
IT 1	554.51	550.34	550.55	550.86	551.36	555.08
IT 4	547.43	544.62	544.5	544.68	545.36	547.91
IT 7	542.25	539.72	540.83	540.78	540.82	543.11
IT 10	539.35	539.6	539.32	538.95	538.87	540.78
IT 13	538.24	540.29	536.4	539.48	539.42	540.59

4.4 Emission Parameters

During the combustion of fuel in IC engine several chemical gases such as CO, CO_2, NO_x, PM, Smoke, Unburned Hydrocarbons etc. are produced as byproducts besides generation of higher amount of enthalpy. These gases are released in the environment after combustion stroke. All these gaseous elements are harmful for the ecosystem and pollutes the air. Hence, the emissions of these gases should be minimum as possible. Combustion of fuel has significant impact on emissions. In the current study, the emissions of CO_2, NO_x, PM, and Smoke are measured numerically. The emission parameters are available in the 'Table of engine parameters' section under the heading 'ECOLOGICAL PARAMETERS' as shown in Fig. 4.3. The measured quantities of the emission of these gases are demonstrated in Table 4.7 to 4.10. Emissions of these gases for each test fuel are determined at various ITs.

```
------------------------ ECOLOGICAL PARAMETERS ----------------------
 4.5439     - Hartridge- Hartridge Smoke Level
0.49783     - Bosch    - Bosch Smoke Number
0.10860     - K,m-1    - Factor of Absolute Light Absorption, 1/m
0.18270     - PM       - Specific Particulate Matter emission, g/kWh
0.77813     - PM,g/kgf - Particulate Matter emission, g/kg_inj.fuel
 746.02     - CO2      - Specific Carbon dioxide emission, g/kWh
 851.02     - NOx.w,ppm- Fraction of wet NOx in exh. gas, ppm
 11.971     - NO       - Specif. NOx emiss. reduc. to NO, g/kWh (Zeldovich)
 1.9538     - SE       - Summary emission of PM and NOx
 0.0000     - SO2      - Specific SO2 emission, g/kWh
```

Figure 4.3. Calculated values of CO_2 emission for different test fuels at various ITs.

Table 4.7. Calculated values of CO_2 emission for different test fuels at various ITs.

Operating Conditions	**D100**	**BD100**	**BD80MB20**	**BD60MB40**	**BD40MB60**	**BD20MB80**
IT 1	792.03	746	746.49	747.79	747.38	746.62
IT 4	787.34	746.06	746.25	746.07	745.04	743.19
IT 7	788.64	751.75	751.67	751.26	749.19	745.53
IT 10	795.89	762.7	762.9	760.51	757.71	753.34
IT 13	806.98	778.75	784.16	776.26	772.32	764.66

Table 4.8. Calculated values of NO_x emission for different test fuels at various ITs.

Operating Conditions	**D100**	**BD100**	**BD80MB20**	**BD60MB40**	**BD40MB60**	**BD20MB80**
IT 1	409.89	699.69	777.07	825.58	824.12	986.69
IT 4	529.37	851.86	909.4	978.13	976.36	987.02
IT 7	670.55	1052.5	1098	1172.3	1163.7	1193.4

IT 10	804.13	1254.7	1326.1	1343.8	1352.3	1365.5
IT 13	1017.2	1492.7	1499.6	1523.1	1572.1	1500.6

Table 4.9. Calculated values of PM emission for different test fuels at various ITs.

Operating Conditions	**D100**	**BD100**	**BD80MB20**	**BD60MB40**	**BD40MB60**	**BD20MB80**
IT 1	0.27927	0.21763	0.21487	0.20613	0.17988	0.1317
IT 4	0.2226	0.18275	0.17865	0.17026	0.14692	0.09293
IT 7	0.18421	0.15778	0.15547	0.14911	0.12779	0.07268
IT 10	0.16235	0.14209	0.13958	0.1342	0.11615	0.0626
IT 13	0.14498	0.12967	0.12957	0.09953	0.05504	0.02194

Table 4.10. Calculated values of smoke emission for different test fuels at various ITs.

Operating Conditions	**D100**	**BD100**	**BD80MB20**	**BD60MB40**	**BD40MB60**	**BD20MB80**
IT 1	0.69626	0.57303	0.56686	0.54769	0.4901	0.38114
IT 4	0.58163	0.49799	0.48848	0.46972	0.41666	0.28698
IT 7	0.49935	0.4415	0.43668	0.42181	0.37175	0.23475
IT 10	0.45073	0.40622	0.39999	0.38714	0.34398	0.20775
IT 13	0.41107	0.37677	0.36828	0.30336	0.1867	0.08764

Chapter 5

Results and Discussion

5.1 Spray and Combustion Characteristics

5.1.1 Fuel Spray Visualization

Fig. 5.1 illustrates the spray pattern of the test fuels injected into the engine cylinder at IT of 4° CA bTDC. The total fuel spray consists of three key regions: the dilute outer sleeve in free spray, the core of the free spray, and the fractions deposited on the piston wall, cylinder wall, and cylinder liner surfaces. A higher proportion of fuel in the dilute outer sleeve enhances the best evaporation conditions, as it significantly improves air entrainment, facilitating efficient combustion. Conversely, fuel in the spray core is denser, leading to poorer evaporation conditions.

Fuel impingement on the piston wall generally supports better evaporation, as the high surface temperature aids in vaporizing fuel droplets. In contrast, fuel deposited on the cylinder head has a moderate influence on evaporation, while fuel sprayed onto the cylinder liner exhibits the least favorable conditions for evaporation. Therefore, minimizing fuel deposition on the cylinder liner is crucial. In this study, no fuel was observed to be deposited on either the cylinder head or liner for any of the tested fuels.

Among the fuels tested, neat BTL diesel exhibited a higher fraction of fuel in the dilute outer sleeve region while showing a lower fraction in both the spray core and on the piston wall compared to conventional diesel. For blends of microalgae biodiesel and BTL diesel, the fraction of fuel in the dilute outer sleeve decreased, whereas the fractions in the spray core and on the piston wall increased as the proportion of microalgae biodiesel in the blend increased. Such spray characteristics indicate that neat BTL diesel produces a spray pattern that promotes more efficient evaporation compared to both conventional diesel and biodiesel blends, potentially leading to improved engine performance.

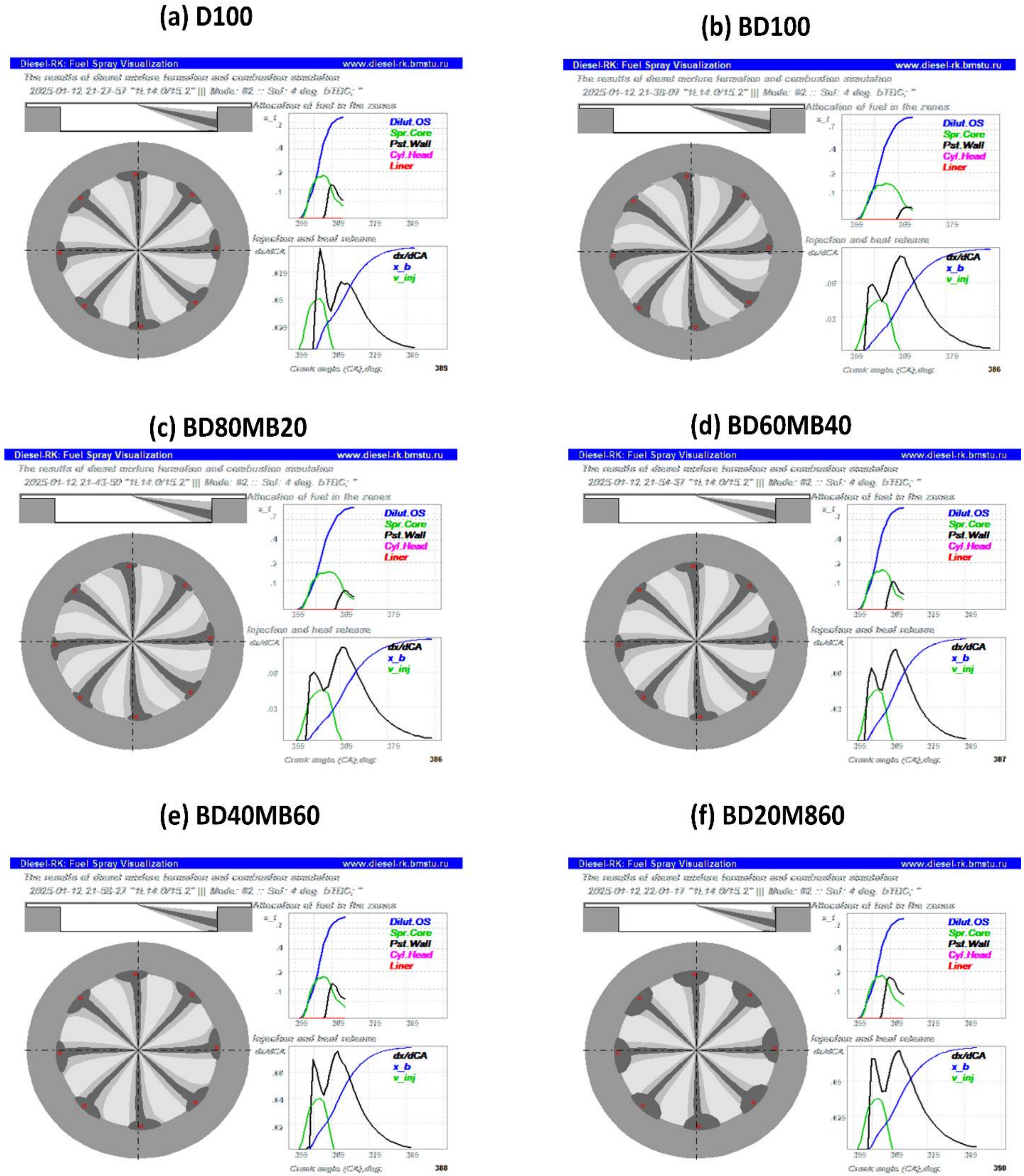

Figure 5.1. Fuel Spray Visualization for IT 4° bTDC.

5.1.2 Sauter Mean Diameter

A crucial metric in diesel engine spray assessment, the SMD is frequently used to characterize the patterns of droplet sizes within fuel sprays. SMD stands for the diameter of the droplets with the same volume-to-surface area ratio throughout the fuel spray. The spray characteristics are strongly affected by the fuel's density, viscosity, and surface tension [134]. For the establishment of clean and effective diesel engines, it is imperative to comprehend the SMD of droplets in sprayed fuel since the fuel injection mechanism dominates the combustion phenomena by regulating the mixing of fuel with entrained air [135]. Fig. 5.2 illustrates the variation of SMD for diesel, BTL diesel, and the blends of BTL diesel/microalgae biodiesel at different ITs.

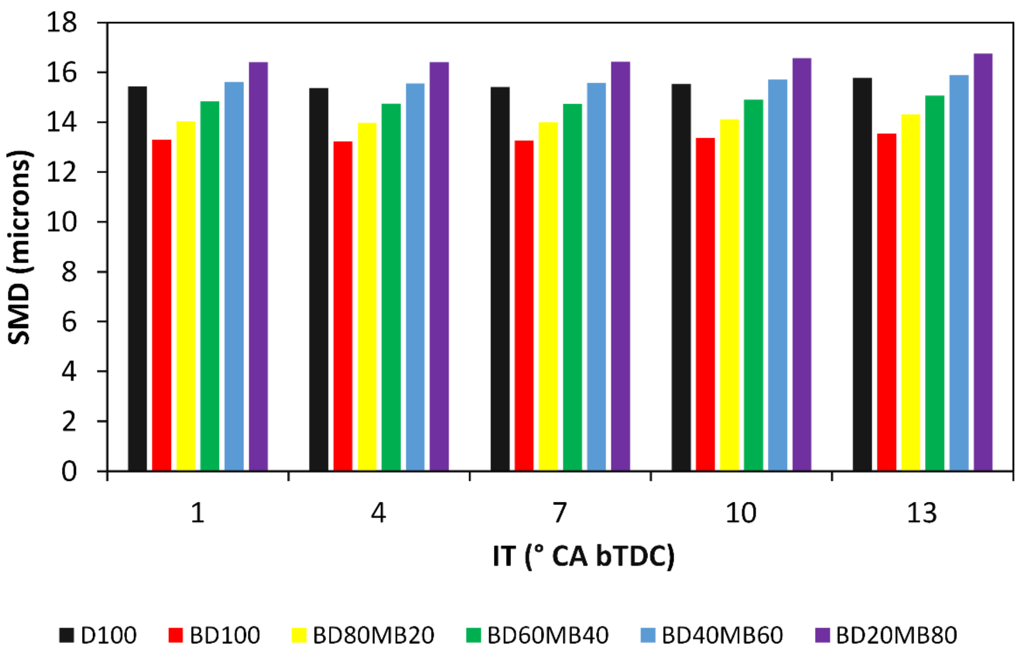

Figure 5.2. Variation of SMD for different test fuels at various ITs.

In comparison to neat diesel, the SMD for neat BTL diesel is reduced by 13.97% on average for the operating conditions. The SMD value reduces in the spray of BTL fuel because of its lower viscosity, density, and surface tension than pure diesel [23,69]. Smaller fuel droplets make it easier for entrained air to mix with fuel, which improves fuel evaporation and promotes favorable combustion [4]. However, when microalgae biodiesel is added to BTL diesel, the SMD values steadily increase compared to pure BTL diesel, and which is caused by the higher viscosity, density, and surface tension of microalgae biodiesel [136–138]. The SMD values for the blends prepared by adding microalgae oil into BTL diesel rise by 5.63-24.07% on average compared to neat BTL diesel. For all conditions, neat BTL diesel poses the lowest, and the BD20MB80 blend, the one with highest proportion of biodiesel poses the highest value of SMD. Among all the cases, the maximum SMD is found for the BD20MB80 blend, and the value is 16.756 µm at IT of 13° CA bTDC, whereas the lowest one is noticed 13.232 µm for pure BTL diesel at IT of 4° CA bTDC. However, the impact of IT on SMD is marginal.

5.1.3 Ignition Delay Period

The interval between when fuel is injected into the combustion chamber and when combustion commences is known as IDP. Engine performance is strongly influenced by IDP, an essential feature that is controlled by both the physical delay of the injection mechanism and the chemical delay during combustion [139,140]. The comparison of the IDP associated with the test fuels at different IT is demonstrated in Fig. 5.3. The neat BTL diesel shortens the IDP consistently for all the other ITs considered in this study compared to other fuel blends. The period of IDP of BTL diesel is shortened by 57.73% on average for the different ITs with respect to conventional diesel. This finding can be attributed to a higher CN, lower viscosity, and surface tension of the BTL diesel compared to conventional diesel [23,69]. A shorter IDP encourages quicker chemical reactions and evaporation, which speeds up combustion [141]. Cai et al. and Ismael et al. also reported that the renewable diesel reduces the duration of IDP compared to regular diesel in their separate studies, and their findings align with this outcome [142,143]. However, the inclusion of microalgae biodiesel into the BTL diesel results in a longer IDP compared to neat BTL diesel. On average, from 11.038% to 67.24% longer IDPs are observed for microalgae biodiesel-blended fuels than neat BTL diesel. The prolonged IDP results from the blended fuels of biodiesel because of its lower CN and higher density and viscosity [144]. The duration of ignition delay prolongs gradually with the increase in the proportion of microalgae biodiesel in the blended test fuels, and the longest IDP is shown by the BD20MB80 blend among the blended fuel of BTL diesel/biodiesel. Pure diesel comes with a longer IDP than BTL diesel and the blended fuels. Similar types of findings were also reported by Krishania et. al. [94].

In addition, The IDP values of the fuel samples decrease first up to 4° CA bTDC and then increase again with the advancement of IT. The IT of 4° CA bTDC poses the lowest IDP. At the most advanced IT (13° CA bTDC) , the pressure and temperature of fuel inside the cylinder is lowest as the volume expands with the advancement of IT. Due to low pressure and temperature, the ignition of fuel takes place lately resulting longer IDP. As the IT retards, the pressure and temperature increase gradually resulting shorter IDP. The IDP shortens up to 4° CA bTDC and increased again for IT of 1° CA bTDC. In case of IT of 1° CA bTDC, the piston starts to go from TDC to BDC again just after 1°CA as the expansion starts that drop the pressure and temperature again leading to longer IDP. At 4° CA bTDC, highest pressure and temperature is generated in engine cylinder resulting the shortest IDP. Therefore, 4° CA bTDC is the optimum IT for IDP.

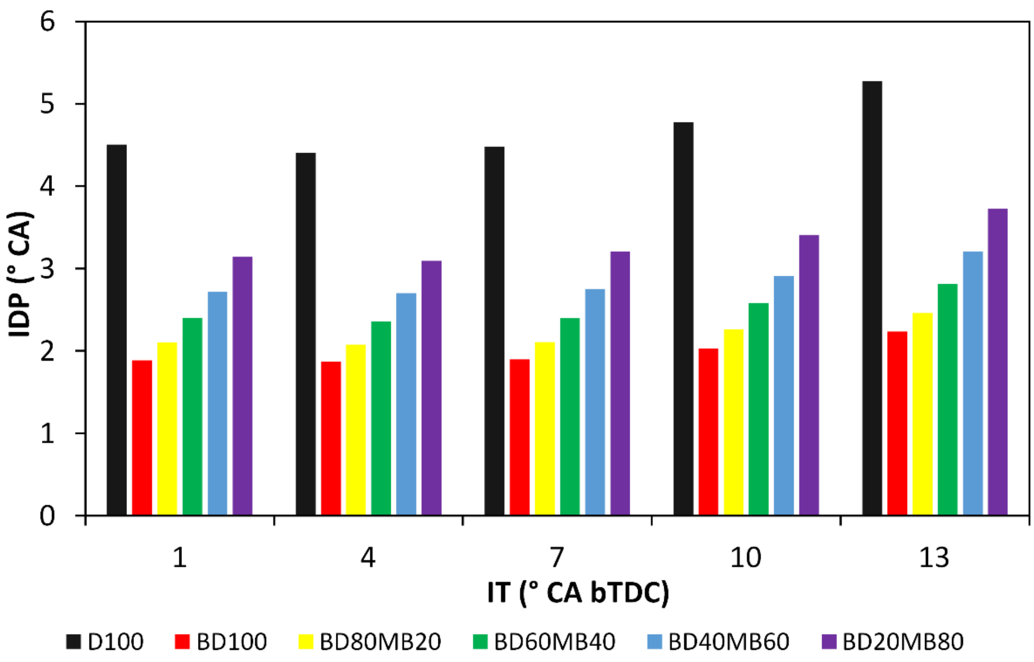

Figure 5.3. Variation of IDP for different test fuels at various ITs.

5.1.4 Heat Release Rate

A diesel engine's HRR is a measurement of how quickly the fuel's chemical energy is transformed into thermal energy during combustion [145]. Fig. 5.4 (a–e) presents a comparative analysis of the HRR for the tested fuels at ITs of 1°, 4°, 7°, 10°, and 13° CA bTDC. The PHRR during the premixed combustion phase for biomass-to-liquid (BTL) diesel is, on average, 39.68% lower than that of conventional diesel. The PHRR is strongly influenced by the IDP, which plays a critical role in shaping the combustion characteristics of diesel engines.

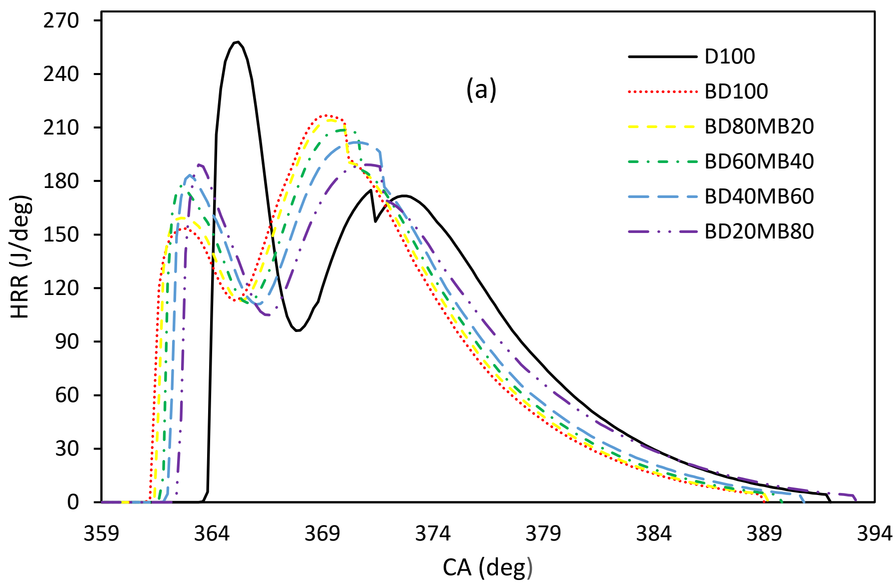

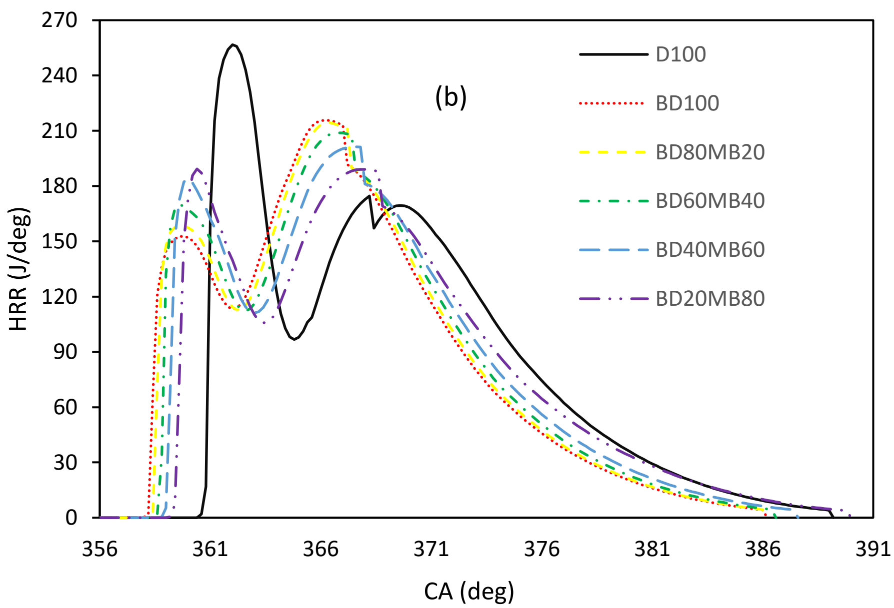

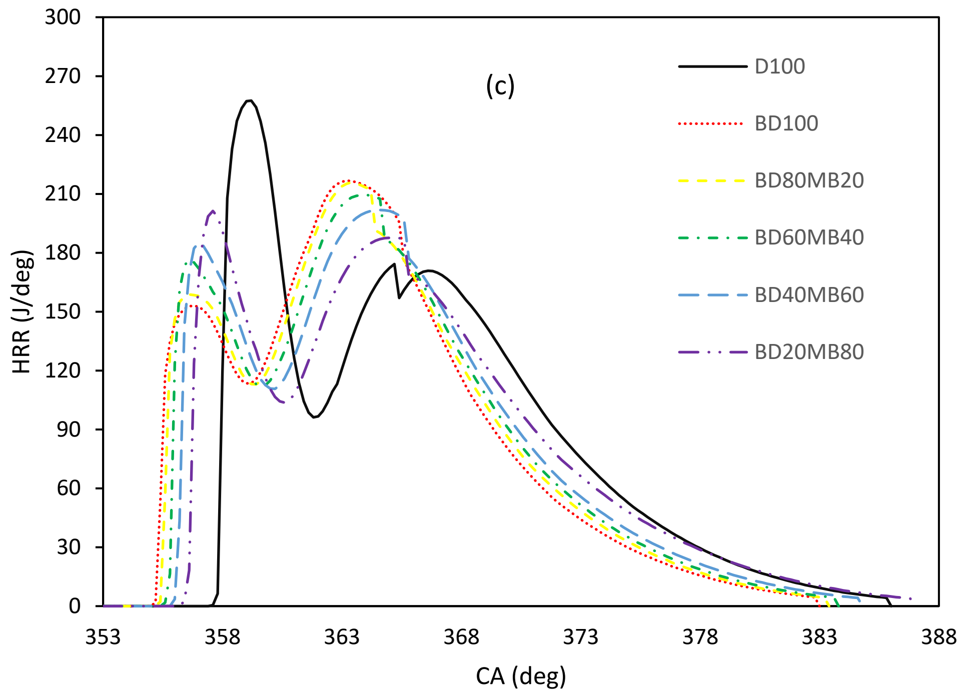
(c)
D100
BD100
BD80MB20
BD60MB40
BD40MB60
BD20MB80
HRR (J/deg)
CA (deg)
0
30
60
90
120
150
180
210
240
270
300
353
358
363
368
373
378
383
388

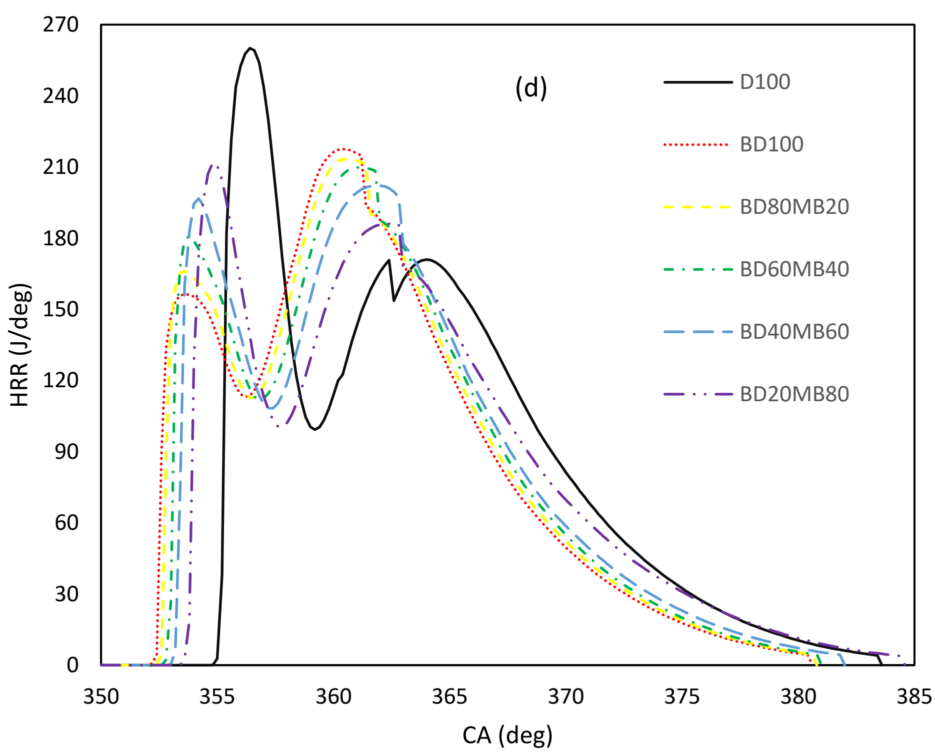
(d)
D100
BD100
BD80MB20
BD60MB40
BD40MB60
BD20MB80
HRR (J/deg)
CA (deg)
0
30
60
90
120
150
180
210
240
270
350
355
360
365
370
375
380
385

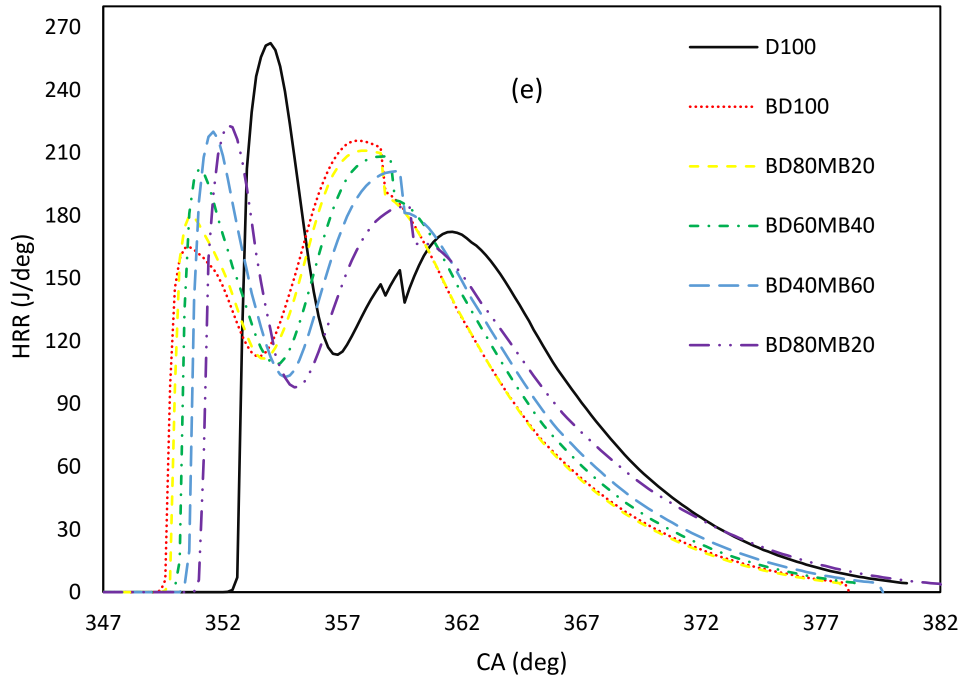

Figure 5.4. Comparison of HRR for different test fuels at IT of (a) 1, (b) 4, (c) 7, (d) 10, and (e) 13° bTDC.

Following injection, the fuel undergoes rapid mixing with air, forming combustible fuel-rich pockets within the combustion chamber. A prolonged IDP allows for better fuel-air mixing, leading to a higher energy release in the premixed combustion phase. This explains why the PHRR of conventional diesel is higher than that of BTL diesel. The IDP for diesel is observed to be longer (see fig. 5.3) than that of BTL diesel, aligning with prior research findings [40]. In contrast, within the diffusion combustion phase, the PHRR of neat BTL diesel consistently exceeds that of conventional diesel under all tested conditions. This suggests that the combustion behavior of BTL diesel shifts towards a more controlled diffusion-dominated mode, potentially improving combustion efficiency and emissions characteristics. However, blending *Spirulina* microalgae biodiesel with BTL diesel results in a noticeable increase in the PHRR within the premixed combustion phase compared to neat BTL diesel. The PHRR of the biodiesel-BTL diesel blends increases by approximately 5.25% to 29.87% relative to BD100. This enhancement is primarily attributed to the longer IDP of the biodiesel-BTL diesel blends, allowing more time for fuel-air mixing before ignition. A similar trend in PHRR has been reported in previous studies [87]. However, increasing the volumetric concentration of microalgae biodiesel with BTL diesel leads to lower HRR during the diffusion combustion phase due to lower volatility, poorer spray attributes (as Fig. 5.1), and atomization (as Fig. 5.2) and lower energy density. With the advancement of IT, the PHRR of the test fuel in premixed zone decrease from IT of 1 to 4° CA bTDC and then it begins to increase gradually form IT 7 to 13° CA bTDC. This trend is resulted by IDP as HRR is significantly impacted by IDP. The IDP similarly decrease first and then rises again with the advancement of IT of fuel spray (as Fig. 5.3). The lowest PHRR is observed for 4° CA bTDC as the shortest IDP was obtained at this IT.

5.1.5 Heat Release Fraction

Fig. 5.5 (a–e) presents the variation in HRF with CA for the tested fuels. The results indicate that HRF for neat BTL diesel remains consistently higher than that of regular diesel under all conditions. The HRF curve for neat BTL diesel exhibits a steeper initial increase, which is primarily attributed to its shorter IDP. A shorter IDP allows the fuel to reach PHRR earlier in the premixed combustion phase, leading to a more rapid conversion of chemical energy into heat energy. As a result, BTL diesel releases a significant portion of its energy earlier, contributing to a higher HRF than regular diesel.

The introduction of BTL diesel/microalgae biodiesel blends demonstrates a clear increasing trend in HRF compared to regular diesel, highlighting the influence of oxygenated fuels on combustion characteristics. However, while the HRF values of the blends surpass those of regular diesel, they remain lower than those of neat BTL diesel across all ITs. This difference arises due to the IDPs of the blends, which are shorter than those of regular diesel but longer than BD100 (ass Fig. 5.3). The intermediate IDP of the blended fuels results in moderate heat release, positioning their HRF between neat BTL diesel and regular diesel. Rajak et al. reported that algae based biodiesel blends have a greater mass fraction burnt compared to regular diesel [128]. Higher mass fraction indicates greater HRF. These findings emphasize the impact of IDP on combustion efficiency, demonstrating that neat BTL diesel achieves superior thermal energy conversion compared to both regular diesel and its biodiesel blends.

From Fig. 5.6, it is observed that with the advancement of IT, the HRF also advances. Advancing the IT allows the fuel to mix with air for longer time before ignition. As the fuel gets longer time to mix with air, a larger quantity of fuel is burnt during the premixed zone leading to higher HRF in the earlier stage with the advancement of IT.

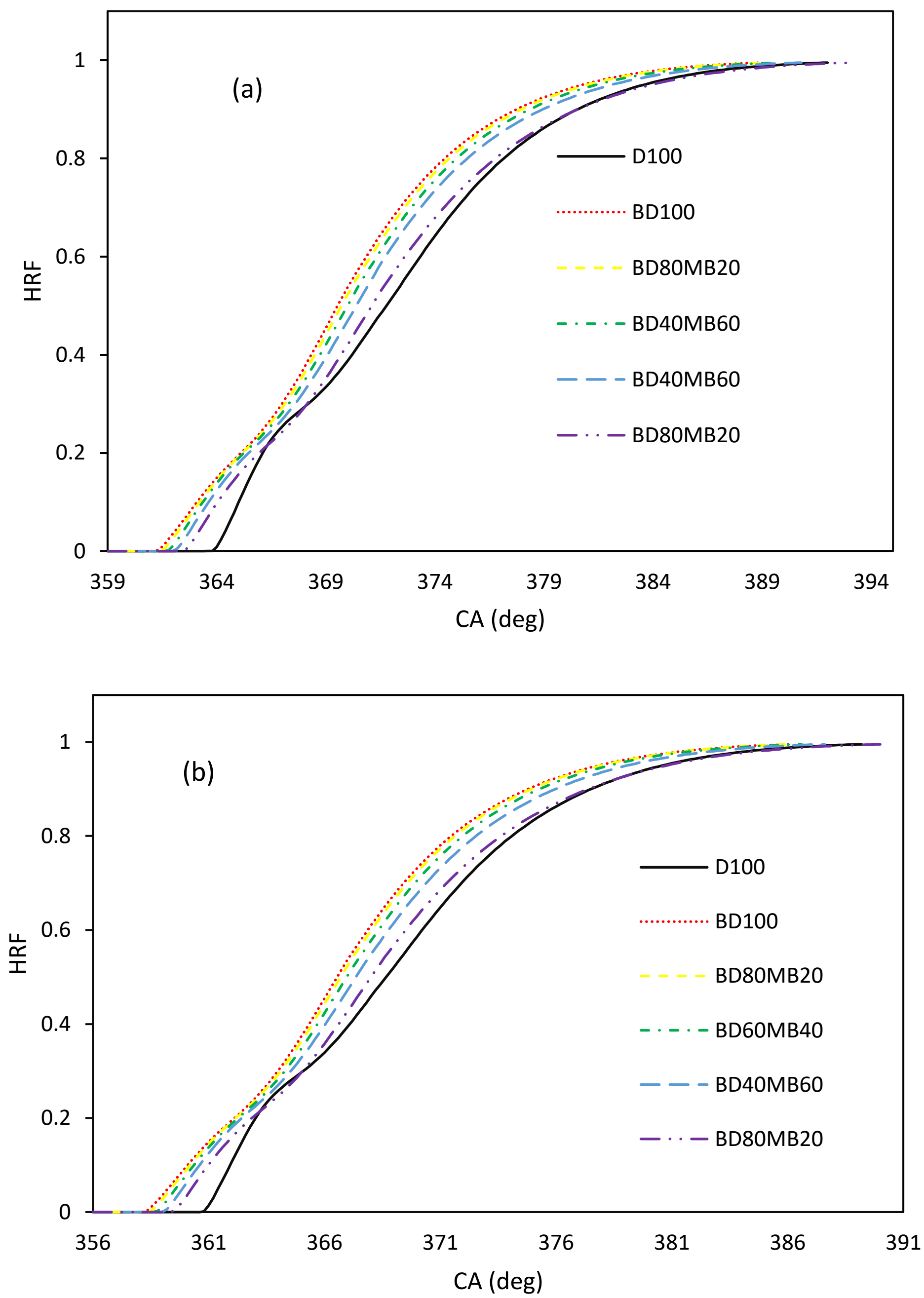

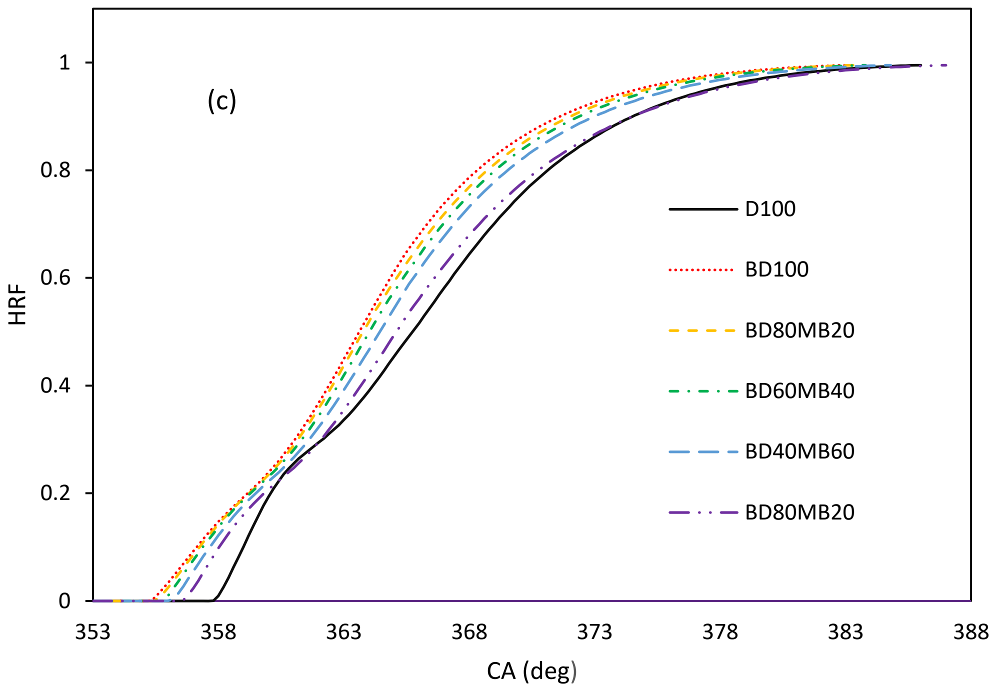
(c)
HRF
1
0.8
0.6
0.4
0.2
0
353
358
363
368
373
378
383
388
CA (deg)
D100
BD100
BD80MB20
BD60MB40
BD40MB60
BD80MB20

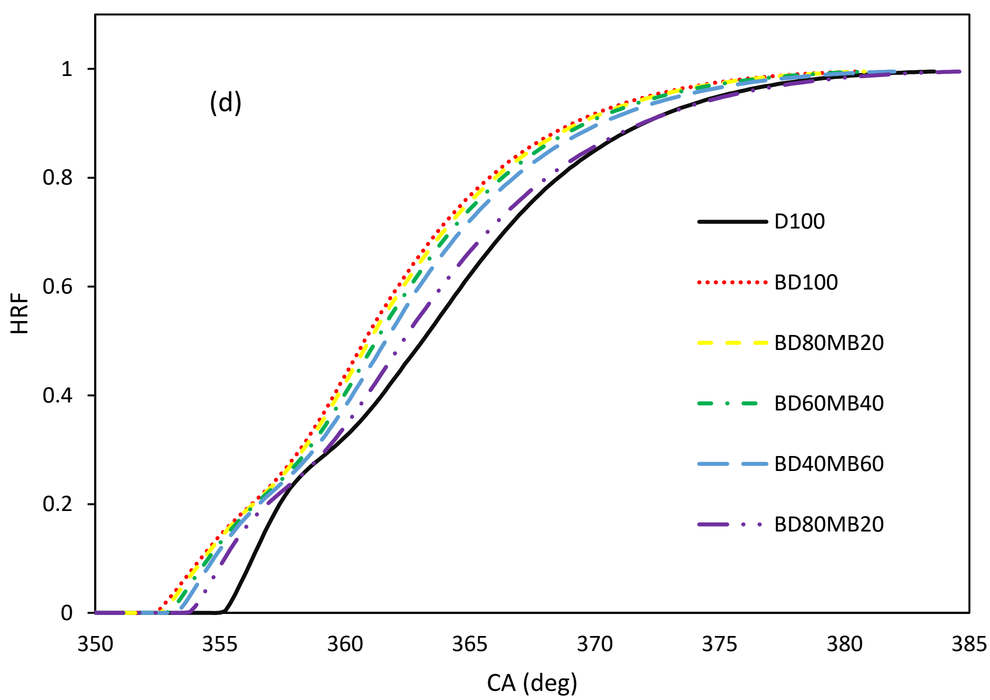
(d)
HRF
1
0.8
0.6
0.4
0.2
0
350
355
360
365
370
375
380
385
CA (deg)
D100
BD100
BD80MB20
BD60MB40
BD40MB60
BD80MB20

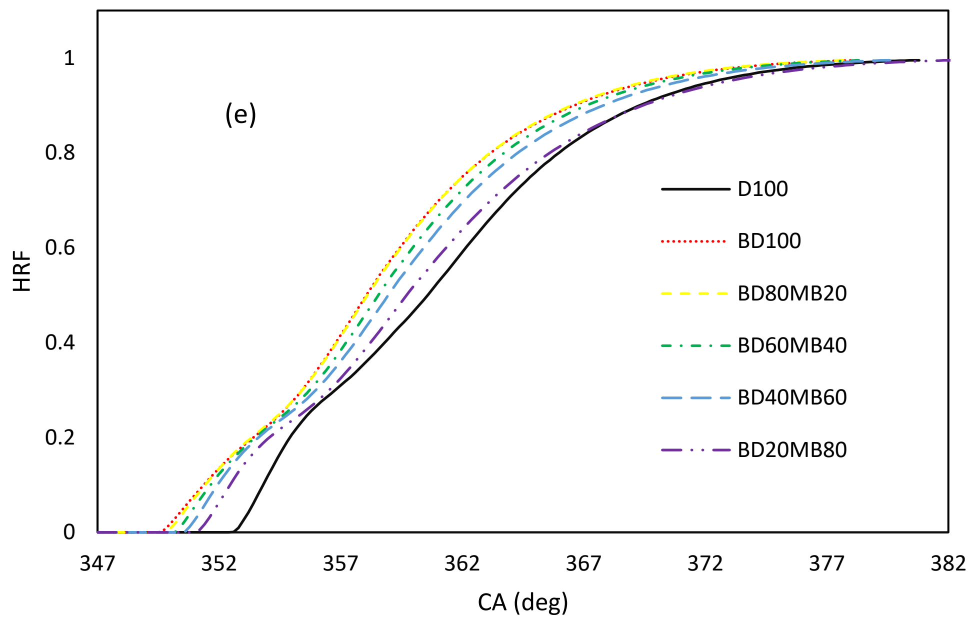

Figure 5.5. Variation of HRF at IT of (a) 1, (b) 4, (c) 7, (d) 10, and (e) 13° bTDC.

5.1.6 Combustion Duration

Fig. 5.7 illustrates the CD of the tested fuels, which refers to the duration from the initiation to the completion of combustion. The results indicate that neat BTL diesel exhibits an average reduction of 8.77% in CD compared to conventional diesel. The shorter CD of BTL diesel can be explained by its physio-chemical properties. Its higher CN makes it more reactive, allowing for quicker ignition and combustion. Additionally, BTL diesel has lower viscosity and surface tension, which promotes finer fuel atomization during injection. Consequently, the fuel droplets in BTL diesel exhibit a smaller SMD than those of conventional diesel (as Fig. 5.2). The smaller SMD facilitates greater air entrainment, leading to the formation of a more reactive fuel-air mixture. Enhanced fuel diffusion within the air results in faster combustion, ultimately reducing CD.

When *Spirulina* microalgae biodiesel is blended with BTL diesel, the CD increases by an average range of 0.66% to 13.03% compared to neat BTL diesel. This can be attributed to the lower CN and higher viscosity and surface tension of biodiesel. The addition of biodiesel gradually lowers the CN of the fuel blends, leading to a delay in ignition (as Fig. 5.3). Furthermore, the higher SMD of the blended fuels extends the CD compared to neat BTL diesel. This trend aligns with previous scholarly findings [137,146].

Among the tested blends, BD20MB80 exhibits the longest CD, surpassing even neat diesel under all conditions. Compared to diesel, its CD increases by 3.03%, 2.41%, 3.03%, 2.98%, and 4.14% for IT of 1, 4, 7, 10, and 13° CA bTDC, respectively. This behavior is primarily due to the high proportion of biodiesel in the blend, which has a lower CN close to that of neat diesel. Additionally, BD20MB80 features a larger SMD than diesel (as Fig. 5.2). The combination of these factors results in a longer CD than D100.

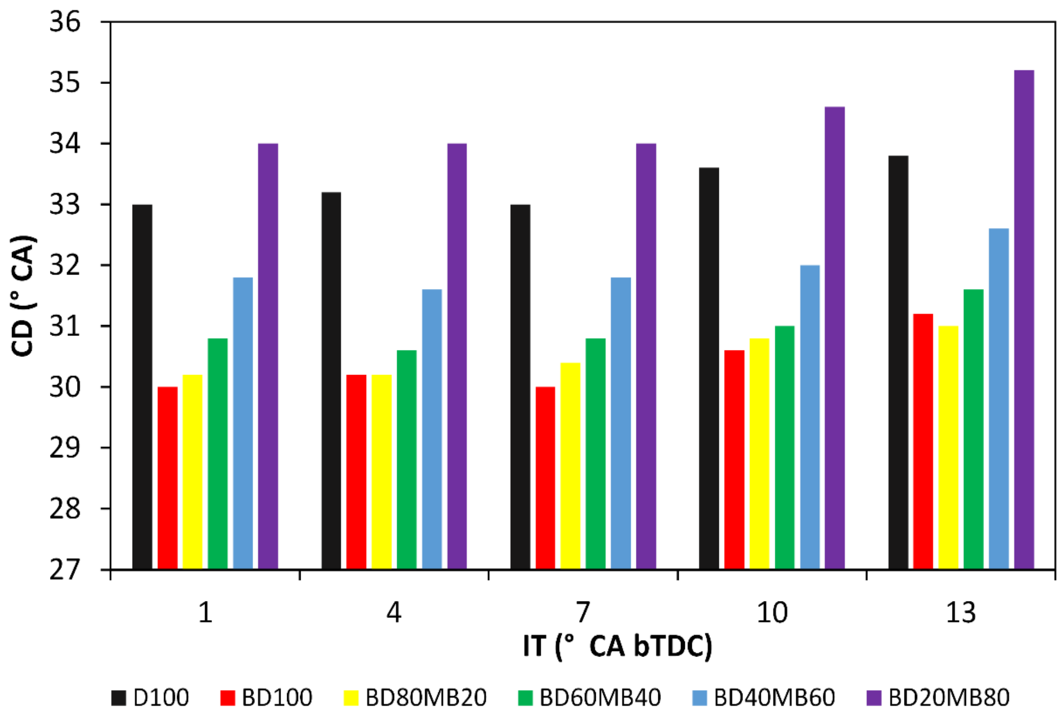

Figure 5.6. Variation of CD for different test fuels at various ITs.

For the earliest IT (13° CA bTDC), the CD is observed highest for all the test fuels. As the IT of spraying the fuel retards, the CD shortens in a gradual manner up to 7° CA bTDC. Such trend is obtained because the pressure as well as the temperature of fuel inside cylinder keep increasing with the retardation of IT. Higher pressure and temperature facilitate to complete the combustion early leading to shorter CD. As the IT retards more than 7° CA bTDC, negligible variation is observed as the CDs of fuel samples at ITs of 1 and 4° CA bTDC are almost similar to those of 7° CA bTDC.

5.1.7 Cylinder Pressure

Throughout the engine's four-stroke cycle, from intake to exhaust, the pressure within the cylinder is referred to as CP [147]. Given that CP history directly influences key engine parameters, in-cylinder pressure measurements in a combustion ignition engine provide critical insights into combustion behavior [148,149].

The variation of CP for the tested fuels at different ITs with respect to CA is depicted in Fig. 5.7 (a-e). The results show that PCP for neat BTL diesel is, on average, 9.61% higher than that of conventional diesel under various operating conditions. This trend is primarily attributed to its greater HRF and shorter CD compared to petrodiesel. The higher CN of BTL diesel makes it a more reactive fuel, leading to enhanced combustion characteristics. The intense fuel-air interaction in BTL diesel results in a shorter IDP, allowing for a greater and earlier heat release than conventional diesel. Additionally, the lower surface tension and viscosity of BTL diesel facilitate improved fuel atomization and mixing, contributing to efficient combustion and reduced CD. As a result, the combination of greater HRF and shorter CD leads to higher CP compared to conventional diesel.

When BTL diesel is blended with *Spirulina* microalgae biodiesel, the PCP increases relative to conventional diesel across all ITs. However, as the proportion of microalgae biodiesel in the blend increases, PCP exhibits a slight decline compared to neat BTL diesel. On average, the PCP for these blends is reduced by 0.72% - 5.26% relative to BD100. This decrease is attributed to slower HRF and prolonged CD compared to neat BTL diesel, as the introduction of biodiesel influences combustion characteristics. The observed trend aligns with previous studies on *Spirulina* microalgae biodiesel, reinforcing its impact on combustion performance [89,94]. A gradual increment in the PCP of all the fuel samples is observed as the IT advances. Previously scholar work shows similar trend for biodiesel [92]. As discussed earlier, the HRF of fuels gets higher in the earlier stage with the advancements of fuel's IT. Such tendency of HRF contributes in raising the PCP with the advancement in the timing of fuel injection. Additionally, advancing the injection of fuel promotes turbulence with in the fuel spray that significantly assist the fuel-air mixing leading to enhanced CP [112,128].

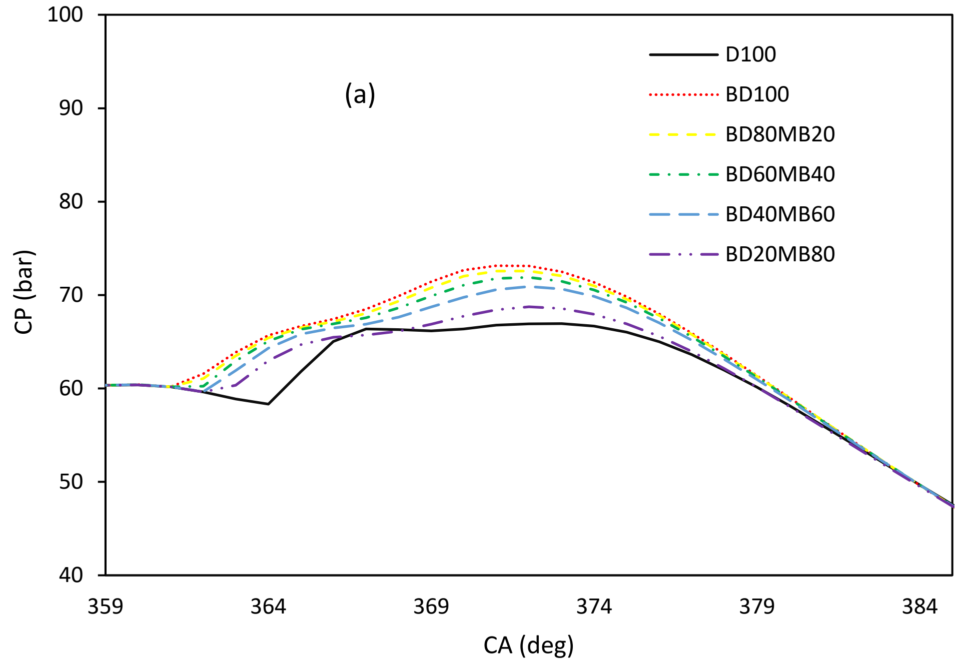

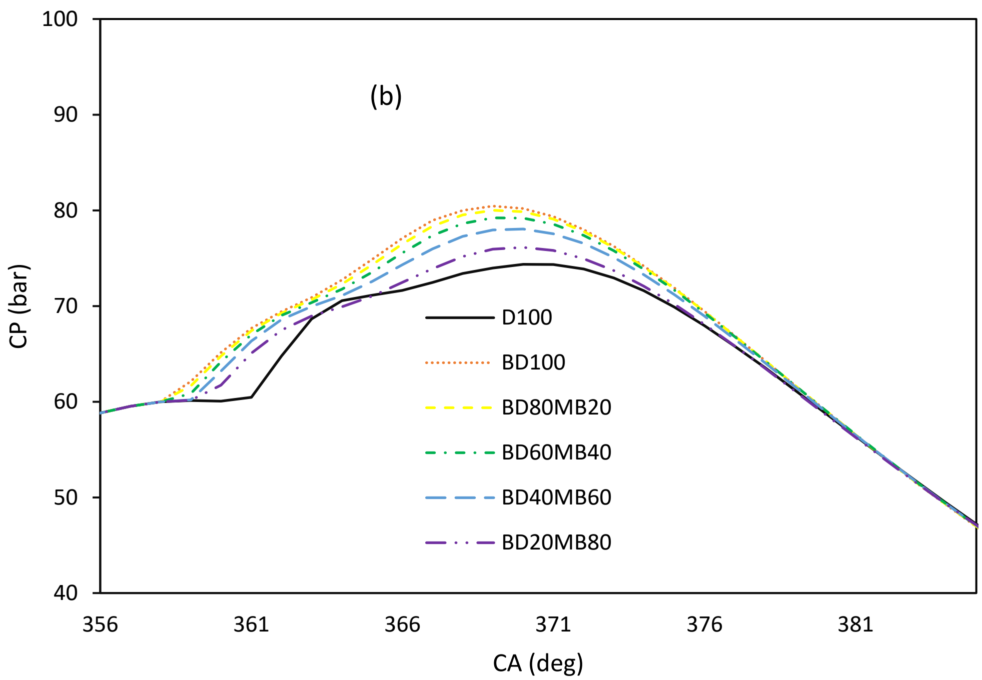

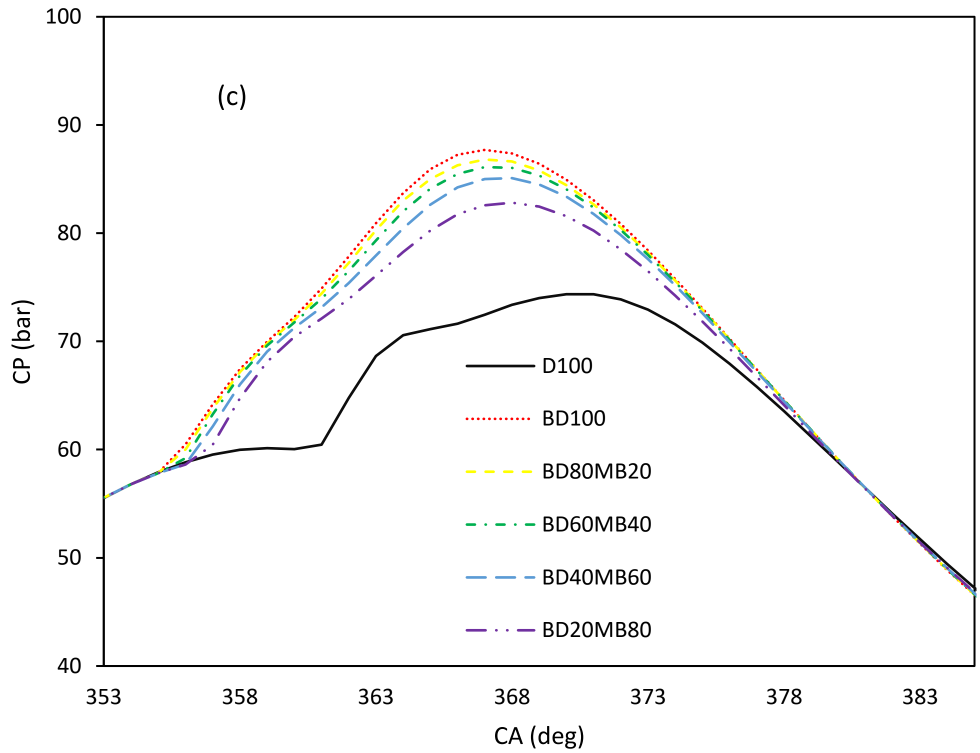
(c)
CP (bar)
CA (deg)
100
90
80
70
60
50
40
353
358
363
368
373
378
383
D100
BD100
BD80MB20
BD60MB40
BD40MB60
BD20MB80

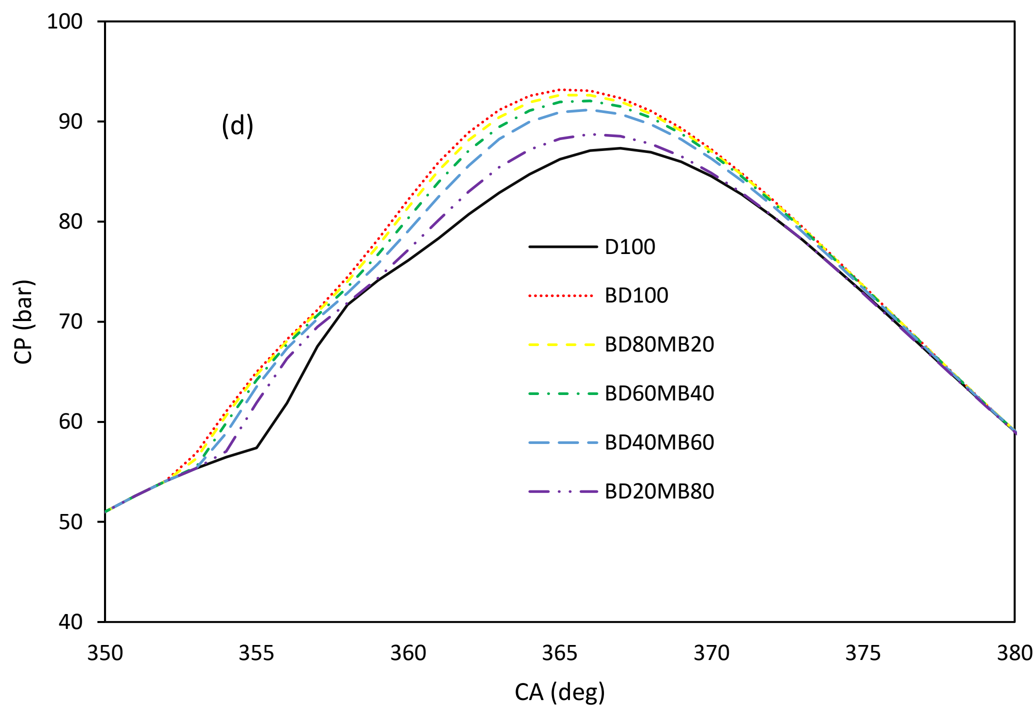
(d)
CP (bar)
CA (deg)
100
90
80
70
60
50
40
350
355
360
365
370
375
380
D100
BD100
BD80MB20
BD60MB40
BD40MB60
BD20MB80

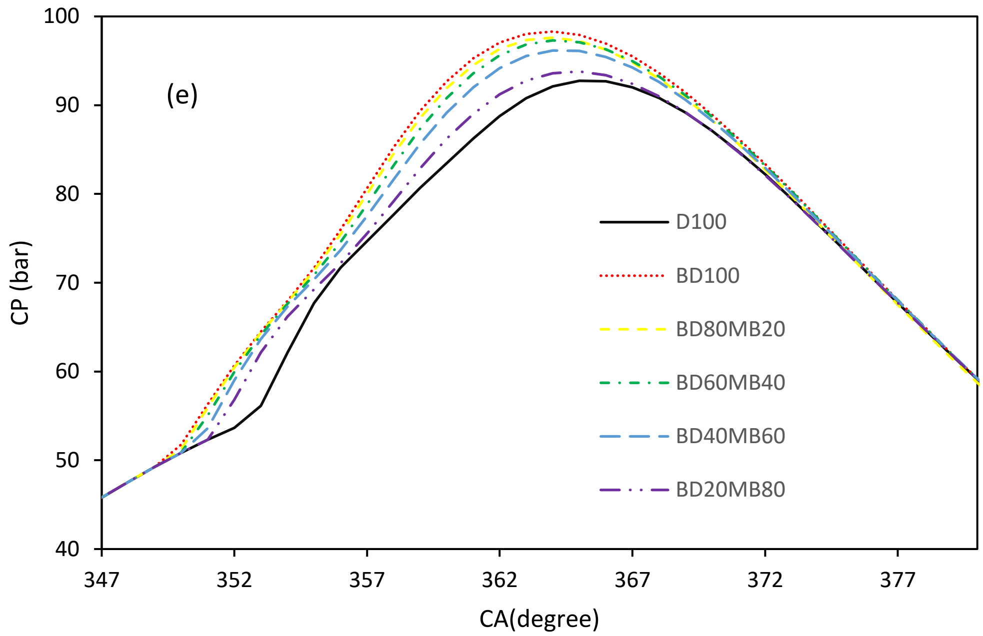

Figure 5.7. Distribution of CP with CA for IT of (a) 1, (b) 4, (c) 7, (d) 10, and (e) 13° bTDC.

5.1.8 Combustion Zone Temperature

In diesel-powered engines, the temperature within the cylinder during combustion is referred to as the CZT. Fig. 5.8 demonstrates the variation of CZT of the test fuels with respect to CA for different ITs. The CZT for BTL diesel is found higher compared to conventional diesel in all operating conditions. The mean value of elevation of CZT for BTL diesel than D100 is 2.96%. PHRR of premixed combustion zone and C/H ratio of fuel are the major factors that dominate the CZT of diesel engine. Higher PHRR of premixed zone results in higher CZT typically. Conversely, larger C/H ratio of fuel lowers the CZT. Smaller C/H ratio means the presence of hydrogen in greater quantity relatively with respect to carbon in the fuel structure. Presence of higher amount of hydrogen produces higher amount of H*, OH*, and HO_2* etc. free radicals during the combustion of fuel. Such reactive free radicals result in higher amount of water molecule (H_2O) comparatively and improves the cooling effect inside engine cylinder that lowers the CZT. In the present study, the CZT of neat BTL diesel is slightly higher than neat diesel for all ITs. In comparison to neat diesel, the PHRR of premixed phase is lower and C/H is higher for BTL diesel (as Fig. 5.4). The effect of higher C/H ratio is dominating for BTL diesel in the current study that leads to higher CZT. However, the application of microalgae biodiesel and diesel blend slightly increased the CZT by 0.17-0.21% averagely with respect to BD100. This trend attributes to the higher PHRRs of the microalgae blended fuels than those of BTL diesel in the premixed combustion zone.

Moreover, the CZT climbs up gradually as the IT advances. With the advancement of IT, the cumulative HRR rises or the HRF gets higher in the earlier stage leading to the increment in the CZT.

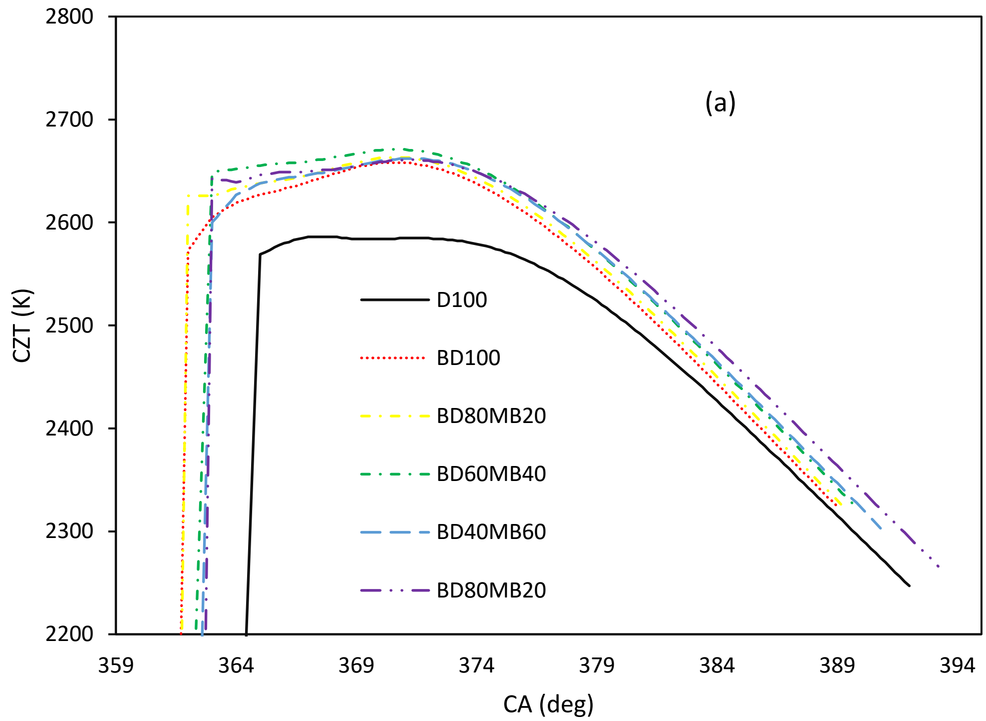

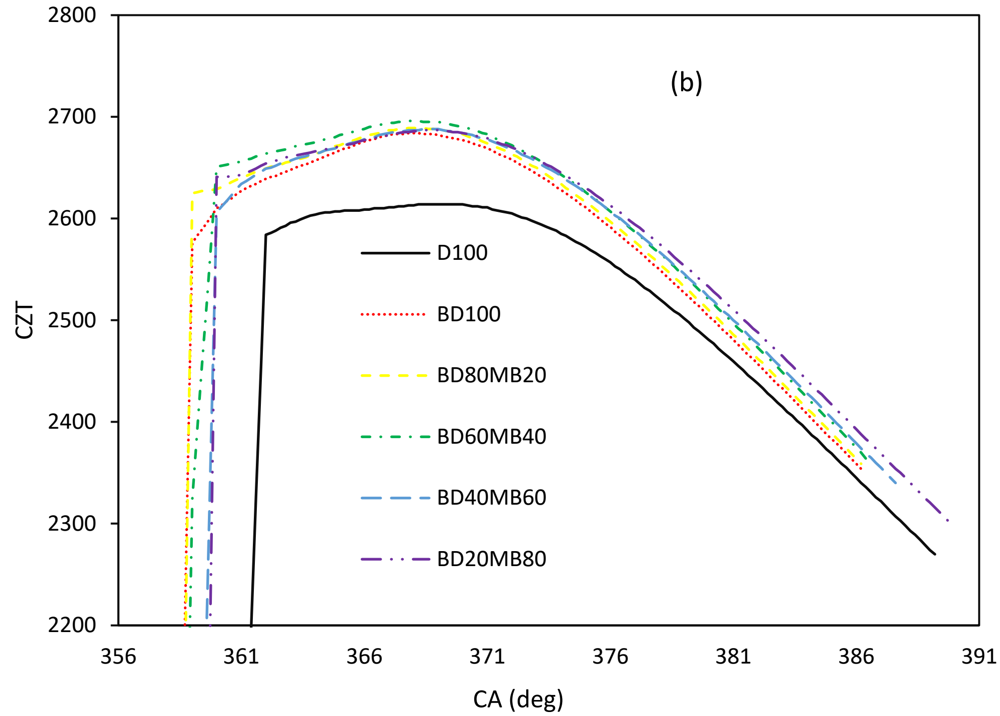
(b)
CZT
CA (deg)
D100
BD100
BD80MB20
BD60MB40
BD40MB60
BD20MB80
2800
2700
2600
2500
2400
2300
2200
356
361
366
371
376
381
386
391

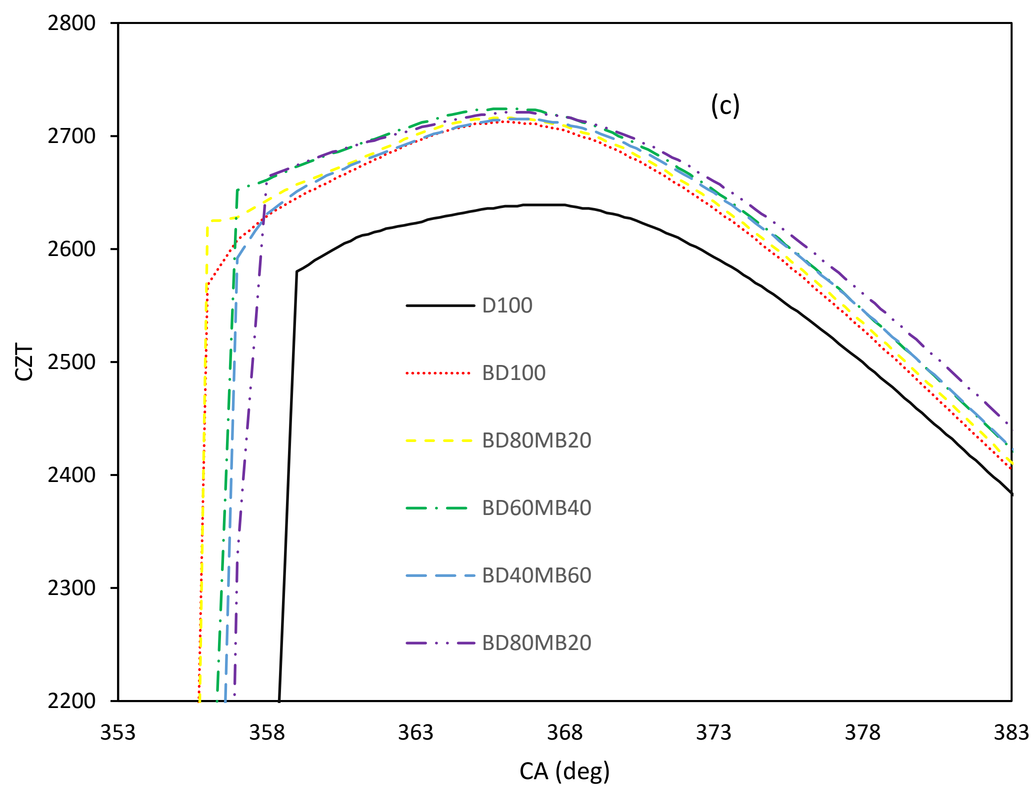
(c)
CZT
CA (deg)
D100
BD100
BD80MB20
BD60MB40
BD40MB60
BD80MB20
2800
2700
2600
2500
2400
2300
2200
353
358
363
368
373
378
383

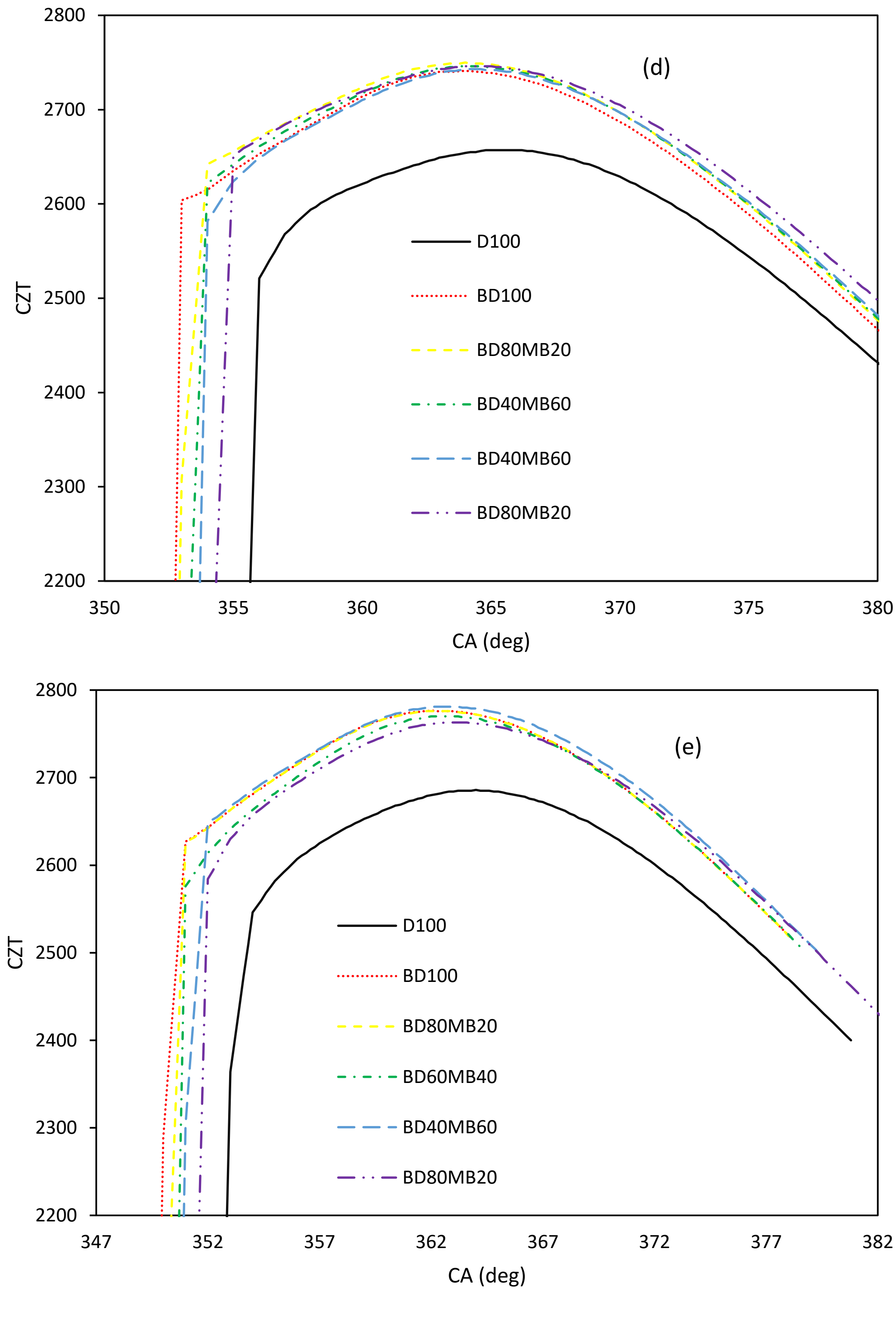

Figure 5.8. Variation of CZT at IT of (a) 1, (b) 4, (c) 7, (d) 10, and (e) 13° bTDC.

5.2 Performance Parameters

5.2.1 Brake Specific Fuel Consumption

BSFC is the amount of fuel consumed per unit of power output per hour in an engine. The values of BSFCs measured for the fuel samples at IT of 1, 4, 7, 10, and 13° CA bTDC are presented in Fig. 5.9.

Neat BTL diesel reduces the engine's BSFC by an average of 3.79% compared to D100, indicating improved fuel economy. This reduction is primarily attributed to BTL diesel's higher CN and lower SMD relative to D100. A higher CN enhances fuel reactivity, leading to improved combustion and greater engine output. Additionally, BTL diesel's lower viscosity and surface tension contribute to the formation of finer fuel droplets, which enhance air entrainment and promote better fuel-air mixing. This improved mixing leads to more efficient combustion, ultimately reducing BSFC. Furthermore, BTL diesel's higher heating value decreases the amount of fuel required to produce the same power output. A similar trend for BTL diesel has been reported by Ogunkoya et al. [24]. However, blending microalgae biodiesel with BTL diesel results in an increase in BSFC under all tested conditions. The BSFC rises by 2.14–7.51% on average compared to neat BTL diesel, primarily due to the lower heating value (LHV), the IDP of biodiesel, and its oxygen content, which does not contribute to energy production. As a result, a higher quantity of fuel is required to maintain the same power output, aligning with previous studies [95].

The variation in BSFC with IT follows a distinct pattern: it decreases from 1° to 4° CA bTDC before increasing from 7° to 13° CA bTDC. This trend can be attributed to heat loss and negative work. When fuel is injected too early (e.g., at 13° CA bTDC), lower CP and CZT delay combustion onset. This delay increases the exposure area of the fuel-air mixture, leading to greater heat loss. Additionally, early IT causes combustion to occur before the piston reaches TDC, raising CP before TDC and generating negative work. At the earliest IT, the combined effects of heat loss and negative work significantly increase BSFC. As IT advances to 4° CA bTDC, the impact of these losses diminishes, leading to the lowest BSFC. At this timing, combustion starts at optimal TDC conditions, minimizing negative work. However, a slight increase in BSFC is observed at 1° CA bTDC. When fuel injection occurs at this timing, combustion begins after the piston starts descending from TDC, increasing the exposure area and heat loss slightly.

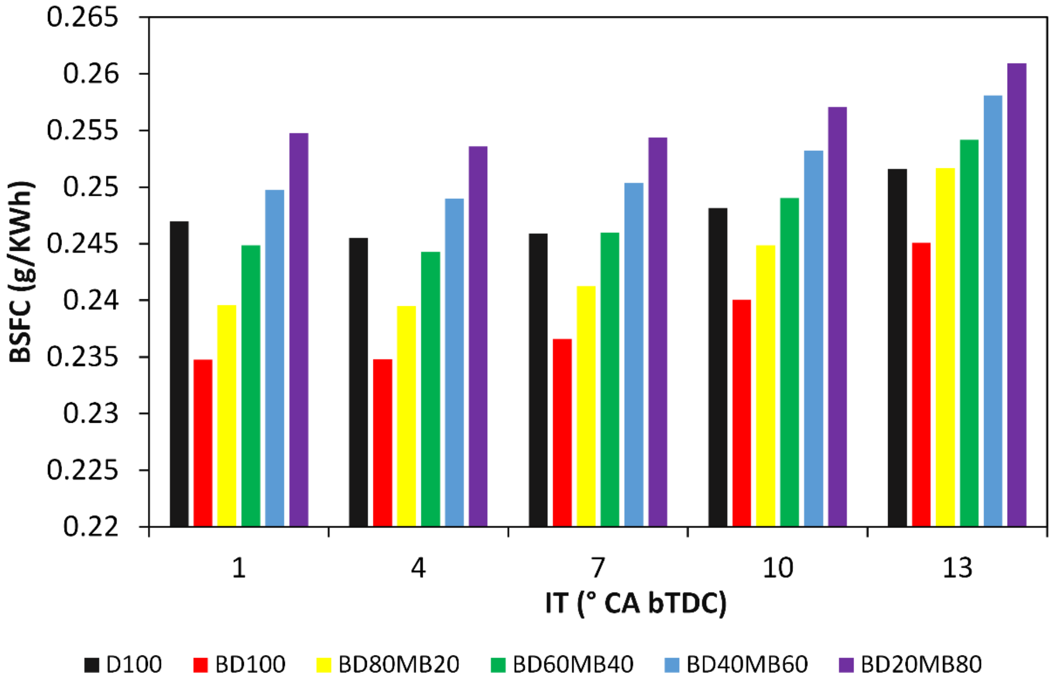

Figure 5.9. Variation of BSFC for different test fuels at various ITs.

5.2.2 Brake Thermal Efficiency

BTE is a crucial parameter for assessing engine performance, as it represents the efficiency with which an engine converts the energy in fuel into usable mechanical power. The comparison of BTE values for different test fuels at varying ITs is depicted in Fig. 5.10. For ITs ranging from 1° to 7° CA bTDC, neat BTL diesel exhibits an average increase of 0.81% in BTE compared to D100. This improvement is primarily due to the reduction in BSFC observed with BTL diesel, which enhances overall efficiency. The higher calorific value and finer spray characteristics of BTL diesel (see fig. 2) contribute to superior fuel-air mixing, ultimately improving combustion efficiency. This trend aligns with findings from previous studies [24].

However, the addition of microalgae biodiesel to BTL diesel results in a decline in BTE for ITs between 1° and 7° CA bTDC. The average reduction in BTE ranges from 0.2% to 1.06% compared to BD100. This decrease is attributed to the inferior spray characteristics and LHV of biodiesel-blended fuels, which negatively impact combustion efficiency.

An opposite trend is observed at ITs of 10° and 13° CA bTDC, where BTL diesel shows an average decrease in BTE of 0.68% compared to conventional diesel. This phenomenon can be attributed to the shorter IDP of BD100 (see fig. 5.3), which causes combustion to initiate earlier, before the piston reaches TDC. As a result, the fuel-air mixture experiences a larger exposed surface area, leading to greater heat loss and an increase in negative work. The premature onset of combustion means that a portion of the energy is expended against the piston while it is still compressing, reducing overall efficiency. Interestingly, when microalgae biodiesel is blended with BTL diesel, BTE gradually improves with increasing biodiesel content. This enhancement can be attributed to the longer IDP of biodiesel-BTL diesel blends. Although fuel injection occurs earlier at ITs of 10° and 13° CA bTDC, the combustion delay caused by the longer IDP allows the piston to move closer to TDC before ignition. This reduced exposure area minimizes heat loss and negative work and subsequently enhances BTE.

The variation in BTE with IT exhibits a distinct pattern, increasing from 1° to 4° CA bTDC before declining from 7° to 13° CA bTDC. This behavior is primarily influenced by heat loss and negative work. At excessively advanced ITs, such as 13° CA bTDC, lower CP and CZT extend the ignition delay, exposing the fuel-air mixture to a larger area and increasing heat dissipation. Furthermore, early combustion initiation before the piston reaches TDC leads to a premature rise in CP, resulting in negative work. These combined effects elevate BSFC and lower BTE. As IT advances to 4° CA bTDC, heat loss and negative work are minimized, yielding the lowest BSFC and highest BTE, as combustion occurs at optimal TDC conditions. However, at 1° CA bTDC, a slight rise in BSFC and a corresponding reduction in BTE are observed due to combustion initiating after the piston begins its descent from TDC, increasing the exposure area and subsequent heat loss.

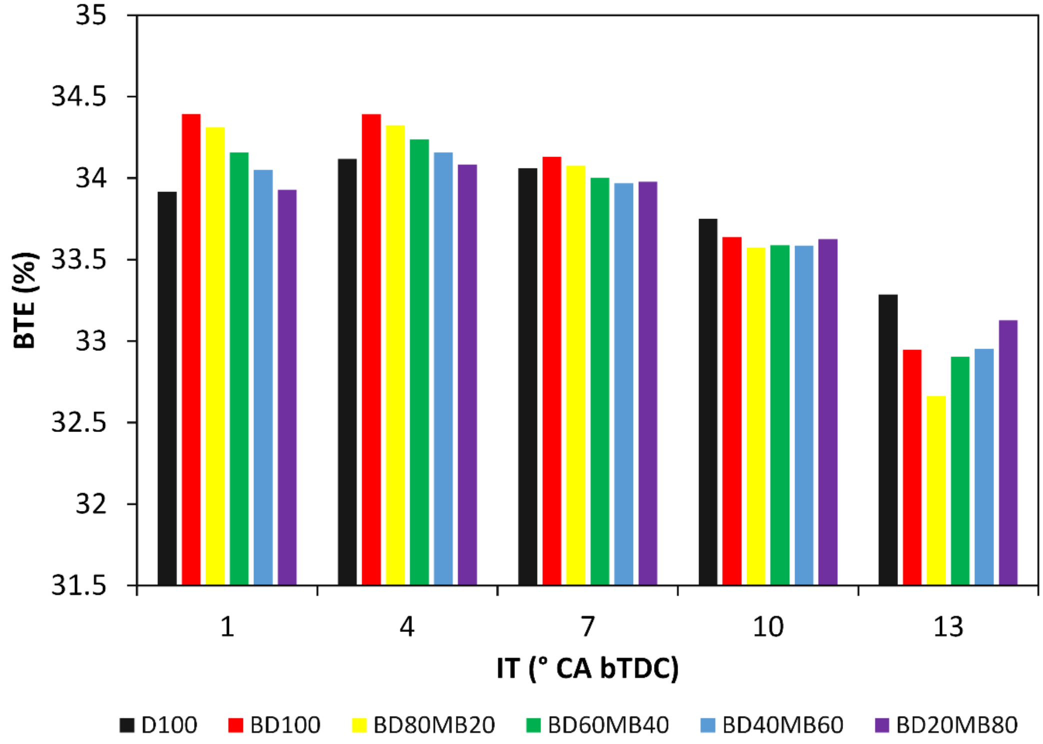

Figure 5.10. Variation of BTE for different test fuels at various ITs.

5.2.3 Exhaust Gas Temperature

The variation in EGT with IT for the test fuels is illustrated in Fig. 5.11. At ITs of 1°, 4°, and 7° CA bTDC, BTL diesel exhibits an average reduction of 0.58% in EGT compared to D100. However, an opposite trend is observed at 10° and 13° CA bTDC, where BTL diesel shows a 0.21% increase in EGT relative to D100. This trend can be attributed to the after-burning effect. At lower ITs (1°–7° CA bTDC), BTL diesel demonstrates improved combustion efficiency and BTE, which reduces the after-burning effect and consequently lowers EGT. Conversely, at 10° and 13° CA bTDC, the BTE of D100 surpasses that of BTL diesel, leading to slightly higher EGT values for BTL diesel.

The addition of microalgae biodiesel to BTL diesel leads to an overall increase in EGT compared to BD100 at ITs between 1° and 7° CA bTDC. This rise can be linked to the higher BSFC associated with biodiesel, which results in relatively incomplete combustion, thereby elevating EGTs due to increased after-burning effect. However, as IT advances further to 10° and 13° CA bTDC, the BTE of blends with lower biodiesel proportions (BD80MB20, BD60MB40, and BD40MB60) remains comparable to or slightly lower than that of neat BTL diesel. Notably, BD20MB80, the blend with the highest microalgae biodiesel content, exhibits a slightly higher EGT than neat BTL diesel at these ITs. This suggests that a higher fraction of biodiesel in the blend sustains the after-burning effect, increasing EGT at advanced ITs.

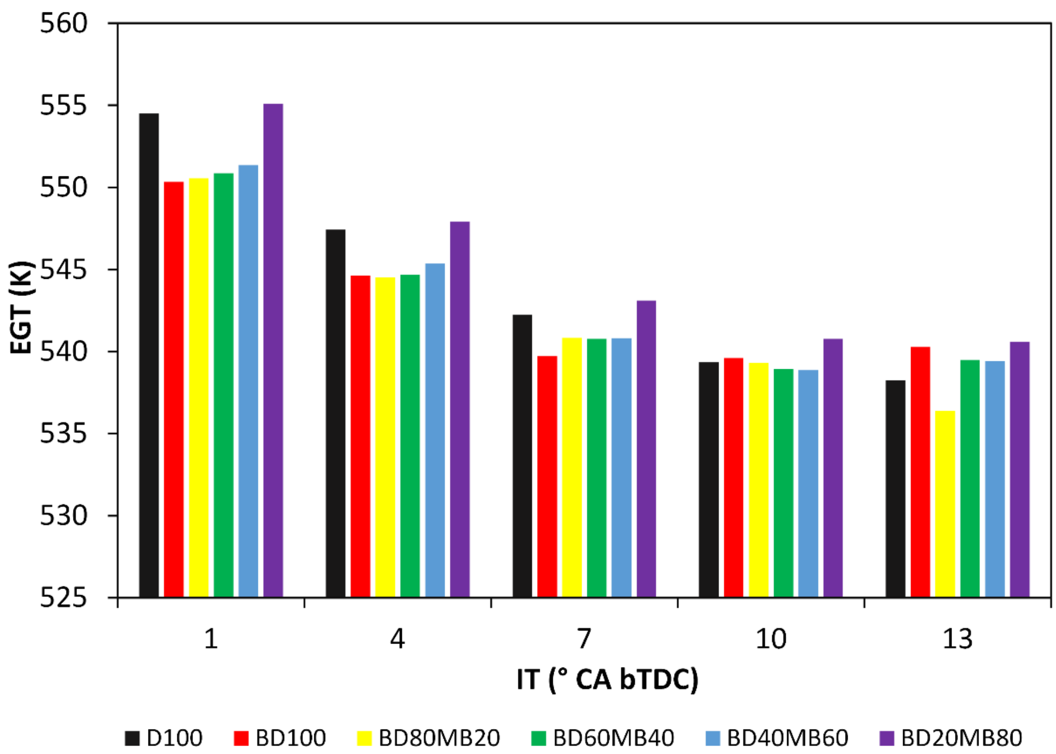

Figure 5.11. Variation of EGT for different test fuels at various ITs.

5.3 Emission Parameters

5.3.1 Carbon Dioxide Emission

The complete combustion of fuel within the engine cylinder produces CO_2 as a byproduct, which is subsequently released in the exhaust stream [144]. The specific CO_2 emissions for the tested fuels at different ITs are illustrated in Fig. 5.12. Among all test conditions, pure diesel exhibits the highest CO_2 emissions at the maximum IT, reaching 806.98 g/kWh. However, neat BTL diesel consistently reduces CO_2 emissions across all ITs compared to pure diesel, with an average reduction of 4.68%. This reduction can be attributed to the lower SFC of BTL diesel (as Fig. 5.9). Since a lower SFC implies that less fuel is required to generate the same power output, the total quantity of CO_2 released into the exhaust is consequently reduced. Similar trends have been reported in previous studies for BTL diesel and Sun diesel [24,106].

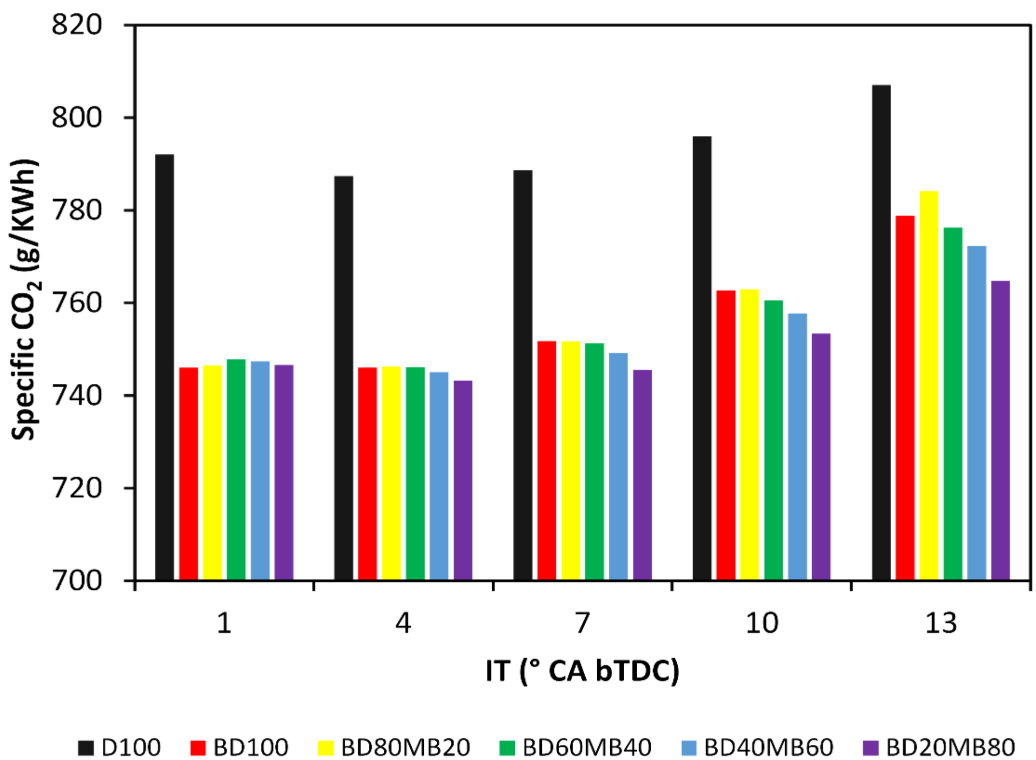

Figure 5.12. Variation of specific CO_2 emissions for different test fuels at various ITs.

Additionally, fuel blends incorporating *Spirulina* microalgae biodiesel with BTL diesel also demonstrate reduced CO_2 emissions compared to conventional diesel. Despite its relatively higher SFC, *Spirulina* biodiesel results in lower CO_2 emissions due to its lower carbon content and reduced carbon-to-hydrogen ratio in its molecular structure compared to conventional diesel. This observation aligns with prior research on microalgae biodiesel, such as the findings of Al-Iwayzy et al. [150]. At lower ITs (1 and 4° CA bTDC), the CO_2 emissions from biodiesel/BTL diesel blends are nearly identical to those of neat BTL diesel. However, at higher ITs (7, 10, and 13° CA bTDC), most of the biodiesel blends exhibit lower CO_2 emissions than BD100, except for BD80MB20 at 13° CA bTDC. With the advancement of IT, CO_2 emissions tend to rise gradually, in parallel with the increasing SFC of the test fuels (as Fig. 5.9).

5.3.2 Nitrogen Oxides Emissions

High-temperature combustion processes contribute to NO_x emissions, which have significant environmental and health consequences, including acid rain formation and ozone layer depletion. In internal combustion engines, NO_x formation is primarily influenced by fuel oxygen content, combustion zone temperature, and residence time [151]. Fig. 5.13 presents the NO_x emissions of the test fuels across different ITs. The results indicate that BTL diesel produces higher NO_x emissions than pure diesel, with an average increase of 58.15%. This trend can be attributed to the elevated CZT observed for BTL diesel in all test conditions (as Fig. 5.8), which enhances thermal NO_x formation.

Furthermore, blending microalgae biodiesel with BTL diesel results in a further increase in NO_x emissions. This is expected due to the combined effect of high CZT (see Fig. 5.8) and the additional intrinsic oxygen content present in biodiesel's molecular structure. On average, NO_x emissions from biodiesel-blended fuels are 5.66_x–15.93% higher than those of BD100. The intrinsic oxygen in biodiesel promotes more complete oxidation of hydrocarbons, leading to localized temperature spikes within the combustion chamber. These elevated temperatures further accelerate the chemical reactions responsible for NO_x formation. This outcome is consistent with findings from prior studies on biodiesel combustion [88,95,152].

Among all ITs, the highest NOx emissions are recorded at the earliest IT (13° CA bTDC). As IT advances, NOx emissions exhibit an increasing trend. This behavior can be explained by the influence of IT on CP (as Fig. 5.8) and CZT (as Fig. 5.8), where earlier ITs result in higher CP peaks and subsequently greater combustion temperatures. Since NO_x formation is highly temperature-dependent, the elevated temperatures associated with earlier ITs promote increased NO_x production. This observed effect of IT on NO_x emissions is in agreement with Ref. [92]. The trend of increasing the NO_x will be continued with the increment of the microalgae biodiesel proportion in the blended fuels. Pure microalgae will show the highest amount of NO_x release.

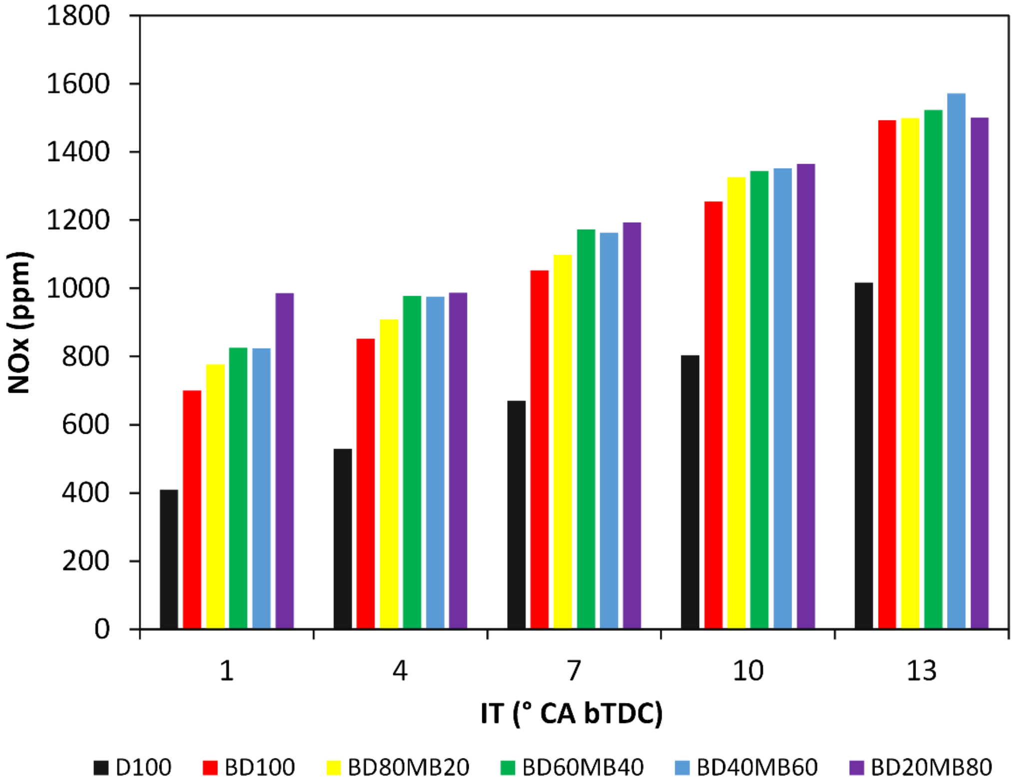

Figure 5.13. Variation of NO_x emissions for different test fuels at various ITs.

5.3.3 Particulate Matter and Smoke Emissions

Monitoring PM emissions and SO in engine exhaust is essential due to their direct association with soot formation and their detrimental impact on both the environment and human health. Figs. 5.14 and 5.15 illustrate the variation of PM emissions and SO with IT for the tested fuel samples, respectively.

On average, BTL diesel demonstrates a 15.32% reduction in PM emissions compared to neat diesel. Additionally, SO decreases by an average of 12.38% when using BTL diesel instead of D100. Several factors contribute to PM emissions, including oxygen content, latent heat of vaporization, chemical composition, and cylinder temperature [153]. Notably, the CZT observed for BTL diesel is higher than that of regular diesel (as Fig. 5.8). Elevated CZT enhances soot oxidation, leading to a significant reduction in both PM emissions and SO.

Blending microalgae biodiesel with BTL diesel further reduces PM emissions and SO beyond the levels observed with pure BTL diesel and pure diesel across all test conditions. On average, PM emissions and SO from biodiesel blends decrease by 1.3–56.17% and 1.61–49.61%, respectively. Similar reductions have been reported in previous studies [88,137,145]. This trend is primarily attributed to the high CZT, lower carbon content and higher oxygen concentration in biodiesel-based fuels compared to conventional diesel and BTL diesel. The high CZT and additional oxygen facilitates more complete combustion, promoting soot oxidation and thereby lowering both PM emissions and SO in the exhaust.

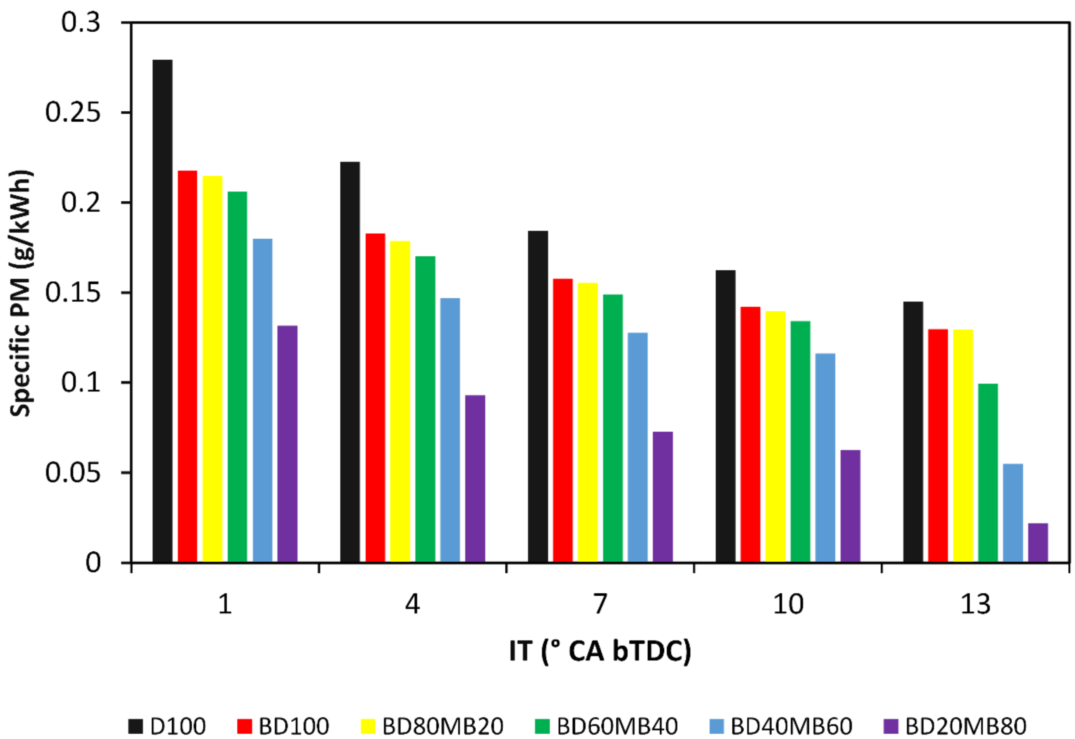

Figure 5.14. Variation of specific PM emissions for different test fuels at various ITs.

Furthermore, as IT advances, a gradual reduction in SO and PM emissions is observed across all fuel samples. The lowest levels of PM emissions and SO occur at the earliest IT. As IT advances, CZT increase, resulting in a progressive reduction in PM emissions. This outcome is consistent with previous literature findings, further confirming the correlation between IT, CZT, and soot formation [92]. Chaurasiya et al. investigated the effect of IT on the characteristics of diesel engine fueled with biodiesel. The authors observed the highest amount of PM & SO in emissions for the latest IT and vice versa. Emission of these compounds observed to decrease gradually with the advancement of IT on their studies. Similar trend is also observed in the current study. The decreasing trend will be continued with the increasing proportion of microalgae due to their intrinsic oxygen content effect.

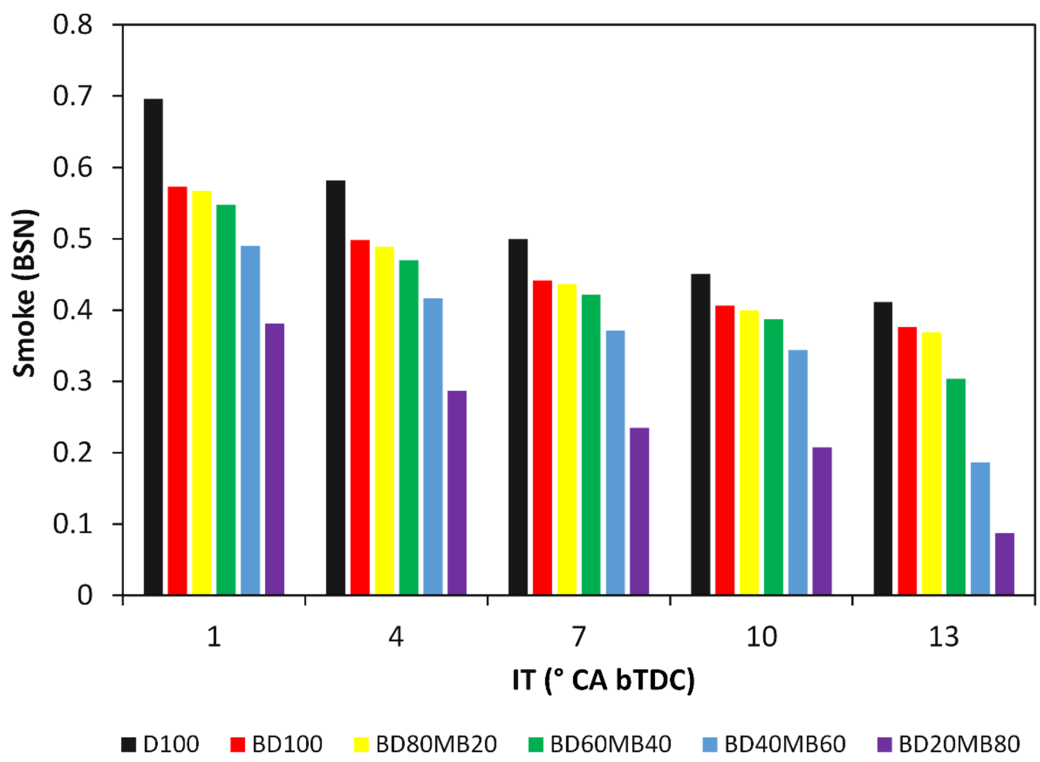

Figure 5.15 Variation of smoke emissions for different test fuels at various ITs.

Finally, a summary of all the results obtained in this study is presented in Table 5.1. The table shows whether the calculated parameters for BTL diesel and blends of microalgae biodiesel-BTL diesel increases or decreases with respect to traditional diesel and neat BTL diesel respectively.

Table 5.1.: Summary table of results.

Parameters	**Effect of BTL diesel (compared to conventional diesel)**	**Effect of BTL diesel-microalgae biodiesel blends (compared to neat BTL diesel)**
SMD	decreased	increased
IDP	shortened	prolonged
PHRR	decreased	increased
HRF	increased	increased
CD	shortened	prolonged
PCP	increased	decreased
CZT	increased	increased
BSFC	decreased	increased
BTE	increased (IT 1-7° CA bTDC) decreased (IT 10-13° CA bTDC)	decreased (IT 1-7° CA bTDC) increased (IT 10-13° CA bTDC)
EGT	increased (IT 1-7° CA bTDC) decreased (IT 10-13° CA bTDC)	increased
CO_2 Emission	decreased	decreased
NOx Emission	increased	increased
PM Emission	decreased	decreased
Smoke Emission	decreased	decreased

Chapter 6
Conclusion

This research explored the impact of Spirulina microalgae and BTL diesel blends on the combustion, performance, and emissions of a CI engine. Based on the results of the numerical investigation, the following conclusions were drawn:

1. For neat BTL diesel, the SMD, IDP, PHRR in the premixed phase, and CD decreased by 13.97%, 57.73%, 39.68%, and 8.77%, respectively, while the PCP increased by 9.61% compared to pure diesel. With the application of microalgae biodiesel-BTL diesel blended test fuels, the SMD, IDP, PHRR, and CD increased by 5.63–24.07%, 11.04–67.24%, 5.25–29.87%, and 0.66–13.03%, respectively, while the PCP decreased by 0.72–5.26% compared to neat BTL diesel.
2. With the advancement of IT, the IDP and HRR for both BD100 and microalgae-BTL diesel blends initially decreased up to 4° CA bTDC and then kept increasing. The CD and PCP for both BD100 and blended fuels gradually increased as the IT advanced.
3. BSFC of the engine decreased by 3.79% using neat BTL diesel with respect to ordinary diesel. The application of microalgae-BTL diesel blends gradually increased the BSFC by 2.14–7.51% compared to neat BTL diesel. For neat BTL diesel, the BTE increased by 0.81% for ITs of 1° to 7° CA bTDC, whereas decreased by 0.68% for ITs of 10° to 13° CA bTDC compared to ordinary diesel. In comparison to BD100, the BTE for the microalgae blended fuels initially decreased for ITs of 1–7° CA bTDC, then improved gradually for ITs of 10° and 13° CA bTDC as the biodiesel content in the blend increased.
4. From ITs of 1 to 4° CA bTDC, the BSFC for all test fuels reduced, and from ITs of 7° to 13° CA bTDC, the BSFC elevated again. The BTE increased up to 4° CA bTDC initially and then gradually decreased as the IT advanced for the fuel samples.
5. Neat BTL diesel reduced the emissions of CO_2, PM, and SO by 4.68%, 15.32%, and 12.38%, respectively, while increasing the NOx emission by 58.15% compared to pure diesel. Further increases in NOx emissions were observed for microalgae biodiesel blended fuel compared to neat BTL diesel. However, PM and SO emissions were significantly

reduced by 1.3–56.17% and 1.61–49.61%, respectively, by the microalgae blended test fuels.

6. The emissions of PM and SO continued to decrease for BD100 and microalgae blended fuel samples as the IT advanced. Gradual increases in NO_x emissions for BD100 and blended fuels were observed as IT varied from 1 to 13° CA bTDC. The CO_2 emissions for BD100 and blends of microalgae biodiesel and BTL diesel were similar for ITs of 1° and 4° CA bTDC, then rose gradually with advanced ITs.

An IT of 4° CA bTDC is shown to be the ideal IT for better performance, lower PM and smoke, and a manageable NO_x trade-off. This study presents critical insights into the influence of varying IT on the combustion, performance, and emissions of CI engines fueled with microalgae biodiesel-BTL diesel blends. The findings underscore the potential of BTL diesel/microalgae-based fuels in improving engine characteristics and reducing certain emissions, particularly PM and smoke. However, challenges remain with respect to NO_x emissions, which increased with higher proportions of microalgae biodiesel. This work serves as a valuable contribution to advancing the development of alternative fuels for cleaner and more efficient diesel engines.

The following recommendations are mentioned for the future researches:

- Further research is recommended to explore the impact of additional parameters such as swirl ratio and piston bowl shape on the engine characteristics.
- Future research is recommended to optimize the fuel blends used in the study.
- Future research work might be conducted for establishing strategies to mitigate the NO_x emissions by BTL diesel and the blended fuels.

References

[1] Shahid EM, Jamal Y. Production of biodiesel: A technical review. Renew Sustain Energy Rev 2011;15:4732–45. https://doi.org/https://doi.org/10.1016/j.rser.2011.07.079.

[2] World Energy Outlook 2007 – Analysis - IEA n.d. https://www.iea.org/reports/world-energy-outlook-2007 (accessed January 28, 2025).

[3] Atabani AE, Silitonga AS, Badruddin IA, Mahlia TMI, Masjuki Hh, Mekhilef S. A comprehensive review on biodiesel as an alternative energy resource and its characteristics. Renew Sustain Energy Rev 2012;16:2070–93.

[4] Adib AR, Rahman MM, Hassan T, Ahmed M, Al Rifat A. Novel biofuel blends for diesel engines: Optimizing engine performance and emissions with C. cohnii microalgae biodiesel and algae-derived renewable diesel blends. Energy Convers Manag X 2024;23:100688.

[5] Mahmudul HM, Hagos FY, Mamat R, Adam AA, Ishak WFW, Alenezi R. Production, characterization and performance of biodiesel as an alternative fuel in diesel engines–A review. Renew Sustain Energy Rev 2017;72:497–509.

[6] Wang B, Yang C, Wang H, Hu D, Wang Y. Effect of Diesel-Ignited Ammonia/Hydrogen mixture fuel combustion on engine combustion and emission performance. Fuel 2023;331:125865.

[7] Gao N, Kamran K, Quan C, Williams PT. Thermochemical conversion of sewage sludge: A critical review. Prog Energy Combust Sci 2020;79:100843.

[8] Rahman MM, Hassan T, Rabbi MF, Shakil MF, Khan MA. Transesterification of vegetable oil with ethanol using different catalysts. AIP Conf. Proc., vol. 2324, AIP Publishing; 2021.

[9] Suresh M, Jawahar CP, Richard A. A review on biodiesel production, combustion, performance, and emission characteristics of non-edible oils in variable compression ratio diesel engine using biodiesel and its blends. Renew Sustain Energy Rev 2018;92:38–49.

[10] Hassan T, Rahman MM, Rahman MA, Nabi MN. Opportunities and challenges for the application of biodiesel as automotive fuel in the 21st century. Biofuels, Bioprod

Biorefining 2022;16:1353–87.

[11] Rakopoulos CD, Antonopoulos KA, Rakopoulos DC, Hountalas DT, Giakoumis EG. Comparative performance and emissions study of a direct injection diesel engine using blends of diesel fuel with vegetable oils or bio-diesels of various origins. Energy Convers Manag 2006;47:3272–87.

[12] Murillo S, Miguez JL, Porteiro J, Granada E, Moran JC. Performance and exhaust emissions in the use of biodiesel in outboard diesel engines. Fuel 2007;86:1765–71.

[13] Stringer FW, Clarke AE, Clarke JS. The spontaneous ignition of hydrocarbon fuels in a flowing system. Proc. Inst. Mech. Eng. Conf. Proc., vol. 184, SAGE Publications Sage UK: London, England; 1969, p. 212–25.

[14] Agarwal AK. Biofuels (alcohols and biodiesel) applications as fuels for internal combustion engines. Prog Energy Combust Sci 2007;33:233–71.

[15] Syafiuddin A, Chong JH, Yuniarto A, Hadibarata T. The current scenario and challenges of biodiesel production in Asian countries: A review. Bioresour Technol Reports 2020;12:100608. https://doi.org/https://doi.org/10.1016/j.biteb.2020.100608.

[16] Thurston GD. Outdoor Air Pollution: Sources, Atmospheric Transport, and Human Health Effects. In: Heggenhougen HK (Kris) BT-IE of PH, editor., Oxford: Academic Press; 2008, p. 700–12. https://doi.org/https://doi.org/10.1016/B978-012373960-5.00275-6.

[17] Sobotowski RA, Porter BC, Pilley AD. The development of a novel variable compression ratio, direct injection diesel engine. SAE Trans 1991;100:776–92.

[18] Yamaki Y, Mori K, Kamikubo H, Kohketsu S, Mori K, Kato T. Application of common rail fuel injection system to a heavy duty diesel engine. SAE Trans 1994;103:1977–88.

[19] Neeft JPA, Makkee M, Moulijn JA. Diesel particulate emission control. Fuel Process Technol 1996;47:1–69.

[20] Koebel M, Elsener M, Kleemann M. Urea-SCR: a promising technique to reduce NOx emissions from automotive diesel engines. Catal Today 2000;59:335–45.

[21] Hassan T, Rahman MM, Adib AR, Meraz RM, Rahman MA, Tushar MSHK. Effect of Ni

and Al nanoadditives on the performance and emission characteristics of a diesel engine fueled with diesel-castor oil biodiesel-n-butanol blends. Case Stud Chem Environ Eng 2023;8:100531.

[22] Hassan T, Rahman MM, Rabbi MS, Rahman MA, Meraz RM. Recent Advancement in the Application of Metal Based Nano-additive in Diesel/Biodiesel Fueled CI Engine: A Comprehensive Review on Nanofluid Preparation and Stability, Fuel Property, Combustion, Performance, and Emission Characteristics. Environ Prog Sustain Energy 2022;42:e13976. https://doi.org/10.1002/ep.13976.

[23] Rimkus A, Žaglinskis J, Rapalis P, Skačkauskas P. Research on the combustion, energy and emission parameters of diesel fuel and a biomass-to-liquid (BTL) fuel blend in a compression-ignition engine. Energy Convers Manag 2015;106:1109–17.

[24] Ogunkoya D, Fang T. Engine performance, combustion, and emissions study of biomass to liquid fuel in a compression-ignition engine. Energy Convers Manag 2015;95:342–51.

[25] Hedden RG. Chapter 12 - Bioheat. In: Dahiya ABT-B (Second E, editor., Academic Press; 2020, p. 223–44. https://doi.org/https://doi.org/10.1016/B978-0-12-815497-7.00012-9.

[26] Tan SX, Lim S, Ong HC, Pang YL. State of the art review on development of ultrasound-assisted catalytic transesterification process for biodiesel production. Fuel 2019;235:886–907. https://doi.org/https://doi.org/10.1016/j.fuel.2018.08.021.

[27] Wan Ghazali WNM, Mamat R, Masjuki HH, Najafi G. Effects of biodiesel from different feedstocks on engine performance and emissions : A review. Renew Sustain Energy Rev 2015;51:585–602. https://doi.org/10.1016/j.rser.2015.06.031.

[28] Diya'Uddeen BH, Abdul Aziz AR, Daud WMAW, Chakrabarti MH. Performance evaluation of biodiesel from used domestic waste oils: A review. Process Saf Environ Prot 2012;90:164–79. https://doi.org/10.1016/j.psep.2012.02.005.

[29] Živković SB, Veljković M V, Banković-Ilić IB, Krstić IM, Konstantinović SS, Ilić SB, et al. Technological, technical, economic, environmental, social, human health risk, toxicological and policy considerations of biodiesel production and use. Renew Sustain Energy Rev 2017;79:222–47.

[30] Janaun J, Ellis N. Perspectives on biodiesel as a sustainable fuel. Renew Sustain Energy Rev 2010;14:1312–20.

[31] Atadashi IM, Aroua MK, Aziz AA. High quality biodiesel and its diesel engine application: a review. Renew Sustain Energy Rev 2010;14:1999–2008.

[32] Sajjadi B, Raman AAA, Arandiyan H. A comprehensive review on properties of edible and non-edible vegetable oil-based biodiesel: Composition, specifications and prediction models. Renew Sustain Energy Rev 2016;63:62–92. https://doi.org/https://doi.org/10.1016/j.rser.2016.05.035.

[33] Balat M, Balat H. Progress in biodiesel processing. Appl Energy 2010;87:1815–35.

[34] Chapagain BP, Yehoshua Y, Wiesman Z. Desert date (Balanites aegyptiaca) as an arid lands sustainable bioresource for biodiesel. Bioresour Technol 2009;100:1221–6.

[35] Azam MM, Waris A, Nahar NM. Prospects and potential of fatty acid methyl esters of some non-traditional seed oils for use as biodiesel in India. Biomass and Bioenergy 2005;29:293–302.

[36] Karmakar A, Karmakar S, Mukherjee S. Properties of various plants and animals feedstocks for biodiesel production. Bioresour Technol 2010;101:7201–10.

[37] Gürü M, Artukoğlu BD, Keskin A, Koca A. Biodiesel production from waste animal fat and improvement of its characteristics by synthesized nickel and magnesium additive. Energy Convers Manag 2009;50:498–502.

[38] Paraíba O, Tsoutsos T, Tournaki S, Antunes D, Lino J, Manning E. Strategies for optimization of the domestic used cooking oil to biodiesel chain. The European project recoil. Proc. 20th Eur. Biomass Conf. Exhib. Milan, Italy, 2012, p. 18–22.

[39] Osman A, Duan Y, Kaftandjian V. Applied Artificial Intelligence in NDE. Handb Nondestruct Eval 40 2021:1–35.

[40] Bhuiya MMK, Rasul MG, Khan MMK, Ashwath N, Azad AK. Prospects of 2nd generation biodiesel as a sustainable fuel—Part: 1 selection of feedstocks, oil extraction techniques and conversion technologies. Renew Sustain Energy Rev 2016;55:1109–28.

[41] Chisti Y. Biodiesel from microalgae. Biotechnol Adv 2007;25:294–306.

[42] Chisti Y. Biodiesel from microalgae beats bioethanol. Trends Biotechnol 2008;26:126–31.

[43] Ananthi V, Raja R, Carvalho IS, Brindhadevi K, Pugazhendhi A, Arun A. A realistic scenario on microalgae based biodiesel production: Third generation biofuel. Fuel 2021;284:118965.

[44] McGinnis KM, Dempster TA, Sommerfeld MR. Characterization of the growth and lipid content of the diatom Chaetoceros muelleri. J Appl Phycol 1997;9:19–24.

[45] Halim R, Gladman B, Danquah MK, Webley PA. Oil extraction from microalgae for biodiesel production. Bioresour Technol 2011;102:178–85.

[46] de Llasera MPG, Santiago ML, Flores EJL, Toris DNB, Herrera MRC. Mini-bioreactors with immobilized microalgae for the removal of benzo (a) anthracene and benzo (a) pyrene from water. Ecol Eng 2018;121:89–98.

[47] Demirbas A. Progress and recent trends in biofuels. Prog Energy Combust Sci 2007;33:1–18.

[48] Patil V, Tran K-Q, Giselrød HR. Towards sustainable production of biofuels from microalgae. Int J Mol Sci 2008;9:1188–95.

[49] Vonshak A. Recent advances in microalgal biotechnology. Biotechnol Adv 1990;8:709–27.

[50] Deshmukh S, Kumar R, Bala K. Microalgae biodiesel: A review on oil extraction, fatty acid composition, properties and effect on engine performance and emissions. Fuel Process Technol 2019;191:232–47.

[51] Kafuku G, Mbarawa M. Biodiesel production from Croton megalocarpus oil and its process optimization. Fuel 2010;89:2556–60.

[52] Singh D, Subramanian KA, Singal SK. Emissions and fuel consumption characteristics of a heavy duty diesel engine fueled with hydroprocessed renewable diesel and biodiesel. Appl Energy 2015;155:440–6.

[53] Meraz RM, Rahman MM, Hassan T, Al Rifat A, Adib AR. A review on algae biodiesel as

an automotive fuel. Bioresour Technol Reports 2023:101659.

[54] Lin L, Cunshan Z, Vittayapadung S, Xiangqian S, Mingdong D. Opportunities and challenges for biodiesel fuel. Appl Energy 2011;88:1020–31.

[55] Kennedy JF, Jumel K. The lipid handbook: Edited by FD Gunstone, JL Harwood and FB Padley, Chapman and Hall, 1986, xii+ 571+ 314 pp. ISBN 0 412 24480 2. Price:£ 95.00 1988.

[56] Balasubramanian S, Allen JD, Kanitkar A, Boldor D. Oil extraction from sheanut (Vitellaria paradoxa Gaertn CF) kernels assisted by microwaves. Bioresour Technol 2011;102:3396.

[57] Dvoretsky D, Dvoretsky S, Temnov M, Akulinin E, Peshkova E. Enhanced lipid extraction from microalgae Chlorella vulgaris biomass: experiments, modelling, optimization. Chem Eng Trans 2016;49:175–80.

[58] Ajala EO, Ajala MA, Akinpelu GS, Akubude VC. Cultivation and processing of microalgae for its sustainability as a feedstock for biodiesel production. Niger J Technol Dev 2021;18:322–43.

[59] Surendhiran D, Vijay M. Effect of various pretreatment for extracting intracellular lipid from Nannochloropsis oculata under nitrogen replete and depleted conditions. Int Sch Res Not 2014;2014:536310.

[60] Kumar M, Sharma MP, Dwivedi G. Algae oil as future energy source in Indian perspective. Int J Renew Energy Res 2013;3:913–21.

[61] Fattah IMR, Noraini MY, Mofijur M, Silitonga AS, Badruddin IA, Khan TMY, et al. Lipid extraction maximization and enzymatic synthesis of biodiesel from microalgae. Appl Sci 2020;10:6103.

[62] Razzak SA, Hossain MM, Lucky RA, Bassi AS, De Lasa H. Integrated CO2 capture, wastewater treatment and biofuel production by microalgae culturing—a review. Renew Sustain Energy Rev 2013;27:622–53.

[63] Hsieh C-H, Wu W-T. Cultivation of microalgae for oil production with a cultivation strategy of urea limitation. Bioresour Technol 2009;100:3921–6.

[64] Pragya N, Pandey KK, Sahoo PK. A review on harvesting, oil extraction and biofuels production technologies from microalgae. Renew Sustain Energy Rev 2013;24:159–71.

[65] Milano J, Ong HC, Masjuki HH, Chong WT, Lam MK, Loh PK, et al. Microalgae biofuels as an alternative to fossil fuel for power generation. Renew Sustain Energy Rev 2016;58:180–97.

[66] Ail SS, Dasappa S. Biomass to liquid transportation fuel via Fischer Tropsch synthesis–Technology review and current scenario. Renew Sustain Energy Rev 2016;58:267–86.

[67] Huber GW, Corma A. Synergies between bio-and oil refineries for the production of fuels from biomass. Angew Chemie Int Ed 2007;46:7184–201.

[68] Swain PK, Das LM, Naik SN. Biomass to liquid: a prospective challenge to research and development in 21st century. Renew Sustain Energy Rev 2011;15:4917–33.

[69] Rantanen L, Linnaila R, Aakko P, Harju T. NExBTL-Biodiesel fuel of the second generation. SAE Technical Paper; 2005.

[70] Tijmensen MJA, Faaij APC, Hamelinck CN, Van Hardeveld MRM. Exploration of the possibilities for production of Fischer Tropsch liquids and power via biomass gasification. Biomass and Bioenergy 2002;23:129–52.

[71] Faaij A, Meuleman B, Van Ree R. Long term perspectives of biomass integrated gasification with combined cycle technology. Costs and efficiency and a comparison with combustion 1998.

[72] Prins MJ. Thermodynamic analysis of biomass gasification and torrefaction 2005.

[73] Metzger JO. Production of liquid hydrocarbons from biomass. Angew Chemie Int Ed 2006;45:696–8.

[74] Iida H, Krische MJ. Catalytic reductive coupling of alkenes and alkynes to carbonyl compounds and imines mediated by hydrogen. Met Catalyzed Reductive C–C Bond Form A Depart from Preformed Organomet Reagents 2007:77–104.

[75] Spielmann M, Bauer C, Dones R, Tuchschmid M. Transport services: Ecoinvent report no. 14. Swiss Cent Life Cycle Invent Dübend 2007.

[76] Edwards R, Mahieu V, Griesemann J-C, Larivé J-F, Rickeard DJ. Well-to-wheels analysis of future automotive fuels and powertrains in the European context. SAE Trans 2004:1072–84.

[77] DIESEL-RK is an engine simulation software. Simulation and optimization of combustion and mixture formation in diesels. Nitrogen oxides NO, soot and particles formation modelling. Common Rail control algorithm development. Turbocharging, supercharging, EGR. Thermodynamic analysis. Valve timing optimization. Bauman Moscow State Technical University (BMSTU). n.d. https://diesel-rk.com/Eng/index.php?page=History (accessed February 4, 2025).

[78] Kartik A, Akhil D, Lakshmi D, Panchamoorthy Gopinath K, Arun J, Sivaramakrishnan R, et al. A critical review on production of biopolymers from algae biomass and their applications. Bioresour Technol 2021;329:124868. https://doi.org/https://doi.org/10.1016/j.biortech.2021.124868.

[79] Wan D, Wu Q, Kuča K. Chapter 42 - Spirulina. In: Gupta RCBT-N, editor., Boston: Academic Press; 2016, p. 569–83. https://doi.org/https://doi.org/10.1016/B978-0-12-802147-7.00042-5.

[80] Ciferri O, Tiboni O. The biochemistry and industrial potential of Spirulina. Annu Rev Microbiol 1985;39:503–26.

[81] Tomaselli L, Palandri MR, Tredici MR. On the correct use of the Spirulina designation. Arch Für Hydrobiol Suppl Algol Stud 1996;117:539–48.

[82] Mostafa SSM, El-Gendy NS. Evaluation of fuel properties for microalgae Spirulina platensis bio-diesel and its blends with Egyptian petro-diesel. Arab J Chem 2017;10:S2040–50.

[83] Morsy OM, Sharoba AM, El-Desouky AI, Bahlol HEM, Abd El Mawla EM. Production and evaluation of some extruded food products using spirulina algae. Ann Agric Sci Moshtohor 2014;52:329–42.

[84] Rajak U, Nashine P, Verma TN. Assessment of diesel engine performance using spirulina microalgae biodiesel. Energy 2019;166:1025–36.

[85] El Shimi HI, Attia NK, Abdel Allah AA, El Sheltawy ST, El Diwani GI. Quality profile of Spirulina platensis Oilgae extraction for biodiesel production. Biotechnology 2015;5:16–21.

[86] Vellaiyan S. Unlocking the potential of Spirulina microalgae: cultivating in wastewater treatment for sustainable biofuel production. Sustain Chem Pharm 2024;41:101705.

[87] Garg J, Mohite AA, Sharma P, Barik D, Medhi BJ, Deka H, et al. Energizing tomorrow: unleashing spirulina's potential in engine performance optimization and emission reduction. Environ Sci Pollut Res 2024:1–19.

[88] Nautiyal P, Subramanian KA, Dastidar MG, Kumar A. Experimental assessment of performance, combustion and emissions of a compression ignition engine fuelled with Spirulina platensis biodiesel. Energy 2020;193:116861.

[89] Rajak U, Nashine P, Verma TN, Pugazhendhi A. Performance, combustion and emission analysis of microalgae Spirulina in a common rail direct injection diesel engine. Fuel 2019;255:115855.

[90] Vellaiyan S. Performance enhancement of a diesel engine using nanoparticle-enriched algae biodiesel-diesel blends with an electrostatic precipitator for nanoparticle emission control. Energy Convers Manag 2025;326:119457.

[91] Munimathan A, Jayabalan J, Shanmugam MK, Majdi HS, Asif M, Ağbulut Ü. Evaluation of RCCI engine combustion, performance, and emissions using spirulina micro-algae biodiesel with methane-enriched hydrogen. Int J Hydrogen Energy 2024;77:712–23.

[92] Chaurasiya PK, Rajak U, Veza I, Verma TN, Ağbulut Ü. Influence of injection timing on performance, combustion and emission characteristics of a diesel engine running on hydrogen-diethyl ether, n-butanol and biodiesel blends. Int J Hydrogen Energy 2022;47:18182–93.

[93] Roy MM, Wang W, Alawi M. Performance and emissions of a diesel engine fueled by biodiesel–diesel, biodiesel–diesel-additive and kerosene–biodiesel blends. Energy Convers Manag 2014;84:164–73.

[94] Krishania N, Rajak U, Chaurasiya PK, Singh TS, Birru AK, Verma TN. Investigations of spirulina, waste cooking and animal fats blended biodiesel fuel on auto-ignition diesel engine performance, emission characteristics. Fuel 2020;276:118123.

[95] Rajak U, Nashine P, Verma TN. Effect of spirulina microalgae biodiesel enriched with diesel fuel on performance and emission characteristics of CI engine. Fuel 2020;268:117305.

[96] Subbiah G, Praveenkumar TR, Ramaraju PJ, Al-Ansari MM, Arun C, Barani B. Assessment of compression ignition engines performance using Spirulina microalgae biodiesel and gaseous fuel blends: A comparative study on efficiency, emissions, and combustion dynamics. J Taiwan Inst Chem Eng 2024:105916.

[97] Samet U, AL-GBURI ASK. Synthesis of spirulina microalgae biodiesel, and experimental research of its effects on compression ignition engine responses with iron II-III oxide (Fe3O4) nanoparticle supplementation. Energy Convers Manag 2023;293:117457.

[98] Alzubaidi MIA, Altawwash ASA, Abbas WN. Study on the performance and emissions of compression ignition engine powered by diesel and biodiesel blends. Int J Thermofluids 2024;24:100869.

[99] Žaglinskis J, Rimkus A. Research on the performance parameters of a compression-ignition engine fueled by blends of diesel fuel, rapeseed methyl ester and hydrotreated vegetable oil. Sustainability 2023;15:14690.

[100] Bezergianni S, Dimitriadis A. Comparison between different types of renewable diesel. Renew Sustain Energy Rev 2013;21:110–6.

[101] Fishcher F, Tropsch H. The synthesis of petroleum at atmospheric pressures. Brennstoff-Chemie 1926;7:97–104.

[102] Niemi S, Vauhkonen V, Mannonen S, Ovaska T, Nilsson O, Sirviö K, et al. Effects of wood-based renewable diesel fuel blends on the performance and emissions of a non-road diesel engine. Fuel 2016;186:1–10.

[103] Miers SA, Ng H, Ciatti SA, Stork K. Emissions, performance, and in-cylinder combustion

analysis in a light-duty diesel engine operating on a fischer-tropsch, biomass-to-liquid fuel. SAE Technical Paper; 2005.

[104] Soltic P, Edenhauser D, Thurnheer T, Schreiber D, Sankowski A. Experimental investigation of mineral diesel fuel, GTL fuel, RME and neat soybean and rapeseed oil combustion in a heavy duty on-road engine with exhaust gas aftertreatment. Fuel 2009;88:1–8.

[105] Mizushima N, Kawano D, Ishii H, Takada Y, Sato S. Evaluation of real-world emissions from heavy-duty diesel vehicle fueled with FAME, HVO and BTL using PEMS. SAE Technical Paper; 2014.

[106] Ng H, Biruduganti M, Stork K. Comparing the performance of SunDiesel™ and conventional diesel in a light-duty vehicle and heavy-duty engine. SAE Technical Paper; 2005.

[107] Gomes RJ. Testing of Diesel, BTL and Jet-A Fuel using a 1.8 L Heavy Duty Optical Engine Test-Bed with High Speed Visualization Techniques 2017.

[108] Grunberg L, Nissan AH. Mixture law for viscosity. Nature 1949;164:799–800.

[109] Arrhenius S. Über die Dissociation der in Wasser gelösten Stoffe. Zeitschrift Für Phys Chemie 1887;1:631–48.

[110] Schoo R, Hoxie A. Basic properties of refined, bleached and deodorized soybean oil–butanol blends. Fuel 2012;102:701–8.

[111] Clements LD. Blending rules for formulating biodiesel fuel. Liq Fuels Ind Prod from Renew Resour Third Liq Fuel Confersnce 1996:44–53.

[112] Le AT, Tran DQ, Tran TT, Hoang AT, Pham VV. Performance and combustion characteristics of a retrofitted CNG engine under various piston-top shapes and compression ratios. Energy Sources, Part A Recover Util Environ Eff 2024;46:13417–33.

[113] Ramírez-Verduzco LF, Rodríguez-Rodríguez JE, del Rayo Jaramillo-Jacob A. Predicting cetane number, kinematic viscosity, density and higher heating value of biodiesel from its fatty acid methyl ester composition. Fuel 2012;91:102–11.

[114] Singh S, Reitz RD, Musculus MPB. Comparison of the characteristic time (CTC), representative interactive flamelet (RIF), and direct integration with detailed chemistry combustion models against optical diagnostic data for multi-mode combustion in a heavy-duty DI diesel engine. SAE Trans 2006:61–82.

[115] Woschni G. A universally applicable equation for the instantaneous heat transfer coefficient in the internal combustion engine. SAE Technical paper; 1967.

[116] Fiveland SB, Assanis DN. A four-stroke homogeneous charge compression ignition engine simulation for combustion and performance studies. SAE Trans 2000:452–68.

[117] Kuleshov AS. Model for predicting air-fuel mixing, combustion and emissions in DI diesel engines over whole operating range. SAE Technical Paper; 2005.

[118] Heywood JB. Internal combustion engine fundamentals. (No Title) 1988.

[119] Alkidas AC. Relationships between smoke measurements and particulate measurements. SAE Technical Paper; 1984.

[120] Razleytsev NF. Combustion simulation and optimization in diesels. Kharkov: Vischa Shkola 1980.

[121] Homan HS. Conversion factors among smoke measurements. SAE Trans 1985:533–47.

[122] Datta A, Mandal BK. Impact of alcohol addition to diesel on the performance combustion and emissions of a compression ignition engine. Appl Therm Eng 2016;98:670–82.

[123] McAulay KJ, Wu T, Chen SK, Borman GL, Myers PS, Uyehara OA. Development and evaluation of the simulation of the compression-ignition engine. SAE Trans 1966:560–93.

[124] Kuleshov AS. Multi-zone DI diesel spray combustion model and its application for matching the injector design with piston bowl shape. SAE Technical Paper; 2007.

[125] Al-Dawody MF, Bhatti SK. Optimization strategies to reduce the biodiesel NOx effect in diesel engine with experimental verification. Energy Convers Manag 2013;68:96–104.

[126] Kuleshov AS. Use of multi-zone DI diesel spray combustion model for simulation and optimization of performance and emissions of engines with multiple injection. SAE

Technical Paper; 2006.

[127] Kuleshov AS. Multi-zone DI diesel spray combustion model for thermodynamic simulation of engine with PCCI and high EGR level. SAE Int J Engines 2009;2:1811–34.

[128] Rajak U, Nashine P, Verma TN, Pugazhendhi A. Alternating the environmental benefits of Aegle-diesel blends used in compression ignition. Fuel 2019;256:115835.

[129] Bayındır H, Işık MZ, Argunhan Z, Yücel HL, Aydın H. Combustion, performance and emissions of a diesel power generator fueled with biodiesel-kerosene and biodiesel-kerosene-diesel blends. Energy 2017;123:241–51.

[130] Omidvarborna H, Kumar A, Kim D-S. Recent studies on soot modeling for diesel combustion. Renew Sustain Energy Rev 2015;48:635–47.

[131] Roy CJ, Oberkampf WL. A comprehensive framework for verification, validation, and uncertainty quantification in scientific computing. Comput Methods Appl Mech Eng 2011;200:2131–44. https://doi.org/https://doi.org/10.1016/j.cma.2011.03.016.

[132] Oberkampf WL, Trucano TG. Verification and validation in computational fluid dynamics. Prog Aerosp Sci 2002;38:209–72. https://doi.org/https://doi.org/10.1016/S0376-0421(02)00005-2.

[133] EL-Seesy AI, He Z, Hassan H, Balasubramanian D. Improvement of combustion and emission characteristics of a diesel engine working with diesel/jojoba oil blends and butanol additive. Fuel 2020;279:118433.

[134] Jawad BA, Riedel CH. Analysis of Sauter Mean Diameter (SMD) for Fuel Sprays. Fluids Eng. Div. Summer Meet., vol. 42894, 2007, p. 1213–22.

[135] Martinez GL, Poursadegh F, Magnotti GM, Matusik KE, Duke DJ, Knox BW, et al. Measurement of Sauter mean diameter in diesel sprays using a scattering–absorption measurement ratio technique. Int J Engine Res 2019;20:6–17.

[136] Van Iersel S, Flammini A. Algae-based biofuels: applications and co-products 2010.

[137] Rajak U, Nashine P, Verma TN, Pugazhendhi A. Performance and emission analysis of a diesel engine using hydrogen enriched n-butanol, diethyl ester and Spirulina microalgae

biodiesel. Fuel 2020;271:117645.

[138] Gopinath S, Devan PK, Sabarish V, Babu BVS, Sakthivel S, Vignesh P. Effect of spray characteristics influences combustion in DI diesel engine–a review. Mater Today Proc 2020;33:52–65.

[139] Dorado MP, Ballesteros E, Arnal JM, Gomez J, Lopez FJ. Exhaust emissions from a Diesel engine fueled with transesterified waste olive oil☆. Fuel 2003;82:1311–5.

[140] Salam S, Verma TN. Appending empirical modelling to numerical solution for behaviour characterisation of microalgae biodiesel. Energy Convers Manag 2019;180:496–510.

[141] Syed A, Quadri SAP, Rao GAP, Mohd W. Experimental investigations on DI (direct injection) diesel engine operated on dual fuel mode with hydrogen and mahua oil methyl ester (MOME) as injected fuels and effects of injection opening pressure. Appl Therm Eng 2017;114:118–29.

[142] Ismael MA, Rosli MAF, Aziz ARA, Mohammed SE, Opatola RA, El-Adawy M. Gas to liquid (GTL) role in diesel engine: Fuel characteristics and emission: A review. Clean Eng Technol 2024;18:100706.

[143] Cai P, Zhang C, Jing Z, Peng Y, Jing J, Sun H. Effects of Fischer-Tropsch diesel blending in petrochemical diesel on combustion and emissions of a common-rail diesel engine. Fuel 2021;305:121587.

[144] Mubarak M, Shaija A, Suchithra T V. Experimental evaluation of Salvinia molesta oil biodiesel/diesel blends fuel on combustion, performance and emission analysis of diesel engine. Fuel 2021;287:119526.

[145] Elkelawy M, Bastawissi HA-E, Esmaeil KK, Radwan AM, Panchal H, Sadasivuni KK, et al. Experimental studies on the biodiesel production parameters optimization of sunflower and soybean oil mixture and DI engine combustion, performance, and emission analysis fueled with diesel/biodiesel blends. Fuel 2019;255:115791.

[146] Li B, Li Y, Liu H, Liu F, Wang Z, Wang J. Combustion and emission characteristics of diesel engine fueled with biodiesel/PODE blends. Appl Energy 2017;206:425–31.

[147] Guardiola C, Pla B, Bares P, Barbier A. An analysis of the in-cylinder pressure resonance excitation in internal combustion engines. Appl Energy 2018;228:1272–9.

[148] Bora BJ, Saha UK, Chatterjee S, Veer V. Effect of compression ratio on performance, combustion and emission characteristics of a dual fuel diesel engine run on raw biogas. Energy Convers Manag 2014;87:1000–9.

[149] Wamankar AK, Satapathy AK, Murugan S. Experimental investigation of the effect of compression ratio, injection timing & pressure in a DI (direct injection) diesel engine running on carbon black-water-diesel emulsion. Energy 2015;93:511–20.

[150] Al-lwayzy SH, Yusaf T. Diesel engine performance and exhaust gas emissions using Microalgae Chlorella protothecoides biodiesel. Renew Energy 2017;101:690–701.

[151] Şahin Z, Aksu ON. Experimental investigation of the effects of using low ratio n-butanol/diesel fuel blends on engine performance and exhaust emissions in a turbocharged DI diesel engine. Renew Energy 2015;77:279–90.

[152] Nabi MN, Akhter MS, Shahadat MMZ. Improvement of engine emissions with conventional diesel fuel and diesel–biodiesel blends. Bioresour Technol 2006;97:372–8.

[153] Kesharvani S, Verma TN, Dwivedi G. Computational analysis of chlorella protothecoides biofuels on engine combustion, performance and emission. Sustain Energy Technol Assessments 2023;55:102972.

Appendix – A

M

ORIGINALITY REPORT

17%	8%	16%	4%
SIMILARITY INDEX	INTERNET SOURCES	PUBLICATIONS	STUDENT PAPERS

PRIMARY SOURCES

1	Tafsirul Hassan, Md. Mizanur Rahman, Abidur Rahman Adib, Redoy Masum Meraz et al. "Effect of Ni and Al nanoadditives on the performance and emission characteristics of a diesel engine fueled with diesel-castor oil biodiesel-n-butanol blends", Case Studies in Chemical and Environmental Engineering, 2023 Publication	1%
2	coek.info Internet Source	1%
3	Tafsirul Hassan, Md. Mizanur Rahman, Md. Arafat Rahman, Md Nurun Nabi. " Opportunities and challenges for the application of biodiesel as automotive fuel for 21 century ", Biofuels, Bioproducts and Biorefining, 2022 Publication	1%
4	Tafsirul Hassan, Md. Mizanur Rahman, Md. Arafat Rahman, Md Nurun Nabi. "Opportunities and challenges for the application of biodiesel as automotive fuel in the 21st century", Biofuels, Bioproducts and Biorefining, 2022 Publication	1%
5	www.researchgate.net Internet Source	1%
6	Tafsirul Hassan, Md. Mizanur Rahman, Md. Sanaul Rabbi, Md. Arafat Rahman, Redoy	1%

Masum Meraz. " Recent Advancement in the Application of Metal Based Nano-additive in Diesel/Biodiesel Fueled Engine: A Comprehensive Review on Nanofluid Preparation and Stability, Fuel Property, Combustion, Performance, and Emission Characteristics ", Environmental Progress & Sustainable Energy, 2022
Publication

7	worldwidescience.org Internet Source	1 %
8	link.springer.com Internet Source	<1 %
9	Ambarish Datta, Bijan Kumar Mandal. "Impact of alcohol addition to diesel on the performance combustion and emissions of a compression ignition engine", Applied Thermal Engineering, 2016 Publication	<1 %
10	Ambarish Datta, Bijan Kumar Mandal. "Engine performance, combustion and emission characteristics of a compression ignition engine operating on different biodiesel-alcohol blends", Energy, 2017 Publication	<1 %
11	Alfredas Rimkus, Justas Žaglinskis, Paulius Rapalis, Paulius Skačkauskas. "Research on the combustion, energy and emission parameters of diesel fuel and a biomass-to-liquid (BTL) fuel blend in a compression-ignition engine", Energy Conversion and Management, 2015 Publication	<1 %
12	Upendra Rajak, Prerana Nashine, Tikendra Nath Verma. "Effect of spirulina microalgae biodiesel enriched with diesel fuel on	<1 %